

**UCSF**

**UC San Francisco Electronic Theses and Dissertations**

**Title**

Molecular Mechanisms of Dendrite Development: The Roles of Semaphorin Signaling and Phospholipid Homeostasis in Dendrite Morphogenesis

**Permalink**

<https://escholarship.org/uc/item/7p17994f>

**Author**

Meltzer, Shan

**Publication Date**

2017

Peer reviewed|Thesis/dissertation

Molecular Mechanisms of Dendrite Development: The Roles of  
Semaphorin Signaling and Phospholipid Homeostasis in Dendrite  
Morphogenesis

by

Shan Meltzer

DISSERTATION

Submitted in partial satisfaction of the requirements for the degree of

DOCTOR OF PHILOSOPHY

in

Neuroscience

in the

GRADUATE DIVISION

of the

UNIVERSITY OF CALIFORNIA, SAN FRANCISCO

Copyright 2017

by

Shan Meltzer

## **Acknowledgements**

I feel fortunate to have attended UCSF, which has prepared me well with comprehensive training to do significant research in the field of neuroscience. I would like to thank my mentors Drs. Yuh-Nung Jan and Lily Jan for their excellent mentorship and support during my time in graduate school. Their encouragement and scientific insights were critical to the completion of my PhD study, and the freedom they gave me to explore on my own was critical in developing my ability to do independent research. I would also like to thank the rest of my thesis committee, Drs. John Rubenstein, Graeme Davis, Eric Huang, and Liqun Luo (from Stanford University), for their guidance, support, and constructive criticism.

I would like to thank the current and former members of the Jan lab, who created an excellent environment that is both collaborative and intellectually stimulating. I thank Dr. Yi Rao for mentoring my undergraduate thesis research in Peking University, and inspiring me to enter the neurobiology field. I would like to thank Drs. Chun Han, Yuanquan Song, Woo-Ping Ge, Joshua Bagley, Smita Yadav, Wei Zhang, Susan Younger, Xi Huang, Peng Jin, Cassandra Ori-McKenney, Matthew Klassen, Caitlin O'Brien, and Li Cheng. I thank Drs. Jay Parrish and Peter Soba for their collaboration and guidance during my thesis research. I would also like to thank Dr. Tingting Wang, a postdoctoral fellow from Dr. Graeme Davis' lab, for being a supportive friend and discussing science with me. I am deeply grateful to them for their helpful advice and help on my PhD

research.

None of this would have been possible without the love and support from my friends and family in China and in the US. I would like to thank my parents, grandparents, my sister, and parents-in-law for their support throughout my life. I must also acknowledge my husband and best friend, Eric Meltzer, without whose love and belief in me, I would not have finished this thesis.

## Contributions

Yuh-Nung Jan supervised the research that formed the basis for this dissertation. Portions of this dissertation contain previously published materials. **Chapter 1** and **Chapter 4** are unpublished material. **Chapter 2** is a modified reprint of "Epidermis-Derived Semaphorin Promotes Dendrite Self-Avoidance by Regulating Dendrite-Substrate Adhesion in *Drosophila* Sensory Neurons" by Shan Meltzer, Smita Yadav, Jiae Lee, Peter Soba, Susan H. Younger, Peng Jin, Wei Zhang, Jay Parrish, Lily Yeh Jan, and Yuh-Nung Jan, appearing in Volume 89, Issue 4 of *Neuron* (2016). **Chapter 3** contains an unpublished reprint of "Phospholipid Homeostasis Regulates Dendrite Morphogenesis in *Drosophila* Sensory Neurons" by Shan Meltzer, Joshua A. Bagley, Gerardo Lopez Perez, Caitlin E. O'Brien, Yanmeng Guo, Lily Yeh Jan, and Yuh-Nung Jan. Individual author contributions are noted at the end of each respective chapter.

This work is comparable to work for a standard thesis awarded by the University of California, San Francisco.

**Molecular Mechanisms of Dendrite Development: The  
Roles of Semaphorin Signaling and Phospholipid  
Homeostasis in Dendrite Morphogenesis**

**by**

**Shan Meltzer**

John Rubenstein

Chair, Thesis Committee

## Abstract

Precise dendrite patterning is critical for the wiring and function of the entire nervous system. Proper dendrite morphogenesis determines the properties and strength of synaptic or sensory information a neuron will receive. Furthermore, deficits in dendritic development and function are observed in many neurodevelopmental disorders. Therefore, a better understanding of how the neuron establishes its dendrite morphology during development is necessary and will also provide insights into normal developmental pathways that may be perturbed in certain disorders. Using the *Drosophila* dendritic arborization (da) sensory neurons, we performed a candidate-based genetic screen to identify molecules that can regulate dendritic arbor morphology. This thesis work focuses on the examination of two candidate mutations identified by genetic screens performed in the lab.

In Chapter 2 we examine the role of the semaphorin signaling in regulating dendrite arbor patterning by restricting dendrites in a 2D space. Loss of *semaphorin-2b* (*sema-2b*) led to the detachment of dendrites from extracellular matrix (ECM) during dendrite outgrowth, resulting in failure of dendrites to be confined in a 2D space. Sema-2b proteins are required in epidermal cells, and act through Plexin-B (PlexB) receptor expressed in the neurons. We further show that Tricornered kinase, target of rapamycin complex 2 (TORC2), and integrins act downstream of the Sema-2b/PlexB signaling. Our findings identify a novel role for



semaphorins, which are well-known axon guidance proteins, in regulating dendrite patterning, and several new downstream signaling components of semaphorin signaling.

In chapter 3 we examine the role of *easily shocked* (*eas*), which encodes a kinase with a critical role in phospholipid phosphatidylethanolamine (PE) synthesis, in dendrite morphogenesis. *eas* is required cell-autonomously in da neurons for dendrite growth and stability. Further, we show that the level of Sterol Regulatory Element Binding Protein (SREBP) activity increased in *eas* mutants, and that decreasing the level of SREBP and its transcriptional targets in *eas* mutants largely suppressed the dendrite growth defects. Furthermore, reducing  $Ca^{2+}$  influx in neurons of *eas* mutants ameliorates the dendrite morphogenesis defects. Our study uncovers a novel role for EAS kinase and reveals the *in vivo* function of phospholipid homeostasis in dendrite morphogenesis.

## Table of Contents

<b>Chapter 1: Introduction</b> .....	<b>1</b>
Molecular mechanisms of dendrite development in the nervous system. ....	1
Alterations of dendritic morphogenesis in neurodevelopmental disorders. ....	2
Intrinsic regulators of dendritic arbor development .....	4
Extrinsic regulators of dendritic arbor development .....	8
The <i>Drosophila</i> dendrite arborization (da) neuron as a model to study dendrite morphogenesis .....	11
Significance .....	14
<b>Chapter 2: Semaphorin Promotes Self-avoidance by Restricting Dendrites of Class IV da Neurons into a 2D Space.</b> .....	<b>15</b>
Introduction .....	15
Results .....	17
Discussion .....	31
Author Contributions .....	36
Acknowledgments.....	37
Experimental Procedures .....	37
<b>Chapter 3: Phospholipid Homeostasis Regulates Dendrite Morphogenesis in <i>Drosophila</i> Sensory Neurons</b> .....	<b>43</b>
Introduction .....	43

Results .....	46
Discussion .....	54
Author Contributions .....	57
Acknowledgements.....	57
Experimental Procedures .....	57
<b>Chapter 4: Conclusions and Future Directions .....</b>	<b>61</b>
Semaphorin Regulation of Dendrite Morphology .....	61
Phospholipid Homeostasis During Dendrite Growth.....	63
<b>Figure Legends.....</b>	<b>66</b>
<b>References .....</b>	<b>86</b>
<b>Figures.....</b>	<b>120</b>

## List of Figures

Figure 1.1 Distributions and dendrite morphologies of classes I-IV <i>Drosophila</i> dendritic arborization (da) neurons. ....	120
Figure 2.1 Sema-2b, but not Sema-2a loss of function leads to an increase in dendritic self-crossings.....	121
Figure 2.2 Enclosure of terminal dendrites by epidermal cells in <i>sema-2b</i> mutants .....	122
Figure 2.3 Sema-2b is derived from epidermal cells and acts at short range to regulate dendrite adhesion.....	123
Figure 2.4 Plexin B is the Sema-2b Receptor that regulates dendrite-ECM adhesion.....	124
Figure 2.5 Sema-2b genetically interacts with TORC2 complex and Trc kinase .....	125
Figure 2.6 Trc kinase acts downstream of Sema-2b/PlexB signaling to promote dendrite adhesion.....	126
Figure 2.7 Integrins overexpression suppresses dendrite crossing defects in <i>sema-2b</i> mutant. ....	127
Figure 2.8 Mys, a $\beta$ subunit of integrin, associates with PlexB. ....	128
Figure 2.9 An example of a contacting and a non-contacting dendritic crossing and dendrite phenotype in class I da neuron in the <i>sema-2b</i> mutants.....	129
Figure 2.10 Overall morphology of axonal projections is normal in the <i>sema-2b</i>	

mutant. ....	130
Figure 2.11 Overall morphology of epidermal cells is normal in the <i>sema-2b</i>	
mutant .....	131
Figure 2.12 BAC Sema-2b reporters colocalize with the epidermal cell marker	132
Figure 2.13 PlexB, but not Sema-1a, is required to prevent dendrite-crossing in	
the class IV da neurons.....	133
Figure 2.14 <i>fak56</i> and <i>otk</i> mutants do not show strong genetic interaction with	
<i>sema-2b</i> mutants .....	134
Figure 2.15 Expression of proteins in S2 cells and dendrites of class IV da	
neurons .....	135
Figure 3.1 EAS Is Required in Class IV da Neurons for Dendrite Morphogenesis	
.....	136
Figure 3.2 EAS Regulates Terminal Dendrite Growth Dynamics .....	137
Figure 3.3 Aberrantly High Level of SREBP Transcriptional Activity Contributes to	
the Dendrite Morphogenesis Defects in <i>eas</i> <sup>KO</sup> Mutants .....	138
Figure 3.4 Reducing the level of <i>cacophony</i> partially suppresses dendrite	
morphogenesis defects in <i>eas</i> <sup>KO</sup> mutants .....	139
Figure 3.5 Generation of <i>eas</i> <sup>KO</sup> mutants .....	140
Figure 3.6 Loss of <i>eas</i> also leads to reduced dendritic growth in class I and III da	
neurons .....	141
Figure 3.7 Seizure-like phenotype in <i>eas</i> mutants is not suppressed by reducing	

SREBP signaling ..... 142

## **Chapter 1: Introduction**

### **Molecular mechanisms of dendrite development in the nervous system.**

Neurons were first recognized as the primary functional units of the nervous system in the late 19th century through the work of Santiago Ramón y Cajal (López-Muñoz et al., 2006; Ramón y Cajal, 1909). Neurons are highly polarized and electrically excitable cells comprised of axons and dendrites. Dendrites are the protrusions of a neuron that receive synaptic or sensory input and propagate the information to the cell body of the neuron, whereas an axon is a long protrusion of a neuron that conducts integrated electrical signals from one neuron to the other. The shape of dendritic arbors is one of features that can accurately distinguish different types of neurons from each other (Lefebvre et al., 2015). The morphology and types of input they receive vary dramatically among different types of neurons. Hence, the precise specification of dendrites and axons determines the direction and strength of information transmission, and is critical for the function of the nervous system.

The precise specification of dendrites is critical for neural information processing and computation in the nervous system (Lefebvre et al., 2015; London and Häusser, 2005; Spruston, 2008). First, the number, position, and types of synapses of a neuron are determined by the position and density of its dendrites. Second, the electrical properties of dendrites and the location of synaptic or

sensory inputs are important for the computation performed by the neuron. Therefore, highly diverse dendrite morphologies among distinct neuronal subtypes likely contribute to accommodating a wide range of computational needs in the nervous system. By understanding the molecular mechanisms of how the shape of dendrites is determined during development, we can have a complete picture of what dendrites do, and how they are wired in order to form functional neural circuits.

#### Alterations of dendritic morphogenesis in neurodevelopmental disorders.

Dendritic and synaptic pathology, such as alterations in dendrite branching patterns, reduction of dendritic branches, fragmentation of dendrites, and changes in dendritic spine morphology and number, have been characteristic anatomical features in many neurodevelopmental disorders, including autism spectrum disorders (ASDs), Rett syndrome, Down syndrome, schizophrenia and fragile X syndrome (Kulkarni and Firestein, 2012). For instance, a decrease the complexity of dendritic branching in CA4 and CA1 hippocampal neurons has been observed in autism patients (Raymond et al., 1996), and a reduction in the number of dendrites has been observed in neurons in the prefrontal cortex of autism patients (Mukaetova-Ladinska et al., 2004). Abnormal dendritic branching and synaptic immaturity were also observed in the brains of patients with fragile X syndrome, an inherited neurodevelopmental disorder associated with autism (Rudelli et al., 1985). Although observations obtained from human postmortem



studies suggest a generalized reduction in the number and size of dendrites, much remains to be learned about the pathology of alterations in dendrite development and how it contribute to behavior changes in patients.

Similarly, changes in dendrite morphology have also been observed in animal models of these disorders (Harony-Nicolas and Buxbaum, 2015; Martínez-Cerdeño, 2017). In both genetic and non-genetic models of autism, changes in dendrite morphology have been linked to behavioral defects (Martínez-Cerdeño, 2017). Indeed, genetic and biochemical studies showed that many genes that are associated with related disorders play important roles in regulating dendrite morphogenesis during development (Martínez-Cerdeño, 2017). For example, the gene *TAOK2* encoding serine/threonine kinase carries substantial susceptibility for autism (Weiss et al., 2008), and studies in cultured neurons have revealed that *TAOK2* regulates basal dendrite development in cortical neurons (de Anda et al., 2012), and dendritic spine maturation through phosphorylating cytoskeletal GTPase Septin7 (Yadav et al., 2017). *interleukin-1 receptor accessory protein like 1 (IL1RAPL1)*, a gene associated with intellectual disability and autism, regulates dendrite complexity in both mouse hippocampal neurons and induced pluripotent stem cell-derived neurons (Montani et al., 2017). Hence, elucidating the molecular mechanisms of dendrite morphogenesis will provide a better understanding how defects in dendrite morphogenesis contribute to neural circuit dysfunctions, and provide insights into the treatment of these

related disorders.

### Intrinsic regulators of dendritic arbor development

Intrinsic regulators are proteins that function inside neurons to determine dendrite morphogenesis. Studies of both invertebrates and vertebrates have identified numerous intrinsic regulators, including transcription factors, cytoskeletal factors, vesicular transport pathways, secretory and endocytic pathways, and other signaling cascades (Dong et al., 2015; Jan and Jan, 2010; Parrish et al., 2007b). Intrinsic regulators drive the overall patterning of dendritic arbors, and define unique neuronal responses to particular extrinsic regulators in the environment.

A combination of transcription factors determines the neuronal type-specific dendritic arbor with distinct functions and morphologies. Comprehensive genetic and expression analyses of transcription factors required for dendrite morphogenesis in *Drosophila* and *Caenorhabditis elegans* sensory neurons have identified many transcription factors and their possible target genes (Hattori et al., 2013; Parrish et al., 2006; Smith et al., 2010). For example, in *Drosophila* dendrite arborization (da) neurons, Abrupt (ab), an evolutionarily conserved BTB-zinc finger transcription factor, regulates the dendritic complexity of a subset of sensory neurons in a cell-autonomous and dosage-dependent manner (Li et al., 2004; Sugimura et al., 2004). The homeobox transcription factor Cut is expressed in a complementary pattern in da neurons, and different expression levels of cut

result in distinct type-specific patterns of dendrite arbors (Blochlinger et al., 1990; Grueber et al., 2003). *Cux1* and *Cux2*, the mammalian homologs of *Drosophila* Cut, also regulate dendrite growth, branching and complexity in cortical neurons (Cubelos et al., 2010; Li et al., 2010). Unlike Cut and Abrupt, Spineless, a conserved transcription factor, is expressed in all da neurons, but regulates dendrite morphogenesis in a neuronal type-specific manner (Kim et al., 2006). The *Drosophila* Forkhead transcription factor FOXO is also expressed in all da neurons and promotes dendrite growth and maintenance by regulating microtubule polymerization (Sears and Broihier, 2016). In addition, the Collier/Olfactory-1/early B cell factor Knot, is only expressed and required in class IV da neurons to regulate dendrite complexity (Crozatier and Vincent, 2008; Hattori et al., 2007; Jinushi-Nakao et al., 2007). These studies suggest that complicated networks of transcriptional regulators operate in concert to regulate type-specific dendrite arborization.

These transcriptional regulators represent promising candidates for studying dendrite morphogenesis in mammalian neurons in the future. The mammalian homologs of some of these transcription factors we introduced above have already been shown to regulate dendritic morphogenesis during development. For example, *Cux1* and *Cux2*, the mammalian homologs of *Drosophila* Cut, promote dendrite branching in layer II-III cortical neurons (Cubelos et al., 2010). During sensory cortex development, BTB/POZ domain-containing 3 (BTBD3), the

mammalian homolog of *Drosophila* Abrupt, translocates to the nucleus to remodel dendritic arbor shape in an activity-dependent manner (Matsui et al., 2013).

Coordinated polymerization of cytoskeletal components allows for directed transport of vesicles, and cytoskeletal growth during dendrite morphogenesis. Cytoskeletal components provide structural support and coordinated transport of cellular cargo for initial dendrite growth during early development, and later also provide mechanisms for the finely-tuned control of the length and position of dendrite arbors. Important factors that regulate the dynamics of the cytoskeleton include Ras-related small GTPases such as RhoA, Rac1, and Cdc42 (Lee, 2003; Lee et al., 2000; Li and Gao, 2003; Li et al., 2000; Nakayama et al., 2000; Ng et al., 2002; Scott et al., 2003; Stankiewicz and Linseman, 2014). Acentrosomal nucleation of microtubules initiated from Golgi outposts can also directly determine the location and growth stability of new dendrite branches in *Drosophila* class IV da neurons (Ori-McKenney et al., 2012). In class I da neurons, this dynamic process is suppressed by Centrosomin, a centrosome-associated protein regulated by Abrupt. Centrosomin recruits microtubule nucleation to Golgi outposts and counteracts anterograde microtubule growth to restrict dendrite growth (Yalgin et al., 2015). In mammalian neurons,  $\gamma$ -Tubulin-dependent nucleation also regulates dendrite branch formation by generating noncentrosomal microtubules in dendrites (Yau et al., 2014).

Vesicular transport is important for proper dendrite morphogenesis. Proteins

in dynein- or kinesin-associated motor complexes have been reported to regulate dendrite arborization. In vivo studies in *Drosophila* da neurons have identified *dynein light intermediate chain 2 (dlic2)*, *dynein intermediate chain (dic)* (Zheng et al., 2008), a dynein subunit gene *dynein light intermediate chain (dlic)* and *kinesin heavy chain (khc)* (Sato et al., 2008) as regulators of dendrite-specific localization of Golgi outposts and dendritic branch positioning. The Dynein motor complex also regulates the transport of cargo during dendritic branching in *C. elegans* mechanosensory neurons (Aguirre-Chen et al., 2011). In mammals, glutamate receptor interacting protein 1 (GRIP1) regulates dendrite growth by functioning as an adaptor protein for kinesin-dependent transport of cargo to dendrites. (Geiger et al., 2014; Hoogenraad et al., 2005).

Last but not least, secretory and endocytic pathways play important roles in supporting dendrite development. It was first observed that dendrites containing Golgi outposts are longer and more complex, and secretory trafficking is required for dendritic outgrowth (Horton et al., 2005). Genetic screens from *Drosophila* sensory neurons further identified *dar2*, *dar3*, and *dar6* (*dar*, dendritic arbor reduction), which encode proteins that function in COPII-mediated transport from the endoplasmic reticulum to the Golgi (Ye et al., 2007). In these mutants, impaired ER-to-Golgi transport led to decreased membrane supply from soma to dendrites, whereas membrane supply from soma to axons was not affected, suggesting that dendrites, but not axons, rely on the secretory pathway to

establish their different morphologies.

### Extrinsic regulators of dendritic arbor development

In this section, we will briefly review our current knowledge of how extrinsic regulators influence local and global decisions during dendrite development. In the nervous system, there are three major classes of extrinsic regulators: secreted cues, contact-mediated cues, and neuronal activity (Dong et al., 2015; Valnegri et al., 2015). Similar to intrinsic regulators, extrinsic regulators influence various aspects of dendrite morphogenesis, such as growth, branching, patterning, pruning, and maturation. Further, extrinsic molecules may function by modulating the intrinsic pathways we mentioned above to regulate dendrite morphogenesis.

First, secreted proteins outside the neurons play important roles in all aspect of dendrite morphogenesis. Neurotrophins (Chao, 2003; Joo et al., 2014; McAllister et al., 1995; Xu et al., 2000; Yacoubian and Lo, 2000; Zhou et al., 2012), Semaphorins (Koropouli and Kolodkin, 2014), Netrins and Slits (Furrer et al., 2003; Gibson et al., 2014; Godenschwege et al., 2002; Smith et al., 2012; Teichmann and Shen, 2011; Whitford et al., 2002), Wnts (Pino et al., 2011; Rosso et al., 2005; Wu et al., 2014), Ephrins (Anzo et al., 2017; Clifford et al., 2014; Hoogenraad et al., 2005; Xu et al., 2011) and Bone Morphogenetic Proteins (BMP) (Majdazari et al., 2013; Osório et al., 2013; Podkova et al., 2013) are examples of secreted cues which regulate dendrite development (Valnegri et al., 2015). For instance,

semaphorins, a large family containing both secreted and transmembrane proteins, regulate both axon guidance and dendrite patterning (Koropouli and Kolodkin, 2014). Secreted semaphorins, Sema2A, Sema2B, and Sema3A regulate dendrite branching and targeting in fly olfactory neurons as well as mammalian cortical neurons (Komiyama et al., 2007; Polleux et al., 2000; Sweeney et al., 2011). Sema3A also regulates apical dendrite formation in hippocampal neurons (Nakamura et al., 2009), and basal dendrite growth together with neuropilin1 (NRP1) and TAO kinase 2 (TAOK2) (de Anda et al., 2012). In addition, secreted proteins can act both over a long distance to orient dendritic growth and targeting, and locally to specify dendrite growth and patterning.

Second, an ever-growing list of contact-mediated regulators are also important for instructing dendrite morphogenesis. Many of these regulators mediate the interaction between dendrites and their local environment, such as axons, dendrites and glia, to regulate dendrite morphogenesis. Cadherins (Gao et al., 2000; Matsubara et al., 2011; Shima et al., 2007; 2004), protocadherins (Deans et al., 2011; Garrett et al., 2012; Lefebvre et al., 2012; Rubinstein et al., 2015), Down syndrome cell adhesion molecule (Dscam) (Fuerst et al., 2008; Hughes et al., 2007; Matthews and Grueber, 2011; Matthews et al., 2007; Soba et al., 2007; Yamagata and Sanes, 2008; Zhu et al., 2006), Teneurins (Hong et al., 2012), adhesion G-protein-coupled receptors (Lanoue et al., 2013), Integrins (Han

et al., 2012; Kim et al., 2012a), a multi-protein receptor-ligand complex containing SAX-7, MNR-1, DMA-1 and LECT2 (Díaz-Balzac et al., 2016; Dong et al., 2013; Salzberg et al., 2013; Zou et al., 2016) are examples of contact-mediated cues which regulate dendrite growth, targeting, maintenance, patterning (i.e. self-avoidance and tiling), and pruning.

Last but not the least, sensory and synapse-evoked neuronal activity plays important roles in regulating dendrite development, and their effects are mediated by calcium signals (Wong and Ghosh, 2002; Dong et al., 2015; Valnegri et al., 2015). Calcium influx mediated by voltage-gated calcium channels (VGCCs) or N-methyl-D-aspartate (NMDA) receptors activates calcium/calmodulin-dependent protein kinases (CaM, CaMKI, CaMKII, and CaMKIV) (Wayman et al., 2009) and calcium-responsive transcriptional activators, such as cAMP response element binding protein (CREB) and calcium-responsive transactivator (CREST) (Redmond and Ghosh, 2005), which regulate many aspects of dendrite morphogenesis (reviewed in Dong et al., 2015 and Valnegri et al., 2015). For example, in cerebellar granule neurons, VGCCs stimulate the activity of the  $\alpha$  isoform of CaMKII, turning on the activation of the basic helix-loop-helix transcription factor NeuroD to induce dendrite growth (Gaudillière et al., 2004). In *Drosophila* sensory neurons, calcium influx mediated by VGCCs is required for generating compartmentalized calcium transients to trigger dendrite pruning during pupal development (Kanamori et al., 2013). In addition to CaMKs,



mitogen-activated protein kinase (MAPK) also mediates the effect of neuronal activity on dendrite extension and stabilization (Redmond et al., 2002; Vaillant et al., 2002; Wu et al., 2001). In primates, the expression of activity-dependent secreted factor Osteocrin is induced by calcium influx to restrict dendrite growth (Ataman et al., 2016).

Overall, developing dendrites coordinate extrinsic and intrinsic cues to make global and local decisions about their number, length and position.

### **The *Drosophila* dendrite arborization (da) neuron as a model to study dendrite morphogenesis**

*Drosophila* dendrite arborization (da) sensory neurons are a powerful system to elucidate the molecular mechanisms behind dendrite development. The da neurons are a group of multidendritic sensory neurons in peripheral nervous system that can be separated into four classes (classes I, II, III and IV), based on the position of their cell bodies, dendritic morphologies and central axon projections (Grueber et al., 2002; 2007). Specifically, class I da neurons have simple comb-like dendritic patterns, class II da neurons show a slightly higher number of dendrites and larger dendritic territories, class III da neurons have many short actin-based terminal branches extending from their major branches, and class IV da neurons have the most complex dendritic arbor shape and non-redundantly innervate the entire epidermis (Figure 1.1) (Giangrande et al., 1993; Jan and Jan, 2010; Parrish et al., 2007b). The four classes also have

distinct functions: class I da neurons function as proprioceptors (Guo et al., 2016; Song et al., 2007), class III da neurons as gentle touch receptors (Yan et al., 2013) (Tsubouchi et al., 2012), and class IV da neurons as proprioceptors (Gorczyca et al., 2014; Song et al., 2007), light receptors (Xiang et al., 2010), and polymodal nociceptive (noxious heat and mechanical stimulus) neurons (Kim et al., 2012b; Tracey et al., 2003).

da neurons have been successfully used to study the molecular mechanisms of various interrelated steps during dendrite morphogenesis, including dendrite outgrowth and branching, guidance and targeting, dendritic arbor scaling and remodeling, tiling and self-avoidance. Mutagenesis screens, genome-wide RNAi screens, and candidate gene studies have discovered many genes that determine their type-specific dendritic morphologies (Corty et al., 2009; Jan and Jan, 2010; Parrish et al., 2007b; Singhanian and Grueber, 2014).

Among these interesting developmental processes, two key mechanisms that specify the spatial patterning of dendritic branches in the peripheral nervous system are self-avoidance and tiling (Singhanian and Grueber, 2014). Self-avoidance ensures complete and non-redundant coverage of sensory and synaptic inputs, while tiling prevents dendrites of sensory neurons of the same type from overlapping with each other. In both vertebrates and invertebrates, contact-mediated self-repulsion is a well-studied mechanism underlying self-avoidance (Jan and Jan, 2010). In *Drosophila*, Down Syndrome Cell

Adhesion Molecule (Dscam) mediates contact-dependent dendritic repulsion through homophilic interactions between identical isoforms of the protein on the dendrites of the same neuron (Hughes et al., 2007; Matthews et al., 2007; Soba et al., 2007). Each *Drosophila* neuron expresses a unique subset of Dscam isoforms (Wojtowicz et al., 2004), allowing dendrites of the same neuron to repel each other by isoform-specific homophilic interactions. A similar mechanism is found in mammalian retinal neurons where protocadherins (Pcdhs) mediate self-avoidance through isoform-specific homophilic interactions (Lefebvre et al., 2012). In addition, Sema6A/PlexA2-mediated repulsion between dendrites of the onset (On) starburst amacrine cell in the retina is also required for proper self-avoidance (Sun et al., 2013).

Self-avoidance and tiling does not depend entirely upon interactions between two-dimensional arbors (in the X-Y plane). In *Drosophila*, dendrite-ECM adhesion, which ensures that dendrites are properly restricted into layers along the Z axis, also facilitates contact-mediated self-avoidance and tiling (Han et al., 2012; Kim et al., 2012a). Dendrites of sensory neurons are tethered to the basal membrane to prevent non-contacting crossings between dendrites in different positions along the Z axis. Mutations in integrin subunits cause dendrites to detach from the extracellular matrix, resulting in excessive non-contacting crossings between dendrites (Han et al., 2012; Kim et al., 2012a). However, the regulatory components of dendrite-ECM adhesion in vivo remain poorly understood.

## Significance

This dissertation aims to better understand the molecular mechanisms of dendrite morphogenesis during development. Beginning with Chapter 2, we will examine the role of one extrinsic regulator, semaphorin signaling, in regulating dendrite stratification in *Drosophila* sensory neurons. Although semaphorins are known as a highly-conserved family of axon guidance cues, how they regulate dendrite patterning during development remains poorly understood. In Chapter 3, we will determine the role of phospholipid homeostasis in dendrite growth during development. Although phospholipid homeostasis is a fundamental process that happens in every cell, our understanding of its role in regulating dendrite development in vivo is lacking. Importantly, most of the genes examined in this dissertation are highly-conserved from fly to vertebrates, which make them interesting candidates to study in mammalian neurons in the future. Thus, this dissertation highlights the importance of highly-conserved genes in regulating dendrite morphogenesis, and provides insights in understanding the pathology of neurodevelopmental disorders that are linked to dendrite morphogenesis defects.

## **Chapter 2: Semaphorin Promotes Self-avoidance by Restricting Dendrites of Class IV da Neurons into a 2D Space.**

### **Introduction**

Precise patterning of dendritic arbors is crucial for the development and function of the nervous system, but the mechanisms that instruct dendrite patterning are only beginning to be elucidated (Dong et al., 2015; Jan and Jan, 2010; Puram and Bonni, 2013). In humans, defects in dendritic morphology are linked to neurodevelopmental disorders including autism, Down syndrome, and Fragile X syndrome (Kaufmann and Moser, 2000; Kulkarni and Firestein, 2012). To refine the location and strength of synaptic or sensory inputs, neurons use various strategies to organize their dendritic arbors, including self-avoidance and tiling (Jan and Jan, 2010; Zipursky and Sanes, 2010).

Self-avoidance, the phenomenon in which dendritic branches of the same neuron avoid overlapping with one another, ensures the non-redundant coverage of sensory or synaptic inputs. Tiling is the phenomenon in which the dendrites of neighboring neurons of the same type avoid overlapping with each other. In both vertebrates and invertebrates, contact-mediated self-repulsion is a well-studied mechanism underlying self-avoidance (Jan and Jan, 2010; Zipursky and Sanes, 2010; Zipursky and Grueber, 2013). In *Drosophila*, Down syndrome cell adhesion molecule (Dscam) mediates contact-dependent dendritic repulsion through homophilic interactions between identical isoforms of the protein on dendrites of the same neuron (Matthews et al., 2007; Soba et al., 2007; Hughes et al., 2007).

In mammalian neurons, protocadherins (Pcdhs) mediate self-avoidance through isoform-specific homophilic interaction (Chen and Maniatis, 2013; Lefebvre et al., 2012).

Importantly, self-avoidance and tiling require not only contact-mediated interactions between dendrites, but also dendrite-ECM adhesion to restrict the dendrites onto a 2D X-Y plane so that dendrites can not stray along the Z-axis and escape contact-mediated repulsion (Han et al., 2012; Kim et al., 2012). Similar spatial restriction of dendrites has been found in *Drosophila* sensory neurons, fish somatosensory neurons, and within the mammalian retina (Jan and Jan, 2010; Lawrence Zipursky and Grueber, 2013; Perry and Linden, 1982; Sagasti et al., 2005; Zipursky and Sanes, 2010). In the mammalian retina, laminar stratification of the neurites of retinal neurons is regulated by semaphorins (Matsuoka et al., 2011a; 2011b; Sun et al., 2013). However, how dendrite-ECM adhesion is regulated *in vivo* remains largely unknown.

*Drosophila* dendrite arborization (da) sensory neurons are a powerful model system to study the molecular mechanisms underlying dendrite-ECM adhesion. *Drosophila* da neurons can be divided into four classes (classes I-IV), based on dendritic morphology and central axon projections (Grueber et al., 2002; Grueber et al., 2007). During development, dendrites of da neurons extend mainly in a 2D plane. Defects in dendrite-ECM adhesion lead to a detachment from the ECM and therefore to an increase in the number of non-contacting crossings (Kim et al., 2012; Han et al., 2012). Loss-of-function mutations in integrin subunits cause dendrites to detach from the ECM and become enclosed by the epidermal cell

membrane, resulting in excessive non-contacting self-crossings between dendrites (Kim et al., 2012; Han et al., 2012). Additionally, target of rapamycin complex 2 (TORC2) and the evolutionarily conserved protein kinase Tricornered (Trc) as well as its adaptor protein Furry (Fry) were found to be important for self-avoidance and tiling (Emoto et al., 2004), and were shown to function by regulating dendrite-ECM adhesion (Han et al., 2012). To gain insight into how dendrite-ECM adhesion is regulated, we conducted a genetic screen in *Drosophila* class IV da neurons to examine the contribution of cell surface proteins.

In this study, we show that mutations in the secreted semaphorin ligand *sema-2b* cause detachment of dendrites from the ECM, leading to an increase in non-contacting dendritic crossings in class IV da neurons. Sema-2b protein is expressed and secreted from epidermal cells, and signals locally through the PlexB receptor in neurons. Moreover, we show that the TORC2 complex and the Trc/Fry signaling pathway act downstream of the Sema-2b/PlexB signaling pathway, and that the PlexB receptor associates with Mys, a  $\beta$  subunit of integrins *in vitro* and *in vivo*. Our results reveal an important role for semaphorins in the precise arrangement of dendrites during development and show how epidermis-derived cues shape neural circuit assembly.

## **Results**

### **Sema-2b Prevents Dendritic Crossings in Class IV da Neurons**

In a screen designed to identify cell surface proteins important for the development of sensory neuron dendrites *in vivo*, we discovered that mutations in

*sema-2b*, which encodes a secreted semaphorin ligand, led to a fully penetrant phenotype in which dendrites of class IV da neurons overlap with each other excessively (Figure 2.1B-D and 2.1H), whereas they normally avoid each other in wild-type larvae (Figure 2.1A and 2.1H). We examined the phenotypes of two mutant alleles of *sema-2b*: a P-element insertion called *sema-2b<sup>f02042</sup>* (Figure 2.1B) (Thibault et al., 2004), and a FRT-derived genomic deletion called *sema-2b<sup>C4</sup>* (Figure 2.1C) (Wu et al., 2011), which showed a stronger dendritic self-crossing phenotype than *sema-2b<sup>f02042</sup>* (Figure 2.1H). We also examined a heteroallelic combination of *sema-2b<sup>f02042/C4</sup>* mutants, which had an intermediate severity of the self-crossing phenotype in between that of *sema-2b<sup>f02042</sup>* and *sema-2b<sup>C4</sup>* mutants (Figure 2.1D and 2.1H). The *Drosophila* genome encodes two secreted semaphorin ligands, *Sema-2a* and *Sema-2b*, both of which often act in the same system (Joo et al., 2013; Wu et al., 2011). To determine if *Sema-2a* is required for preventing dendritic crossings, we examined *sema-2a* loss-of-function mutants and found that the loss of *sema-2a* did not lead to any increase in dendritic crossings (Figure 2.1E and 2.1H). Moreover, a double mutant of *sema-2a* and *sema-2b* did not show a more severe phenotype than *sema-2b* mutants alone (Figure 2.1F and 2.1H), suggesting that *Sema-2b*, but not *Sema-2a*, plays a major role in preventing dendritic self-crossings in class IV da neurons.

Dendrites of class IV da neurons are tightly confined between the basal surface of epidermal cells and the ECM, and branch out in a 2D plane, facilitating contact-mediated dendritic self-avoidance (Han et al, 2012; Kim et al., 2012). Loss of attachment to the ECM leads to enclosure of dendrites into epidermal



cells and thus to an increase in the number of non-contacting dendritic crossings (Han et al, 2012; Kim et al., 2012). To understand the nature of the dendritic crossings we observed in the *sema-2b* mutants, we tested whether these crossings involve direct contact between dendrites using *in vivo* high-resolution confocal imaging (Figure 2.1G; Figure 2.9A). In all mutants examined, we observed no significant increase in contacting crossings compared to wild-type controls (Figure 2.1H). However, the number of non-contacting crossings increased in *sema-2b* mutants and *sema-2a, sema-2b* double mutants (Figure 2.1H). In addition, we also found an increase in the number of non-contacting crossings in the class I da neurons in *sema-2b* mutants (Figures 2.9B-2.9D). By contrast, we found no detectable defects in the overall axonal projections of class IV da neurons in the ventral nerve cord of the *sema-2b* mutants (Figure 2.10). These observations suggest that the loss of Sema-2b leads to non-contacting dendritic crossings, possibly by an impairment of dendrite-ECM adhesion.

To determine whether Sema-2b is required in class IV da neurons to prevent dendritic crossings, we generated single neuron clones homozygous for a *sema-2b* mutation in an otherwise heterozygous background using the mosaic analysis with a repressible cell marker (MARCM) technique {Lee:1999bw}. Surprisingly, reducing Sema-2b function in class IV da neurons had no significant effect on dendritic self-crossings (Figures 2.1I-2.1K). Therefore, Sema-2b is not required in class IV da neurons for preventing self-crossing of dendrites (also see Figures 2.3J-2.3L).

## **Loss of Sema-2b Function Leads to a Progressive Increase in Detachment of Terminal Dendrites from the ECM**

To investigate the spatial distribution of dendrites in relation to the ECM, we visualized class IV da neuron dendrites using a class IV-specific membrane marker *ppk-CD4-tdTom* (Han et al., 2011) and the ECM using *viking-GFP* (*vkg-GFP*) (Han et al., 2012) in live third instar larvae. Using a combination of high-resolution confocal imaging and 3D deconvolution, we reconstructed the positions of each dendrite relative to the ECM. At 120 hr after egg laying (AEL), wild-type dendrites of class IV da neurons at the dorsal midline were tightly attached to the ECM (Figure 2.2C and 2.2E). In *sema-2b* mutants, however, the percentage of enclosed dendritic length greatly increased (Figure 2.2D and 2.2E), suggesting that defects in dendrite-ECM adhesion contribute to increased non-contacting dendritic crossings.

Enclosure of growing dendrites by epidermal cells is a dynamic process that takes place during development (Han et al., 2012). To determine the stage during which Sema-2b is required for dendrite-ECM attachment, we characterized the dendrite enclosure in wild-type and *sema-2b* mutant larvae at different time points throughout development. In wild-type larvae, class IV da neuron dendrites establish their receptive fields by tiling the body wall completely and non-redundantly at 48 hr AEL (Parrish et al., 2007a). We found that wild-type dendrites were tightly attached to the ECM from 48 hr AEL to 120 hr AEL (Figure 2.2A and 2.2E). Interestingly, in the *sema-2b* mutants, dendrites initially exhibit normal dendrite-ECM attachment at 48 hr AEL (Figure 2.2B and 2.2E). Defects in

dendrite-ECM attachment of *sema-2b* mutants became evident at 72 hr AEL and became worse at 96 hr AEL, revealing that *sema-2b* mutants exhibit progressive loss of dendrite-ECM attachment after neurons have established their receptive fields (Figure 2.2E).

Since it has been shown that terminal dendrite branching increases between 72 hr and 96 hr AEL (Parrish et al., 2007a), we reasoned that loss of terminal dendrite attachment to the ECM could be the main contributor to the observed increase in dendrite enclosure in the epidermis in *sema-2b* mutants. Indeed, we found that 72.2% of the enclosed dendrites (n=72) were terminal dendrites in *sema-2b* mutants, whereas only 25.0% of the enclosed dendrites (n=24) were terminal dendrites in wild-type animals (Figure 2.2F). In addition, we found that the overall morphology and total number of epidermal cells in the *sema-2b* mutants were the same as wild-type animals, suggesting that *Sema-2b* is not required for the development of epidermis (Figure 2.11).

Collectively, these data reveal that *Sema-2b* is required for the maintenance of dendrite attachment to the ECM in order to reduce non-contacting crossings (Figure 2.1G) and ensure non-overlapping coverage of dendritic fields.

### ***Sema-2b* is Secreted From Epidermal Cells to Regulate Dendrite-ECM Adhesion**

Next, we examined the localization of *Sema-2b* proteins in the *Drosophila* larval body wall using a polyclonal antibody specific for *Sema-2b* (Sweeney et al., 2011). We found that *Sema-2b* was evenly distributed throughout the wild-type

larval body wall (Figure 2.3A), and was completely absent in *sema-2b<sup>C4</sup>* null mutants (Figure 2.3B).

To pinpoint the source of Sema-2b, we employed a Sema-2b reporter, *2b<sup>L</sup>- $\tau$ GFP*, with the  $\tau$ GFP expression driven by the *sema-2b* promoter (Wu et al. 2011). The *2b<sup>L</sup>- $\tau$ GFP* reporter resided in epidermal cells (Figure 2.3C) and colocalized with an epidermal-cell specific marker (Figure 2.12). We further confirmed the expression pattern using a more selective Sema-2b reporter, *2b- $\tau$ Myc* (Wu et al. 2011). This reporter uses a shorter fragment of the *sema-2b* promoter to drive the expression of  $\tau$ Myc and labels a subset of cells in the developing *Drosophila* embryo that normally express a high level of Sema-2b (Wu et al. 2011). We found that *2b- $\tau$ Myc* labeled a subset of epidermal cells in the midline of each abdominal hemisegment, suggesting that these cells express a high level of Sema-2b (Figures 2.3D and 2.12). These results suggest that Sema-2b is expressed in epidermal cells, with a high level of expression in the midline of each segment.

We next tested if restoring Sema-2b in epidermal cells would be sufficient to rescue the dendrite crossing phenotype in the *sema-2b* mutants. To do this, we used the Gal4/UAS system in *Drosophila* to specifically express secreted Sema-2b in the epidermal cells using the epidermis-specific driver *Gal4<sup>A58</sup>* in the *sema-2b* mutant background (Galko and Krasnow, 2004). Indeed, expression of Sema-2b specifically in the epidermis, but not in class IV da neurons, rescued the crossing defects observed in the *sema-2b* mutants (Figures 2.3E-2.3G). To test if the release of Sema-2b protein into the extracellular space is required for dendrite

self-avoidance, we expressed a membrane-tethered *Sema-2b*<sup>TM</sup> in all the epidermal cells. We found that *Sema-2b*<sup>TM</sup> also rescued dendritic crossing defects in *sema-2b* mutants (Figure 2.3H-2.3I), suggesting that secretion of *Sema-2b* is not required for mediating dendrite self-avoidance. To further examine if locally produced *Sema-2b* is required to prevent dendrite crossing, we performed MARCM analysis to remove *Sema-2b* from epidermal cells and we found that dendrites innervating mutant *sema-2b* clones showed an increase in dendritic crossings ( $1.1 \pm 0.2$ , N=26), compared to control clones ( $0.3 \pm 0.1$ , N=26; Figures 2.3J-2.3L). Together, these results strongly suggest that *Sema-2b* is derived from epidermal cells and functions locally to regulate dendrite-ECM adhesion. Further, the fact that a clone of a single *sema-2b* mutant epidermal cell can produce the dendritic crossing phenotype in adjacent class IV da neuron dendrites strongly suggests that *Sema-2b* cannot diffuse substantially for a distance longer than the diameter of an epidermal cell.

### **PlexB functions in the Sensory Neurons to Regulate Dendrite-ECM Adhesion**

We next explored the mechanisms by which *Sema-2b* regulates dendrite-ECM adhesion in class IV da neurons. *PlexB* and *Sema-1a* have been shown to be receptors for *Sema-2a* and *Sema-2b* (Ayoob, 2006; Joo et al., 2013; Sweeney et al., 2011; Wu et al., 2011). *Sema-1a* loss-of-function mutants had normal dendrite morphology with no defects in dendritic crossing (Figure 2.13B). However, *plexB* loss-of-function mutants showed a large increase in the number

of dendritic crossings (Figures 2.4A, 2.4B and 2.4E), suggesting that reducing PlexB function leads to a defect in dendrite-ECM adhesion.

PlexB is expressed in class IV da neurons during the embryonic stages of development (Zlatic et al., 2009). Therefore, we investigated if the PlexB receptor is required cell-autonomously in class IV da neurons to mediate dendrite-ECM adhesion. We used Gal4/UAS-based RNA interference (RNAi) to knock down PlexB in class IV da neurons using *Gal4<sup>21-7</sup>* (Song et al., 2007). Using two different RNAi lines, we observed a strong increase in the number of dendritic crossings (Figures 2.4C-2.4E, and Figures 2.13C-2.13F), demonstrating that *plexB* acts cell-autonomously in class IV da neurons to regulate dendrite-ECM adhesion. Additionally, we found an increase in the number of non-contacting crossings when we knocked down *plexB* in class I da neurons (Figures 2.12G-2.13I).

To determine if *sema-2b* and *plexB* function in the same genetic pathway, we examined *sema-2b/+*, *plexB/+*, and *sema-2b/plexB* animals and found an increase in non-contacting crossings but not in contacting crossings in the *sema-2b/plexB* animals compared to *sema-2b/+* and *plexB/+* animals (Figures 2.4F-2.4I). In addition, we did not find genetic interaction between *sema-2b* and a null allele of a transmembrane protein Off-track (Otk), which mediates downstream signaling of Sema-1a and PlexinA {Winberg:2001dg}, suggesting that *otk* is not involved in regulating dendrite-ECM adhesion (Figures 2.14E-2.14G).

### **Sema-2b Genetically Interacts with TORC2 Complex and Trc/Fry**

To uncover the components of Sema-2b/PlexB signaling involved in dendrite-ECM adhesion, we assayed for genetic interactions between *sema-2b* and other known regulators of dendrite-ECM adhesion, including TORC2 complex and the Trc/Fry signaling pathway (Han et al. 2012). Trc kinases are a subclass of the protein kinase A (PKA)/protein kinase G (PKG)/protein kinase C (PKC) (AGC) group of serine/threonine kinases (Hergovich et al., 2006). In *Drosophila*, components of the TORC2 complex function in the same pathway by phosphorylating and activating Trc (Koike-Kumagai et al., 2009). In class IV da neurons, loss of components in the TORC2 complex, or the loss of Trc or Fry leads to an increase in dendritic self-crossings and defects in dendrite-ECM adhesion (Emoto et al., 2004; Han et al., 2012; Koike-Kumagai et al., 2009). We tested if Target of Rapamycin (*tor*), SAPK-interacting protein 1 (*sin1*), or rapamycin-insensitive companion of Tor (*rictor*), three components of TORC2 complex, genetically interact with *sema-2b*. We found strong genetic interactions between *sema-2b* and all three loss-of-function alleles (Figures 2.5A-2.5F and 2.5K). We further found that *sema-2b* also interacts genetically with *trc* and *fry* (Figures 2.5G-2.5K). These genetic interaction results suggest that the Sema-2b/PlexB signaling pathway likely functions together with TORC2 complex and Trc/Fry pathway to regulate dendrite-ECM adhesion.

### **Sema-2b/PlexB Signaling Regulates Dendrite-ECM Adhesion through Tricornered Kinase Activation**

Next, we investigated whether Sema-2b/PlexB signaling functions upstream or downstream of the Trc/Fry signaling pathway. The function of the Trc/Fry

signaling pathway is evolutionarily conserved, controlling dendrite growth and morphology in worms (Gallegos and Bargmann, 2004), flies (Emoto et al., 2004), and mammals (Ultanir et al., 2012). It has been previously shown that mammalian substrates of Trc/NDR1/2 kinase all contain the consensus sequence HXRXXS/T (Ultanir et al., 2012), which is absent in the *Drosophila* PlexB receptor. Therefore, we reasoned that PlexB is unlikely to be a direct substrate of Trc kinase.

To assess whether the Sema-2b/PlexB signaling pathway influences Trc kinase activity *in vivo*, we used a previously generated antibody that specifically detects phosphorylation on threonine residue 449 (T449) of Trc kinase, which is associated with maximal Trc kinase activation {Tamaskovic:2003dv}{Lee:2014if}. In the larval body wall, Trc P-T449 immunoreactivity was present at high levels in the axons, dendrites and cell bodies of class IV da neurons (Figures 2.6A and 2.6D). In the *sema-2b* and *plexB* mutants, overall Trc P-T449 levels were greatly reduced (Figures 2.6B-2.6D), whereas we did not see any difference in the overall Trc expression levels in class IV da neurons of the *sema-2b* and *plexB* mutants (data not shown). Together, these results suggest that Sema-2b/PlexB signaling is required for Trc phosphorylation and activation in class IV da neurons.

If Sema-2b/PlexB signaling functions by promoting Trc kinase activation to regulate dendrite-ECM adhesion, we hypothesized that ectopic Trc activation in class IV da neurons of *sema-2b* mutants would mitigate the dendritic crossing phenotype. First, we tested if overexpressing wild-type Trc could rescue the dendritic crossing phenotype in *sema-2b* mutants. It has been shown that overexpressing wild-type Trc in a wild-type background is sufficient to activate Trc



(Wu et al., 2013). Therefore, if overexpressing wild-type Trc could rescue the *sema-2b* mutant crossing phenotype, it would suggest that Trc functions downstream of Sema-2b/PlexB signaling, and that its activation is independent of Sema-2b/PlexB signaling. On the other hand, if overexpressing Trc does not rescue the *sema-2b* mutant crossing phenotype, it would suggest that Sema-2b/PlexB signaling is not only upstream of Trc, but is also required for its activation. Consistent with the second scenario, overexpressing wild-type Trc in *sema-2b* mutant background led to a more severe dendritic crossing defect (Figures 2.6E and 2.6H). Next, we overexpressed dominant negative Trc (S292AT449A), with alanine substitutions of Serine 292 (S292A) and Threonine 449 (T449A) to prevent phosphorylation and activation of Trc (Emoto et al., 2004). Consistent with our hypothesis, overexpressing dominant negative Trc in *sema-2b* mutants also led to a more severe dendritic crossing defect (Figures 2.6F and 2.6H). Finally, overexpressing a constitutively active myristoylated Trc (Myr-Trc), which targets Trc to the membrane (Koike-Kumagai et al., 2009), significantly suppressed the dendritic crossing defects of the *sema-2b* mutants (Figures 2.6G and 2.6H).

Together, these results suggest that Sema-2b/PlexB signaling regulates dendrite-ECM adhesion through the Trc/Fry signaling pathway.

### **Mys Associates with PlexB and Likely Acts Downstream of the Sema-2b/PlexB Signaling Pathway**

Loss of integrins in class IV da neurons causes defects in dendrite-ECM adhesion similar to those found in *sema-2b* and *plexB* mutants (Han et al., 2012;

Kim et al., 2012). Because Trc promotes integrin-mediated adhesion in class IV da neurons (Han et al., 2012), we hypothesized that defects in integrin-mediated adhesion contribute to the increased dendrite-ECM detachment seen in *sema-2b* and *plexB* mutants. If so, we reasoned that increasing the level of integrin expression should rescue the *sema-2b* mutant dendritic crossing defects, since integrin overexpression is able to suppress dendritic crossing defects of Trc/Fry pathway mutants (Han et al., 2012). To test this prediction, we overexpressed an integrin  $\alpha$  subunit encoded by *multiple edematous wings* (*mew*), and an integrin  $\beta$  subunit encoded by *myospheroid* (*mys*), both of which are required in class IV da neurons for dendrite-ECM adhesion (Han et al., 2012). In fact, overexpressing these two integrin subunits reduced the number of total dendritic crossings in *sema-2b* mutants to wild-type levels (Figures 2.7A-2.7C). It is worth noting that overexpressing integrins greatly reduced the number of non-contacting crossings, suggesting that dendrites become tightly attached to the ECM.

To test whether Mys and PlexB localize to dendrites, we expressed Mys-FLAG together with Myc-PlexB in class IV da neurons, and found that Mys-FLAG and Myc-PlexB strongly colocalize in the dendrites of class IV da neurons (Figure 2.7D; Pearson correlation coefficient  $0.71 \pm 0.02$ ,  $n=5$ ).

In mammals, activation of integrins signals through focal-adhesion kinase (FAK) family proteins to promote outgrowth of neurites (Ivankovic-Dikic et al., 2000), and semaphorin treatment has been shown to exert changes on Fak phosphorylation (Cho et al., 2012). Therefore, we tested if Fak is also required for dendrite-ECM adhesion in class IV da neurons. We examined the *fak56*<sup>CG1</sup> null

allele and found no significant difference in the number of dendritic crossings (Figures 2.14A and 2.14D). Moreover, we did not find any significant genetic interaction of *fak56* and *sema-2b* mutations (Figures 2.14B-2.14D). Our results suggest that Fak is not essential for regulating dendrite-ECM adhesion in class IV da neurons.

Plexin receptors have been shown to associate with various other receptors to mediate unique downstream signaling processes (Pasterkamp, 2012; Pasterkamp and Kolodkin, 2013). Whether the *Drosophila* PlexB receptor associates with other transmembrane receptors is unknown. Therefore, we asked if PlexB could associate with integrins by co-immunoprecipitations. We expressed FLAG-tagged Mys (Mys-FLAG) and Myc-tagged full-length PlexB (Myc-PlexB) in the *Drosophila* S2 cell line (Schneider, 1972). As a control, we expressed Myc-tagged Dscam, a guidance receptor required for contact-mediated self-avoidance in class IV da neurons (Matthews et al., 2007; Soba et al., 2007; Hughes et al., 2007), to examine if Dscam interacts with Mys. All proteins were expressed robustly and colocalized with membrane tagged GFP (Figures 2.15A and 2.15B). We immunoprecipitated Myc-PlexB and Dscam-Myc and found that Mys-FLAG co-immunoprecipitated with Myc-PlexB, but not with Dscam-Myc (Figure 2.8A). Consistent with these results, immunoprecipitation of Mys-FLAG revealed robust co-immunoprecipitation of both the full-length Myc-PlexB (250kDa) and the cleaved extracellular region of Myc-PlexB (150kDa) (Ayoob, 2006), but not Dscam-Myc (Figure 2.8B), demonstrating that the interaction between PlexB and Mys is specific.

To define the regions of Mys that interact with PlexB, we generated three FLAG-tagged Mys constructs encoding: the full-length Mys (FLAG-Mys), the Mys extracellular region with transmembrane domain (FLAG-MysEctoTM), and the Mys intracellular region with transmembrane domain (FLAG-MysEndoTM). Surface staining confirmed that these proteins were trafficked to the surface of S2 cells (Figure 2.15C). We found that immunoprecipitation of Myc-PlexB strongly co-immunoprecipitated FLAG-Mys and FLAG-MysEctoTM, but not FLAG-MysEndoTM (Figure 2.8C), suggesting that the formation of a complex between Mys and PlexB requires the extracellular region of Mys.

To test if Mys and PlexB interact on the surface of the cells, we performed surface staining and used an *in situ* proximity ligation assay (PLA), which can visualize specific protein-protein interactions (Söderberg et al., 2006). As a negative control, we generated FLAG-Dscam and confirmed its expression by western blotting and its membrane localization by surface staining (Figures 2.15D and 2.15E). We performed surface labeling of FLAG and Myc and found strong PLA signals only in the FLAG-Mys and Myc-PlexB co-expressed condition, and not in FLAG-Dscam and Myc-PlexB co-expressed condition (Figures 2.8E and 2.8F), demonstrating that Mys and PlexB interact on the surface of S2 cells.

Next, we examined if Mys and PlexB interact *in vivo* in dendrites of class IV da neurons. We expressed FLAG-Mys and Myc-PlexB (both tagged at the N-terminus) in class IV da neurons and performed *in situ* PLA (Figure 2.8G). As a negative control, coexpressing Mys-FLAG (tagged at the C-terminus) and Myc-PlexB should not give strong signals (Figure 2.8H). Indeed, even though

FLAG-Mys is expressed at a lower level than Mys-FLAG (Figure 2.15F), we found a significantly higher level of PLA signals in dendrites expressing FLAG-Mys and Myc-PlexB, compared to those expressing Mys-FLAG and Myc-PlexB (Figure 2.8I). We found PLA signals in both the proximal regions and the distal regions of the dendritic fields, suggesting the interactions of Mys and PlexB occur in these areas.

## **Discussion**

Self-avoidance and tiling are critical mechanisms governing the patterning of dendritic arbors. In *Drosophila* sensory neurons, these mechanisms depend on the dendrites being restricted onto a 2D plane through dendrite-ECM adhesion. We have uncovered a new role for Sema-2b/PlexB signaling in regulating dendrite-ECM adhesion to promote contact-mediated self-avoidance. We demonstrate that Sema-2b secreted from epidermal cells acts on neuronal PlexB receptors. Furthermore, we identified the TORC2 complex, the Trc/Fry signaling pathway and integrins as components of a Sema-2b/PlexB signaling pathway (Figures 2.8J and 2.8K). Our study uncovers previously unknown functions of semaphorin in regulating dendrite-ECM adhesion in neurons to promote dendrite self-avoidance.

### **Epidermis Secreted Cues Shape Neuron Circuit Formation**

Neurons interact with the complex environment that surrounds them at every step of neural development. For example, neuron-glia interaction has been studied in a variety of model organisms from worms to mammals (Corty and Freeman, 2013). Glia-secreted factors play an active role in neuronal migration,

axon guidance, and synapse formation during development, and have been implicated in many neurodevelopmental disorders (Sloan and Barres, 2014). In vertebrates and *Drosophila*, the secretion of TGF- $\beta$  ligands from glia regulates neuromuscular junction synapse formation and growth (Fuentes-Medel et al., 2012).

Compared to the extensive inquiries into neuron-glia interactions, the importance of neuron-epidermis interactions in neural circuit formation has only begun to be studied. Sensory neurons innervate the epidermis of both invertebrate and vertebrate organisms, and precise innervation must require diverse extrinsic signals. Two recent studies in *C.elegans* show that the epidermis generates pre-patterned cues to regulate sensory dendrite development (Dong et al., 2013; Salzberg et al., 2013). Our study provides evidence that semaphorin is an epidermis-derived ligand that instructs spatial patterning of sensory dendrites in *Drosophila*. In mammals, many members of the semaphorin family are expressed in sensory neurons, including those in dorsal root ganglia (O'Malley et al., 2014; Pasterkamp, 2012). It will be of great interest to determine whether epidermis-derived semaphorin also regulates morphogenesis of mammalian sensory neurons.

### **Role for Semaphorins in Regulating Dendrite-ECM Adhesion to Promote Self-Avoidance**

For self-avoidance involving homotypic repulsion, spatial restriction is critical to ensure that contact-mediated interaction between neurites occurs (Zipursky and Grueber, 2013). Similar to class IV da neurons, spatially restricted systems

for tiling and self-avoidance also exist in vertebrates, such as fish somatosensory neurons (Sagasti et al., 2005), mammalian cerebellar Purkinje cells (Kaneko et al., 2011), and mammalian retina (Sanes and Zipursky, 2010; Wässle, 2004). Indeed, semaphorin signaling is required for the stratification and symmetric arborization of starburst amacrine cell (SAC) dendrites in the developing mouse retina (Sun et al., 2013). Interestingly, SACs with defects in laminar stratification also show an increase in the number of self-crossings (Sun et al., 2013). In this study, we show that the spatial restriction mediated by dendrite-ECM adhesion is itself modulated by Sema-2b/PlexB signaling, thereby promoting contact-mediated self-avoidance in *Drosophila*. Our data suggests that Sema-2b/PlexB signaling does not directly promote contact-mediated dendritic repulsion, because the number of contacting crossings did not increase in the *plexB* mutants (Figure 2.4B and 2.4E). Conceptually, the problem of laminar stratification of neurites in vertebrate retina (Kim et al., 2010; Sanes and Zipursky, 2010) and the tethering of dendrites of *Drosophila* da neurons to the ECM are somewhat similar. In both cases, the growth of the neurites has to be constrained to a 2D space to allow the contact-mediated self-avoidance mechanism to operate. It is therefore very intriguing that semaphorins are involved in both situations (Sun et al., 2013 and this study). In the future, it will be of interest to determine whether the semaphorin regulated dendrite-substrate adhesion observed in our study also occurs in the dendrites of mammalian neurons, and if so whether it also contributes to self-avoidance and tiling in that context.

### **New Insights into the Semaphorin Signaling Pathway**

Semaphorin family proteins play essential roles in refinements of neural circuitry, including neuronal polarization, topographical mapping, dendrite arborization and axon sorting (Koropouli and Kolodkin, 2014; Pasterkamp, 2012). How a small number of proteins can generate such a diverse set of neuronal connections is an intriguing question. One mechanism by which semaphorins may achieve this feat is through activation of divergent downstream signaling pathways at different times during development. In the *Drosophila* embryonic central nervous system, PlexB receptors in mechanosensory axon terminals mediate both Sema-2b attraction and Sema-2a repulsion (Wu et al., 2011). At the embryonic stage, Sema-2a also acts through PlexB receptor to guide precise axon terminal projections of class IV da neurons (Zlatic et al., 2009). In our study, we found that Sema-2b, but not Sema-2a, acts on PlexB receptor to mediate dendrite adhesion to the ECM. How PlexB binding to Sema-2a and Sema-2b activates distinct downstream pathways is a question that awaits future studies.

*Drosophila* PlexB receptor has been shown to have opposite effects on cytoskeletal components by simultaneously inhibiting active Rac and enhancing RhoA signaling (Hu et al., 2001). Yet other components downstream of PlexB receptor are less well understood. Our study found that the activation of the Trc/Fry signaling pathway requires Sema-2b/PlexB signaling and provided genetic evidence that TORC2 and Trc activation is downstream of Sema-2b/PlexB signaling (Figure 2.8K). Our finding is consistent with a previous study that showed TORC2 complex associates with Trc and promotes its



activation possibly by recruiting Trc to the membrane in the class IV da neurons (Koike-Kumagai et al., 2009).

The phenotype of the *plexB* mutants we observed was weaker than the phenotype of *sema-2b* mutants. It is possible that the *plexB* allele we used is not a complete null allele (Ayoob, 2006), or that there is an unidentified Sema-2b receptor that also mediates Sema-2b/PlexB signaling (Figure 2.8K). It was recently shown that Ret receptor mediates dendrite-ECM adhesion and that Ret also associates with Mys (Soba et al., 2015), and it would be interesting to determine if Ret mediates part of Sema-2b signaling.

In our model, we proposed that Trc/Fry signaling is upstream of integrins, based on three lines of evidence (Figure 2.8K). First, overexpressing integrins in *trc* and *fry* mutant background rescued their dendrite-ECM adhesion defect (Han et al., 2012). Second, the mammalian homologue of Trc, NDR2 kinase, can induce phosphorylation at the activity and trafficking-relevant site of  $\beta$ 1-integrin to stimulate their trafficking to the cell membrane in neurons {Rehberg:2014ca}. Third, our previous study identified AAK1 (AP-2 associated kinase) and Rabin8, a GDP/GTP exchange factor (GEF) of Rab8 GTPase as two direct substrates of NDR1 kinase in mammals, both of which function in intracellular vesicle trafficking (Ultanir et al., 2012). Thus, it is possible that Trc/Fry signaling is important for regulating membrane turnover of integrins in neurons. In the future, it will also be important to determine whether the mammalian NDR kinases mediate semaphorin signaling.

Previous studies show that crosstalk between semaphorin and integrin signaling leads to inhibition of integrin-mediated adhesion in both invertebrates and vertebrates (Cho et al., 2012; Kruger et al., 2005; Tamagnone and Comoglio, 2004). For example, semaphorin-mediated signaling decreases integrin-mediated attachment during vascular morphogenesis (Serini et al., 2003). It has also been observed that semaphorin 4D promotes the formation of focal adhesion complexes through RhoA and Rho kinases (Basile et al., 2007). Here, we found that in *Drosophila* sensory neurons Sema-2b/PlexB signaling acts in the same pathway as integrins, and showed that PlexB and Mys form a complex (Figure 2.8). The biological relevance of this association would be of interest for future studies. It is possible that the physical association of PlexB and Mys stabilizes the surface expression of integrins for binding to laminins in the ECM. It is also possible that the interaction induces conformational changes to facilitate signaling pathways downstream of PlexB and/or integrins.

Overall, our results demonstrate that epidermis-secreted semaphorins regulate contact-dependent self-avoidance by promoting dendrite-ECM association and provide insights into the downstream components of semaphorin signaling pathway.

### **Author Contributions**

S.M. designed and performed a genetic screen, confocal imaging, genetic and statistical analysis, co-immunoprecipitations, and PLAs and wrote the manuscript with help from other authors. S.Y. co-designed and performed co-immunoprecipitations. J.L. co-designed and performed immunohistochemistry

with P-Trc antibody. S.H.Y. contributed to generating fly lines. P.S., P.J. and W.Z. contributed to generating several constructs. J.P., L.Y.J., and Y.-N.J. supervised the project development.

## Acknowledgments

We thank Drs. Chun Han, Matthew Klassen, Mu He, and William Joo for technical assistance; Drs. Alex Kolodkin, Liqun Luo, Bingwei Lu, and Tadashi Uemura for reagents; Bloomington Stock Center and VDRC Stock Center for fly stocks; and all members of the Jan lab for discussions. S.M. is the recipient of a National Science Foundation Graduate Research Fellowship under grant number 1144247. This work was supported by NIH grant number R37NS040929 to Y.-N.J. L.Y.J. and Y.-N.J. are investigators of the Howard Hughes Medical Institute.

## Experimental Procedures

### Fly Stocks

These following mutant alleles were used: a piggyBac insertion *sema-2b*<sup>f02042</sup> (Thibault et al., 2004), a FRT-mediated deletion *sema-2b*<sup>C4</sup> (Wu et al., 2011), a loss of function allele *sema-2a*<sup>03021</sup> (Matthes et al., 1995), an FRT-mediated deletion *sema-2b*<sup>B65</sup> (Wu et al., 2011), a loss of function allele *sema-2a*<sup>P2</sup> (Ayoob, 2006), a FRT-mediated deletion *sema-2ab*<sup>A15</sup> (Wu et al., 2011), *plexB*<sup>KG00878</sup> (Ayoob, 2006), *otk*<sup>3</sup> (gift from Denise Montell), *fak56*<sup>CG1</sup> (Chun-Jen Lin et al., 2011), *sin1*<sup>e03756</sup> (Han et al., 2012), *ric1*<sup>A2</sup> (Wu et al., 2013), *tor*<sup>AP</sup> (Wu et al., 2013), *trc*<sup>1</sup> (Geng et al., 2000), *fry*<sup>1</sup> (Cong et al., 2001). *UAS-plexB-RNAi* (v27220, v12167) were obtained from the Vienna *Drosophila* RNAi Center (VDRC). Other

transgenic flies used in this study were: *Gal4<sup>21-7</sup>* (Song et al., 2007), *Gal4<sup>A58</sup>* (Galko and Krasnow, 2004), *ppk-CD4-tdTom* (Han et al., 2011), *UAS-dcr-2* (Dietzl et al., 2007), *UAS-βPS (UAS-mys)* (Beumer et al., 1999), *vkg-GFP<sup>G00205</sup>* (Morin et al., 2001), *UAS-αPS1 (UAS-mew)* (Martin-Bermudo, 1997), *UAS-trc* (Emoto et al., 2004), *UAS-trc<sup>S292AT449A</sup>* (Emoto et al., 2004), *UAS-myr-trc* (Wu et al., 2013), *UAS-plexB* (Ayoob, 2006), *UAS-sema-2b-TM* (Wu et al., 2011). *UAS-sema-2b* flies were generously provided by Dr. Alex Kolodkin (Johns Hopkins University).

### **Live Imaging and Image Processing**

Animals were reared at 25°C and 29°C for RNAi experiments in density-controlled vials. Third instar larvae were mounted in glycerol and dendrites of class IV da neurons were imaged using a Leica SP5 laser scanning confocal microscope. For high-resolution imaging in the z axis, images were collected as described in Han et al., 2012. To quantify dendrite enclosure, images were deconvoluted using Autoquant (MediaCybernetics) and analyzed in Imaris (Bitplane) as described in Han et al., 2012.

### **Immunohistochemistry**

Third instar larvae were dissected in PBS, fixed in 4% PFA for 20 min at room temperature, blocked with 5% normal goat serum, and stained with the primary antibodies in a 0.3% Triton X-100 solution overnight at 4°C, and subsequently with secondary antibodies in a 0.3% Triton X-100 solution for 3 hours at room temperature.

### **Statistical analysis**

Two-tailed Student's t-tests were used to compare two samples. A one-way ANOVA test was used to compare multiple samples.

### **Molecular Biology.**

To generate N-terminally tagged proteins, we first generated pUAST-FLAG vector with the IgK-chain leader sequence from the pSecTagB vector (Invitrogen, Carlsbad, CA) followed by a FLAG tag. The amino-terminal fragment of Dscam and Mys was amplified by PCR to remove the signal peptide sequences and cloned into the pUAST-FLAG vector. FLAG-Mys was then cloned into a pACU2 vector (Han et al., 2011) to generate transgenic flies. Mys (amino acids 1-846) deletions were made according to its annotation in UniProt: MysEcto<sup>TM</sup> (1-804) and Endo<sup>TM</sup> (769-846). MysEcto<sup>TM</sup> and Endo<sup>TM</sup> fragments were amplified using PCR and cloned into the pUAST-FLAG vector. cDNA of Dscam (3.36.25.1) isoform (Wang et al., 2004) was cloned into a pUAST-Myc vector. Mys-FLAG was cloned from pUAST-Mys-FLAG (Soba et al., 2015) into pJFRC81-10XUAS-IVS-Syn21-GFP-p10 vector (Pfeiffer et al., 2012) for making transgenic flies. All constructs were fully sequenced and plasmids were injected by Rainbow Transgenic Flies.

### **Immunohistochemistry**

Primary antibodies and dilutions used in this study were mouse anti-tMyc (1:1000, Santa Cruz Biotechnology, Cat#sc-40), chicken anti-GFP (1:500, Aves Labs, Cat#GFP-1020), rabbit anti-Sema-2b (preabsorbed against larval brains from homozygous *sema-2b*<sup>C4</sup> mutants, 1:100, Sweeney et al, 2011), mouse anti-FLAG (1:100, Sigma), rabbit anti-Myc (1:500, Sigma, RRID:AB\_439680),

goat anti-HRP (1:500, Jackson Labs, Cat# 123-165-021), rabbit anti-pTrcT449 {Lee:2014if}, Mouse anti-Fasciclin III (1:100, 7G10, Developmental Studies Hybridoma Bank, RRID:AB\_528238).

For S2 cell surface staining, cells were incubated in primary antibody for 30 min without detergent, fixed in 4% PFA for 15 min at 4°C, blocked with 5% normal goat serum, and stained with other primary antibodies in a 0.1% Triton X-100 solution overnight at 4°C, and subsequently with secondary antibodies in a 0.1% Triton X-100 solution for 30 min at room temperature.

### **Colocalization Analysis**

Third instar larval filets immunostained for Mys, PlexB and GFP were imaged by confocal microscopy with high resolution and confocal stacks, which were deconvoluted using AutoQuant software. Colocalization analysis was performed on the deconvoluted confocal stacks using the Imaris software as described in Soba et al., 2015. Briefly, the GFP signals were used to create a mask to specifically analyze neuronal Mys and PlexB signals, which were automatically thresholded. A colocalization channel was then built and we performed Costes randomization for all samples to ensure that the colocalization coefficients between Mys and PlexB were non-random.

### **Quantification of P-Trc levels**

The P-Trc antibody signals of class IV da neuron dendrites were quantified using ImageJ and the averaged background signals were subtracted from each image. To obtain background signal levels, four areas in each image with no dendrites in them were used to calculate the mean pixel intensity for both the

P-Trc channel and the Tomato channel. The equation used for the subtraction is shown below:

$$\begin{aligned} & \text{Normalized - pTrc level} \\ &= \frac{\text{pTrc MeanInt (a. u.)} - \text{pTrc MeanBackground (a. u.)}}{\text{Tomato MeanInt (a. u.)} - \text{Tomato MeanBackground (a. u.)}} \end{aligned}$$

MeanInt refers to mean intensity and a.u. stands for arbitrary unit. Statistical analysis for three genotypes was performed in Prism software using one-way ANOVA test.

### ***In situ* Proximity Ligation Assay**

Drosophila S2 cells were transfected 48 hours before plating on ConA-coated (Sigma) glass coverslips. Cells were incubated with primary antibodies for mouse anti-FLAG (Sigma, 1:300, RRID:AB\_262044) and rabbit anti-Myc (Sigma, 1:300, RRID:AB\_439680) for 30 min prior to fixation in 4% PFA for 15 min at 4°C. Cells were then blocked for 30 min and Duolink® *in situ* PLA was performed according to manufacturer's protocol (Sigma). Cover slips were mounted using Duolink® *in situ* mounting medium with DAPI (Sigma). Slides were imaged by confocal microscope and PLA signal intensities in GFP positive cells (transfected cells) were quantified using imageJ.

For *in situ* PLA in dendrites, larval body walls were fixed in 4% PFA for 20min, blocked for 1 hour, and incubated with mouse anti-FLAG (Sigma, 1:500, RRID:AB\_262044) and rabbit anti-Myc (Sigma, 1:500, RRID:AB\_439680). Duolink® *in situ* PLA was then performed according to manufacturer's protocol (Sigma). Body walls were mounted and imaged with a confocal microscope. The number of PLA dots were counted and normalized to dendritic length.

## MARCM Analysis

MARCM analyses of *sema-2b* were performed as described in Grueber et al., 2002. *sema-2b<sup>C4</sup>*, *FRT42D* or *FRT42D* flies were crossed with *Gal4<sup>5-40</sup>*, *UAS-venus*, *SOP-flp*; *FRT42D*, *tub-Gal80* (generously provided by Dr. Tadashi Uemura) to generate marked *sema-2b<sup>C4</sup>* mutant class IV da neurons or wild-type neurons. To create epidermal MARCM clones, we crossed *sema-2b<sup>C4</sup>*, *FRT42D*; *ppk-CD4-tdTomato* or *FRT42D*; *ppk-CD4-tdTomato* flies with *tubulin-Gal4*, *UAS-GFP*, *hs-flp*; *FRT42D*, *tub-Gal80*. To induce epidermal clones, we collect embryos at 25°C for 3 hours, wait for 1 hour, and heat shock embryos at 37°C for 1 hour. We then examined late third instar larvae for the presence of mutant clones and live-imaged selected larvae under glycerol and a coverslip.

## Immunoprecipitation and Western Blotting

*Drosophila* S2 cells were grown at 25°C in Schneider's *Drosophila* Medium (Life Technologies) with 10% FBS and Penicillin. Cells were seeded in a 60mm petri dish and were transfected 24 hours after plating with pUAST constructs together with pActin-Gal4 using Effectene Transfection Reagent (Qiagen). Cells were washed in PBS 48 hours after transfection, pelleted and incubated in HKT lysis buffer (10mM HEPES pH7.2, 100mM KCl, 1% TritonX-100, 2mM DTT, PMSF, and protease inhibitors from Roche) for 20 min on ice. Cells were homogenized, and spun at 12000g on a table-top centrifuge to collect the supernatant, which was then incubated with Protein A Sepharose® 4B (Thermo Fisher Scientific) beads for 30 min to inhibit non-specific binding. To immunoprecipitate Mys-FLAG, the pre-cleared supernatant was incubated with



FLAG (M2) affinity sepharose beads (Sigma) overnight. To immunoprecipitate Myc tagged PlexB and Dscam, the pre-cleared supernatant was incubated with rabbit anti-Myc (Sigma) for 3 hours and then Protein A Sepharose® 4B for 2 hours. Beads were washed thrice with HKT buffer and twice with buffer without detergent. Sample buffer was added to the beads, boiled for 10 min and then samples were run on a 4-12% gradient Bis-Tris precast gel (Novex) using Mops-SDS running buffer (Novex). NuPAGE MES SDS Running Buffer (Thermo Fisher Scientific) was used for running Mys samples in the domain mapping experiments. Gel was transferred on PVDF membrane (Millipore) and nitrocellulose membrane for Mys domain mapping experiments. Membranes were blocked with 10% milk in TBST buffer and probed for presence of PlexinB and Dscam using Myc (rabbit polyclonal from Sigma, 1:1000, RRID:AB\_439680, or mouse monoclonal from BD Biosciences, 1:500, Cat#554205), and FLAG (mouse monoclonal from Sigma; 1:1000, RRID:AB\_262044) antibodies.

## **Chapter 3: Phospholipid Homeostasis Regulates Dendrite Morphogenesis in *Drosophila* Sensory Neurons**

### **Introduction**

How neurons achieve the proper wiring pattern during development is an important question, as the dendrite arborization pattern of each neuron is critical for the function of the nervous system (Jan and Jan, 2010; Lefebvre et al., 2015).

Defects in dendrite morphogenesis are common anatomical features of many neurodevelopmental disorders (Kaufmann and Moser, 2000). Although abnormal lipid metabolism has been observed in mouse models as well as patients with neurodevelopmental disorders (Buchovecky et al., 2013; Tamiji and Crawford, 2010; Tint et al., 1994) and 60 percent of the human brain dry mass is lipids (Wong and Crawford, 2014), relatively little is known about the importance of lipid homeostasis for dendrite morphogenesis during neural development.

We have used the dendritic arborization (da) sensory neurons of the *Drosophila* larval peripheral nervous system (PNS) to identify the molecular mechanisms that regulate dendrite morphogenesis of these neurons, which fall into four distinct classes (I–IV) based on their dendrite morphologies and axon projections (Grueber et al., 2002; 2007). From a genetic screen for genes that affect dendritic growth in class IV da neurons, we identified *easily shocked* (*eas*) as an important gene that regulates dendrite morphogenesis in sensory neurons. The *eas* gene encodes a conserved ethanolamine kinase, the first enzyme in the cytidine 5'-diphosphate (CDP)-ethanolamine pathway for the synthesis of the membrane phospholipid phosphatidylethanolamine (PE) (KENNEDY, 1957). PE is the major phospholipid in most dipterans (Fast, 1966) and the second most abundant phospholipid in mammals (Vance, 2014). In *Drosophila*, PE is the predominant phospholipid in membranes (Jones et al., 1992), and regulates the processing and activity of sterol regulatory element-binding protein (SREBP), a

highly conserved basic helix-loop-helix leucine zipper transcription factor that is crucial for lipid homeostasis (Dobrosotskaya et al., 2002). Reduction of the PE level causes SREBP precursor proteins to be transported from the endoplasmic reticulum to the Golgi apparatus, where they are cleaved to release the transcriptionally active domain that translocates to the nucleus to activate the expression of lipogenic genes (Rawson, 2003). Prior to our study, it was unknown how this phospholipid homeostasis process affects dendrite development.

Originally identified by Seymour Benzer in his pioneering work of *Drosophila* neurogenetics, *eas* mutants respond to a mechanical jolt by exhibiting transient paralysis and then recover, whereas wild type flies are unaffected (Benzer, 1971). *eas* mutant flies were subsequently used as a *Drosophila* model of seizure; their seizure-like phenotype could be suppressed by mutations that reduced the hyperexcitability of *eas* mutants (Parker et al., 2011; Pavlidis et al., 1994a). It is unknown whether these mutations that reduce hyperexcitability also affect neural morphogenesis in *eas* mutants. Reducing the level of *cacophony* (*cac*), the *Drosophila* homolog of the Cav2 voltage-gated calcium channel genes and a major mediator of neuronal Ca<sup>2+</sup> influx (Peng and Wu, 2007; Saras and Tanouye, 2016), potently suppresses the seizure phenotype present in *eas* mutants. We found that reducing *cac* gene activity significantly ameliorated the dendrite morphogenesis defects of *eas* mutants.

Here, we show that the dendrite morphogenesis defects of *eas* mutants are

attributable to increased lipogenesis and altered  $\text{Ca}^{2+}$  influx. Our results uncover a previously unknown role for the conserved ethanolamine kinase and for SREBP signaling in dendrite morphogenesis and highlight an important role of phospholipid and lipid homeostasis during neuronal development.

## Results

### **EAS Kinase Acts Cell-Autonomously to Regulate Dendrite Morphogenesis in da Neurons**

From an RNA interference (RNAi) screen for regulators of dendrite development in *Drosophila*, we identified *eas*, which encodes ethanolamine kinase (Pavlidis et al., 1994), as a candidate. To corroborate the RNAi results, we first examined the existing *eas* allele, *eas*<sup>1</sup>, which produces a truncated protein lacking kinase activity (Pavlidis et al., 1994). We further generated knockout mutants, *eas*<sup>KO</sup> (Figures 3.5A and 3.5B), in which the entire coding region is removed via CRISPR/Cas9 (Port et al., 2014). Both alleles showed similar dendrite outgrowth defects at 120 hours (hrs) after egg laying (AEL), with dramatic decreases in the number of branches and the total dendrite length in class IV da neurons (Figures 3.1A-3.1C, 3.1E and 3.1F). Sholl analysis revealed that reductions in dendrite branching occurred uniformly throughout the dendritic arbor in the *eas*<sup>1</sup> and *eas*<sup>KO</sup> mutants (Figure 3.1G). In addition, we found decreases in the number of branches and the total dendrite length in class I and

class III da neurons in the *eas*<sup>1</sup> and *eas*<sup>KO</sup> mutants (Figures 3.6A-3.6H). We further examined the morphology of class IV da neurons at 48, 72, 96, and 120 hrs AEL in wildtype and *eas*<sup>KO</sup> mutants. Dendrites of class IV da neurons normally establish their dendritic territories and completely tile the body wall by 48 hrs AEL, and then continue to grow throughout larval development (Parrish et al., 2007a). Although the patterning of class IV da neurons in *eas*<sup>KO</sup> mutants examined at 48 hrs AEL initially proceeded normally, dendrite growth defects became apparent at 72 hrs AEL (Figures 3.1E and 3.1F), suggesting that *eas* is required for dendrite outgrowth and/or stability after the initial dendrite territory is established.

We next asked whether *eas* was required cell-autonomously in class IV da neurons to regulate dendrite morphogenesis. We were able to rescue the *eas*<sup>KO</sup> and *eas*<sup>1</sup> dendrite morphogenesis defects by expressing *eas* in class IV da neurons (Figures 3.1H and 3.1I). Furthermore, knocking down *eas* only in da neurons led to a similar reduction in number of branches and total dendrite length (Figures 3.1D, 3.1H and 3.1I), suggesting that *eas* is required cell-autonomously in class IV da neurons for proper dendrite morphogenesis.

In *Drosophila*, the *eas* gene encodes an ethanolamine kinase that catalyzes the phosphorylation of ethanolamine to phosphoethanolamine, which is modified by phosphoethanolamine cytidylyltransferase (encoded by *pect*) to produce CDP-ethanolamine. CDP-ethanolamine donates phosphoethanolamine to diacylglycerol to generate PE, which is mediated by CDP-ethanolamine

phosphotransferase (encoded by *bbc*) (Dobrosotskaya et al., 2002). Therefore, we asked whether the dendrite morphogenesis defects were due to insufficient PE synthesis through the CDP–ethanolamine pathway. Compared with control animals, expressing RNAi constructs against *pect* and *bbc* specifically in neurons both led to *eas*<sup>KO</sup>-like decreases in the number of branches and dendrite length (Figures 3.1J-3.1N), suggesting that PE synthesis through the CDP–ethanolamine pathway is important for dendrite growth.

Together, these results reveal that *eas* cell-autonomously regulates dendrite morphogenesis in da neurons after dendrite territories are established. These findings highlight the impact of the CDP-ethanolamine pathway on dendrite development.

### **EAS Kinase Regulates Terminal Dendrite Dynamics**

Dendrites in wildtype animals grow and branch extensively starting from 48 hrs AEL, while displaying dynamic growth and retraction of the terminal dendrites (Parrish et al., 2007a). Since the dendrite defects of *eas*<sup>KO</sup> mutant neurons became apparent during this period, we asked whether *eas* is required for normal terminal dendrite dynamics (Figures 3.2A-3.2F). By performing *in vivo* time-lapse analysis during larval development at 72 hrs and 76 hrs AEL, we detected terminal dendrite growths and retractions while these dendrites formed complete field coverage in wildtype animals (Figures 3.2A-3.2C). The fraction of retracting terminal dendrites in *eas*<sup>KO</sup> mutant class IV da neurons was increased compared

to wildtype controls (Figure 3.2H), while the fraction of growing terminal dendrites was unaltered (Figure 3.2G). As a result, 77.5% of the terminal dendrites were dynamic in *eas*<sup>KO</sup> mutants (n=10), whereas 70.1% of the terminal dendrites were dynamic in wildtype animals (n=10, p<0.05), suggesting that *eas* is required for stabilizing terminal dendrites. Furthermore, the growth/retraction ratio of terminal dendrites was significantly decreased in class IV da neurons in *eas*<sup>KO</sup> mutant, owing to the disproportional increase in retraction compared to growth (Figure 3.2I).

Our findings suggest that *eas* is important for stabilizing terminal dendrites and supporting dendrite growth after the initial dendrite patterning is established.

### **Level of SREBP Activity is Critical for Dendrite Morphogenesis in the Class IV da Neurons**

Previous studies have established a link between low PE levels and increased SREBP activity (Dobrosotskaya et al., 2002; Lim et al., 2011), which is critical for turning on the transcription of downstream genes for lipogenesis (Rawson, 2003). In mice and *Drosophila*, abnormally high SREBP transcriptional activity triggered by reactive oxygen species causes lipid droplet accumulation in glia before the onset of neurodegeneration (Liu et al., 2015). Importantly, *srebp* mutant larvae are auxotrophic for fatty acids and die by the end of the second instar (Kunte et al., 2006). However, it is unknown whether SREBP, a highly conserved transcription factor that is essential for lipid homeostasis, regulates

nervous system development.

To test whether the level of SREBP transcriptional activity is important for dendrite morphogenesis, we first tested the consequence of increased SREBP activity in class IV da neurons by expressing constitutively active forms of SREBP. Indeed, expressing the N-terminal domain containing the first 452 amino acids of SREBP, which mimics the cleaved, active form of SREBP (SREBP.1-452), led to a dramatic decrease in the number of branches (Figure 3.3E) and the total dendrite length (Figure 3.3D) of class IV da neurons. Similarly, expressing another truncated form of constitutively active SREBP (SREBP.Cdel) in class IV da neurons also led to severe dendrite outgrowth defects (Figures 3.3A, 3.3B, 3.3D and 3.3E).

Conversely, we examined whether the reduced level of SREBP activity affects dendrite morphogenesis by expressing a previously-characterized SREBP RNAi in class IV da neurons (Figure 3.3C) (Song et al., 2014). Knocking down SREBP in neurons also led to a dramatic decrease in the number of branches (Figure 3.3E) and the total dendrite length (Figure 3.3D). Taken together, our results demonstrate that SREBP signaling for lipid homeostasis is critical for dendrite outgrowth during larval development.

### **Aberrant Lipid Homeostasis Mediated by SREBP Signaling Contributes to Dendrite Morphogenesis Deficits in *eas*<sup>KO</sup> Mutants**

Given that the level of SREBP activity is critical for dendrite growth, we



tested the hypothesis that SREBP acts downstream of a deficiency in PE synthesis to alter dendrite morphogenesis in *eas*<sup>KO</sup> mutants. First, we determined whether SREBP activity is altered in *eas*<sup>KO</sup> mutants by examining the processing of endogenous SREBP proteins by Western blots using wildtype and *eas*<sup>KO</sup> larval brains. Most of the endogenous SREBP proteins were full-length, membrane-bound precursors (FI-SREBP), and only a trace amount of the cleaved and mature form (m-SREBP) was detected in wildtype larval brains (Figure 3.3F). In contrast, a greater fraction of SREBP proteins were found to be m-SREBP in *eas*<sup>KO</sup> mutant brains (Figure 3.3F). The increase in the level of the mature form of SREBP protein in *eas*<sup>KO</sup> mutants suggests that loss of *eas* results in greater activation of SREBP signaling.

To determine whether the increased transcriptional activity of SREBP contributes to dendrite morphogenesis defects in *eas*<sup>KO</sup> mutants, we reduced the level of SREBP in *eas*<sup>KO</sup> mutants to see whether the severity of dendrite growth defects would be ameliorated. Indeed, removing one copy of the SREBP gene in *eas*<sup>KO</sup> mutants significantly restored dendrite growth (Figures 3.3G and 3.3H). In *Drosophila*, the mature form of cleaved SREBP protein travels to the nucleus to activate the expression of known lipogenic genes (Rawson, 2003), including *acetyl-coA carboxylase (acc)*, *fatty acid synthase (fas)*, *acetyl CoA synthase (acs)* and *fatty acyl CoA synthetase (acsl)* (Seegmiller et al., 2002). Given that the SREBP processing and transcriptional activity is increased in *eas*<sup>KO</sup> mutants, we

reasoned that the dendrite morphogenesis defects could arise from increased expression of SREBP target genes. To test whether reducing the activities of SREBP target genes in *eas*<sup>KO</sup> mutants affects the mutant phenotype, we expressed RNAi constructs targeting *acc* and *fas* in class IV da neurons of *eas*<sup>KO</sup> mutants (Figures 3.3I and 3.3J), and introduced one copy of the *acsl* or *acs* mutant alleles in *eas*<sup>KO</sup> mutants (Figures 3.3K and 3.3L). Indeed, reducing the expression level of the SREBP downstream target genes significantly improved dendrite morphogenesis in *eas*<sup>KO</sup> mutants, leading to increased number of branches and total dendrite length in most cases (Figures 3.3M and 3.3N). While knocking down *fas* in class IV da neurons in *eas*<sup>KO</sup> mutants also increased the number of branches, it did not increase the dendrite length, possibly due to a low RNAi efficiency or the redundancy of the three *fas* genes in the *Drosophila* genome.

Together, these results show that hyperactivation of SREBP signaling contributes to the dendrite growth defects in *eas*<sup>KO</sup> mutants, thus underscoring the importance of lipid homeostasis in dendrite morphogenesis.

### **Reducing the Level of *cacophony* Partially Suppresses Dendrite Morphogenesis Deficits in *eas*<sup>KO</sup> Mutants**

Adult *eas* flies with characteristic seizure-like phenotypes have been used as a model for screening for mutations that could suppress neuronal hyperexcitability and hence bang sensitivity (Parker et al., 2011; Saras and Tanouye, 2016). To

determine whether the bang-sensitive seizure-like phenotype was associated with defects in dendrite development, we asked whether the increased lipid homeostasis mediated by SREBP also contributes to the seizure-like phenotype in *eas*<sup>KO</sup> mutants (Figure 3.7A). Interestingly, removing one copy of the SREBP genes did not suppress the bang-sensitive behavioral phenotype in *eas*<sup>KO</sup> mutants (Figure 3.7B). Similarly, mutations in the transcriptional targets of SREBP, *acs* and *acsl*, which were able to ameliorate the dendrite morphogenesis defects in class IV da neurons, did not suppress the bang-sensitive seizure-like behavior in *eas*<sup>KO</sup> mutants (Figure 3.7B). These results suggest that dendrite morphogenesis defects mediated by the altered lipid homeostasis pathway likely do not contribute to the physiological defects that eventually lead to seizure susceptibility in *eas*<sup>KO</sup> mutant flies.

We then asked whether genes that suppressed the seizure-like phenotype could ameliorate the dendrite morphogenesis defects in *eas*<sup>KO</sup> mutants. Mutations in *cacophony* (*cac*), a gene encoding the  $\alpha 1$  subunit of the voltage-gated  $\text{Ca}^{2+}$  channel that is a major neuronal mediator of neuronal  $\text{Ca}^{2+}$  currents (Peng and Wu, 2007), potently suppress the seizure-like behavior in *eas* mutants (Saras and Tanouye, 2016). Interestingly, *cac* is also required shortly after the larval stage to mediate dendrite  $\text{Ca}^{2+}$  influx and hence pruning of class IV da neurons during metamorphosis (Kanamori et al., 2013). We found that knocking down *cac* by expressing a previously characterized RNAi construct (Saras and Tanouye, 2016)

in class IV da neurons significantly ameliorated the dendrite outgrowth defects in *eas*<sup>KO</sup> mutants (Figures 3.4A and 3.4B), leading to increases in the total dendrite length (Figure 3.4D) and the number of branches (Figure 3.4E). Consistent with previous observation (Kanamori et al., 2013), knocking down *cac* in class IV da neurons in wildtype animals did not cause any significant dendrite growth defects, suggesting that low Ca<sup>2+</sup> influx does not impair dendrite morphogenesis (Figure 3.4C). It thus appears that calcium signaling is abnormally enhanced in *eas*<sup>KO</sup> mutants. Although overexpressing *escargot* (*esg*, a member of the snail family of transcription factors) (Hekmat-Safe et al., 2005) or *kazachoc* (*kcc*, K<sup>+</sup>-Cl<sup>-</sup> cotransporter) (Hekmat-Safe et al., 2010) was able to suppress seizure-like phenotype in *eas* mutants, their overexpression in class IV da neurons could not suppress the dendrite phenotype in *eas*<sup>KO</sup> mutants (Figures 3.7C-3.7F). Therefore, the increased Ca<sup>2+</sup> influx, rather than hyperexcitability *per se*, likely contribute to dendrite morphogenesis defects in *eas*<sup>KO</sup> mutants, indicative of Ca<sup>2+</sup> regulation of dendrite growth.

## Discussion

Here, we provide evidence that impairment in the synthesis of the phospholipid PE in *eas* mutants and the reduction of other enzymes in the PE synthesis pathway lead to defects in dendrite growth after the initial establishment of dendritic fields, accompanied with a reduction in the stability of terminal

dendrites. These defects in dendrite morphogenesis can be attributed to elevated levels of lipid synthesis, mediated by SREBP signaling, and changes in neuronal  $\text{Ca}^{2+}$  influx. Specifically, the dendrite morphogenesis defects of *eas*<sup>KO</sup> mutants are significantly suppressed by reducing the level of lipogenic gene expression or by reducing the expression of *cacophony* encoding a subunit of a voltage-gated calcium channel. To our knowledge, this is the first *in vivo* evidence that EAS kinase and SREBP, two highly conserved molecules involved in lipid homeostasis, play an important role in dendrite morphogenesis.

A growing body of evidence suggests that lipid metabolism and homeostasis is important for nervous system development (Zhang and Liu, 2015). Furthermore, disruptions in the metabolism of lipids including phospholipids have been linked to autism spectrum disorders (Wong and Crawford, 2014), which are also associated with defects in dendrite morphogenesis (Kaufmann and Moser, 2000). Here, we provide evidence that EAS kinase and its downstream SREBP signaling pathway are required for dendrite growth and stability during development. Since the homologues of both genes are highly conserved and expressed in human brain (Uhlén et al., 2015), it will be interesting to determine their roles in dendrite morphogenesis within the developing mammalian central nervous system. Given the importance of *eas* and SREBP signaling in dendrite growth and stability shown in our study, it will also be interesting to investigate the role of phospholipid homeostasis in the dendrite morphogenesis abnormalities

that are present in many neurodevelopmental disorders.

Interestingly, we find that reducing the level of *cacophony*, a subunit of the Cav2 voltage-gated  $\text{Ca}^{2+}$  channel, significantly ameliorates the dendrite morphogenesis defects in *eas*<sup>KO</sup> mutants. In contrast, reducing SREBP signaling significantly rescues the dendrite phenotypes but does not suppress the adult seizure-like phenotype. It is conceivable that the part of the neural circuit that heavily relies on SREBP signaling for dendrite morphogenesis during development does not contribute to the seizure-like behavior. Consistent with this hypothesis, expressing *eas* acutely in neurons in adult *eas* flies largely suppresses the seizure-like phenotype (Kroll and Tanouye, 2013). Our study further suggests that changes in neuronal  $\text{Ca}^{2+}$  influx can significantly affect dendrite morphogenesis. It thus appears that alterations in neuronal  $\text{Ca}^{2+}$  influx contribute to not only adult seizure-like phenotypes but also dendrite morphogenesis abnormalities during larval development.

In summary, our study demonstrates that EAS kinase plays an important role in dendrite morphogenesis by regulating SREBP signaling and affecting neuronal  $\text{Ca}^{2+}$  influx. These findings uncover an important new role for phospholipid PE synthesis in neural development, and they further reveal a molecular pathway involving highly conserved molecules for phospholipid homeostasis as being important in the regulation of dendrite morphogenesis. Extension of these studies to the mammalian nervous system may provide significant insight into the

pathologies of neurodevelopmental disorders linked with alterations in phospholipid and lipid homeostasis.

### **Author Contributions**

S.M., J.A.B., G.L.P., Y.G., and C.E.O., conducted experiments and analyses. S.M., L.Y.J. and Y.-N.J. designed experiments and wrote the paper. J.A.B. conducted the genetic screen.

### **Acknowledgements**

We thank Dr. Mark Tanouye for reagents; Bloomington Stock Center and VDRC Stock Center for fly stocks. Supported by National Science Foundation Graduate Research Fellowship, AAUW American Dissertation Fellowship (to S.M.), NIH grant number R37NS040929 and R35NS097227 (to Y.-N.J.). L.Y.J. and Y.-N.J. are investigators of the Howard Hughes Medical Institute.

### **Experimental Procedures**

#### Experimental Model and Subject Details

These following mutant alleles were used: *eas*<sup>1</sup>, provided by Dr. Mark Tanouye (University of California at Berkeley), *eas*<sup>KO</sup> (generated in this study), and *srebp*<sup>189</sup> (Kunte et al., 2006), *acs*<sup>MI12066</sup> (BL56480), *acs*<sup>KO</sup> (BL32331). Other

transgenic flies used in this study were: *UAS-bbc-RNAi* (VDRRC7989), *UAS-pect-RNAi* (BL63710), *UAS-srebp-RNAi* (BL25975) (Song et al., 2014), *UAS-fas-RNAi* (BL29349), *UAS-acc-RNAi* (VDRRC8105), *UAS-cac-RNAi* (Saras and Tanouye, 2016), *UAS-esg* (Hekmat-Scafe et al., 2005), *UAS-kcc* (Hekmat-Scafe et al., 2010), *Gal4<sup>21-7</sup>* (Song et al., 2007), *Gal4<sup>19-12</sup>* (Xiang et al., 2010), *Gal4<sup>2-21</sup>* (Parrish et al., 2006), *ppk-Gal4* (Grueber et al., 2003), *ppk-CD4-tdTomato* (Han et al., 2011), *UAS-tdTomato* (Han et al., 2011), *UAS-dcr-2* (Dietzl et al., 2007). Animals were reared at 25°C in density-controlled vials or at 29°C for *bbc* and *pect* RNAi experiments. To image *eas* mutants, homozygous *eas* female flies were crossed with male flies carrying *ppk-CD4-tdTomato*. Male larvae from the next generation were imaged 5-7 days after the crosses were made.

### Live Imaging

Animals were reared at 25°C in density-controlled vials or at 29°C for *bbc* and *pect* RNAi experiments. Flies were allowed to lay eggs on food for two hours at 25°C in order to precisely time the developmental stages of their progeny. Larvae at appropriate stages were mounted in glycerol and dendrites of *da* neurons were imaged using a Leica SP5 laser scanning confocal microscope.

### Western Blots

To analyze SREBP protein levels *in vivo*, brains were removed from wandering third instar larvae and homogenized in HKT lysis buffer (10mM HEPES pH7.2, 100mM KCl, 1% TritonX-100, 2mM DTT, PMSF, and protease inhibitors from Roche) at 4 °C. Sample buffer was added to the lysis buffer, and samples



were boiled for 10 min. Equal numbers of brains (3–5) from control and experimental groups were separated by 4-12% gradient Bis-Tris precast gels (Novex) using Mops-SDS running buffer (Novex), and analyzed by Western blot. The primary antibodies used were mouse monoclonal anti-SREBP (1:1000, Cat# 557036, BD Biosciences, RRID: AB\_384985) and mouse monoclonal anti-tubulin (1:1000, Cat# T9026, Sigma, RRID: AB\_477593).

#### Generating *eas* knockout flies

Prior to generating *eas* knockout flies, the *eas* gene in *vasa*-Cas9 flies was sequenced to confirm the presence of guideRNA sites. For the generation of *eas* knockout flies, annealed oligos were ligated with BbsI-digested pU6-BbsI-gRNA, in order to generate targeting guideRNAs. GuideRNAs were then injected into *vasa*-Cas9 fly embryos. *eas* knockout animals were identified with genomic PCR and further confirmed by sequencing.

#### Bang-sensitivity assay

Bang-sensitivity tests were performed as previously described (Pavlidis et al., 1994b). Before testing, flies were raised and aged for at least 3 days at 25 °C. For testing, each group of flies was vortexed at maximum speed for 10 seconds. The number of flies that exhibit temporary paralysis and total number of flies tested were scored for quantification.

#### Quantification of dendrite morphology

Images were collected using Leica SP5 laser scanning confocal microscope, and imported in ImageJ software. Dendrite tracing was performed manually using the “simple neurite tracer” plug-in of ImageJ. Dendrite length and number of

dendrite were obtained from each tracing. Sample sizes (n) indicated in the figure legends corresponds to the number of neurons.

#### Quantification of bang-sensitive phenotype

After applying the mechanical jolt to flies, the number of flies that exhibit temporary paralysis over the total number of flies tested was used to score the bang-sensitivity phenotype. For the bang-sensitivity assay, sample sizes (n) indicated in the figure legend corresponds to the total number of flies.

#### Statistical Analysis

Data were analyzed and plotted with Prism 6.0c software. As stated in the figure legends, data were analyzed statistically using a Student's t test or one-way ANOVA tests. The Tukey's multiple comparison test was used along with one-way ANOVA tests when multiple comparisons was required.

## **Chapter 4: Conclusions and Future Directions**

My research for this dissertation focused on identifying novel molecular regulators of dendrite morphogenesis and study their downstream signaling components. In Chapter 2, we described the identification and characterization of an extrinsic regulator of dendrite development (the Sema-2b/PlexB signaling pathway) in regulating dendrite ECM-adhesion. In Chapter 3, we characterized the role of phospholipid homeostasis pathways in regulating dendrite growth, an intrinsic regulator of dendrite development. There are still many open questions that remain to be explored in future studies, which we will discuss below for each chapter.

### **Semaphorin Regulation of Dendrite Morphology**

Neurons encounter and respond to various guidance cues during development. Interestingly, only a small number of them have been discovered so far, and the nervous system seems to reuse these molecules for many processes, such as axonal fasciculation, pathfinding, dendrite targeting and morphogenesis. Semaphorins are one such example that are famous for their role in regulating both axon and dendrite development (Tran et al., 2007). We showed that Sema-2b/PlexB signaling regulates dendrite-ECM adhesion to restrict dendritic growth and promote contact-mediated self-avoidance during larval development. Interestingly, during embryonic stage, Sema-1a/PlexA and Sema-2a/PlexB signaling pathways specify the termination positions of class IV da neuron axons in the dorso-ventral axis of the nerve cord (Zlatic et al., 2009). How do two

proteins that have high sequence similarity, Sema-2a and Sema-2b, elicit different downstream signaling patterns in axons and dendrites? Moreover, PlexB receptor seems to be required in both axons and dendrites for distinct roles, and it is possible that how neurons interpret the extrinsic cues depends on the polarized and compartmentalized subcellular environment. Hence, comparing cross talk between semaphorin signaling and other regulators which are downstream of guidance cues, such as integrin receptors (this study) and Ret receptor (Soba et al., 2015), in axons and dendrites of class IV da neurons may provide insights into how cells interpret and integrate distinct extrinsic cues to allow for differential regulations of neuronal morphology.

Further genetic analysis of the *plexB* gene in the future will yield more insights in the mechanisms of how Plexin receptors function. The *Drosophila plexA* and *plexB* gene are located on the fourth chromosome, the most intractable chromosome of the fly genome for genetic analysis due to its small size and lack of genetic tools. The *plexB*<sup>KG00878</sup> mutant we used in this study is either a null or a strong hypomorphic allele (Ayoob, 2006), and the dendrite self-crossing phenotype in *plexB*<sup>KG00878</sup> mutants is less severe compared to the *sema-2b* mutants. As we proposed in the discussion session, it is possible that another receptor acts together with PlexB to mediate dendrite-ECM adhesion. Another possibility is that *plexB*<sup>KG00878</sup> is a hypomorphic allele. Hence, generating a knockout *plexB* allele using CRISPR/Cas9 and characterizing the null phenotype in the future will clarify this issue. In addition, the powerful combination of CRISPR/Cas9 and fly genetics genetic and biochemical tools will help us further

characterize the intracellular signaling domains of the Plexin receptors and elucidate the signaling events that define how dendritic and axonal Plexin receptors elicit distinct responses to guidance cues.

### **Phospholipid Homeostasis During Dendrite Growth**

The brain is highly enriched in lipids (Wong and Crawford, 2014) and yet the roles of lipids in neural development in vivo is poorly understood. In Chapter 3, we show that *Drosophila easily shocked (eas)*, a gene encoding a kinase with a critical role in phospholipid phosphatidylethanolamine (PE) synthesis, regulates dendrite morphogenesis by affecting the activity of a lipogenic transcription factor SREBP and by modulating calcium influx in neurons. Interestingly, although the level of phospholipid PE is low in *eas* mutants (Kliman et al., 2010; Nyako et al., 2001; Pavlidis et al., 1994a), our genetic analyses suggest that part of the dendrite morphogenesis defects are due to aberrantly high SREBP activity, which turns on the transcriptions of target genes that are involved in synthesizing new lipids. However, our results do not exclude the possibility that lower PE levels could independently contribute to the dendrite growth defects in *eas* mutants, as PE is one of the major components of cellular membranes (Jackson et al., 2016). A comprehensive analysis of the contribution of phospholipid composition of dendrites at different development stages, and examining how the lack of PE affects dendritic membrane integrity and other signaling molecules may yield insights into how PE regulates dendrite growth.

SREBP is a membrane bound transcription factor that is critical for normal lipid synthesis in both invertebrates and vertebrates (Jeon and Osborne, 2012;

Rawson, 2003). It is conceivable that the lack of lipid synthesis in the neuron leads to a lack of membrane lipid supply, resulting in reduced dendrite growth. Similarly, increased lipid synthesis caused by high level of SREBP activation could lead to dendritic overgrowth. Interestingly, we find that both increased and decreased levels of SREBP lead to dendrite growth defects. Our results suggest that high levels of lipid synthesis may inhibit dendrite growth or even be toxic for dendrites, as it is for neurons prior to the onset of neurodegeneration (Liu et al., 2015). It thus seems that maintaining the proper level of SREBP activity during development is important for dendrite growth. In addition, studies from mammalian liver suggest that the phosphatidylinositol-3-kinase (PI3K) regulates SREBP activity through AKT and the mammalian target of rapamycin complex 1 (mTORC1) (Jeon and Osborne, 2012). It would be of great interest to see if SREBP and PI3K/AKT/mTOR signaling cascade intersect in neurons to regulate dendrite morphogenesis. Determining what other pathways are necessary to regulate the level of SREBP activity, how SREBP-mediated lipid synthesis contributes to dendrite growth, and whether the level of SREBP is different in neurons with different dendritic arbor complexity will be fascinating directions for future studies.

Many intriguing questions regarding the roles of lipids in brain development still remain to be addressed: Where and how phospholipid homeostasis and metabolism pathways intersect with other signaling pathways to regulate dendrite morphogenesis? How are signaling events and the cytoskeleton in dendrites affected by their interactions with membrane lipids? Do neurons utilize different

types of phospholipids to build their primary and terminal dendrites, and if so how does this contribute to the integration of synaptic and sensory signals? Answers to these questions will not only further our understanding of phospholipid homeostasis during neural development, but will also help to elucidate the contributions of lipid imbalances during diseases.

Overall, our study sought to identify novel *in vivo* regulators of dendrite morphogenesis. We succeeded in identifying multiple genes that regulate dendritic arbor patterning and growth, and gained insight into their signaling components. Most of the genes we studied are highly conserved in vertebrates, such as the semaphorins, easily shocked kinase, and lipid homeostasis regulator SREBP, which makes them interesting candidates to further investigate in mammalian neurons in the future. Not only do our findings reveal previously unidentified roles of semaphorins and lipid homeostasis in dendrite morphogenesis, but they also provide insights into the neuronal pathologies of many neurodevelopment disorders that are linked to defects in dendrite development.

## Figure Legends

### Figure 1.1. Distributions and dendrite morphologies of classes I-IV *Drosophila* dendritic arborization (da) neurons.

(A) A schematic representation of *Drosophila* larval body wall showing the distributions of class I-IV da neuron cell bodies (represented by colored dots). (B) Different classes of da neuron exhibit type-specific dendrite morphologies. Scale bars represent 30  $\mu\text{m}$ .

### Figure 2.1. *Sema-2b*, but not *Sema-2a* loss of function leads to an increase in dendritic self-crossings.

(A-F) Dendritic patterns of wild-type (A), *sema-2b*<sup>f02042</sup> (B), *sema-2b*<sup>C4</sup> (C), *sema-2b*<sup>f02042/C4</sup> (D), *sema-2a*<sup>03021/B65</sup> (E), and *sema-2a*<sup>P2</sup>, *2b*<sup>f02042</sup>/*2ab*<sup>A15</sup> (F) class IV da neurons. Dendritic crossings are indicated by blue arrowheads. Scale bars represent 30  $\mu\text{m}$ . Wild-type animals are *w*<sup>1118</sup> carrying one copy of *ppk-CD4-tdTomato*.

(G) Schematic of a contacting crossing (top) and a non-contacting crossing (bottom). In the case of contacting crossings, both dendrites (white bars) are in the same X-Y plane. In the case of non-contacting crossings, one or both dendrites (red bars) detach from ECM (green sheet) and become enclosed by the basal surface of epidermal cells (grey sheet).

(H) Quantification of crossing points normalized to total dendritic length in wild-type (n=6), *sema-2b*<sup>f02042</sup> (n=4), *sema-2b*<sup>C4</sup> (n=4), *sema-2b*<sup>f02042/C4</sup> (n=7), *sema-2a*<sup>03021/B65</sup> (n=4), and *sema-2a*<sup>P2</sup>, *2b*<sup>f02042</sup>/*2ab*<sup>A15</sup> (n=4) mutant neurons.



White bars represent the quantifications of contacting crossings and red bars represent the quantification of non-contacting crossings. Data are plotted as average  $\pm$  SEM. ns, not significant, and \*\*\* $p < 0.001$  as assessed by one-way analysis of variance and Dunnett's test. The comparisons of the total number of crossings are labeled on top of the bars. The comparisons of the contacting crossings and non-contacting crossings are labeled in the white bars and red bars, respectively.

(I-J) Dendritic patterns of control (I) and *sema-2b*<sup>C4</sup> (J) class IV neurons generated with MARCM. Scale bars represent 30  $\mu$ m.

(K) Quantification of total crossing points normalized to total dendritic length in control (n=3) and *sema-2b*<sup>C4</sup> (n=3) class IV da neurons. Data are plotted as average  $\pm$  SEM. ns, not significant as assessed by a Student's t test.

**Figure 2.2. Enclosure of terminal dendrites by epidermal cells in *sema-2b* mutants.**

(A-B) Wild-type (A) and *sema-2b*<sup>f02042/C4</sup> (B) dendritic field imaged at 48 hr AEL.

(C-D) Wild-type (C) and *sema-2b*<sup>f02042/C4</sup> (D) dendritic field imaged at 120 hr AEL.

Wild-type animals are *w*<sup>1118</sup> carrying one copy of *ppk-CD4-tdTomato*. Dendrites attached to the ECM are labeled in green and enclosed dendrites are labeled in magenta. The arrowheads point to terminal dendrites that are enclosed by epidermal cells. Scale bars represent 30  $\mu$ m.

(E) Quantification of percentages of enclosed dendrites at 48 hr, 72 hr, 96 hr and 120 hr AEL in wildtype and *sema-2b*<sup>f02042/C4</sup> neurons. Data are plotted as average

± SEM. \*\*\*p < 0.001 as assessed by a Student's t test.

(F) Percentages of detached dendrites that are terminal dendrites in class IV da neurons in wild-type and *sema-2b* mutants.

**Figure 2.3. Sema-2b is derived from epidermal cells and acts at short range to regulate dendrite adhesion.**

(A-A') Anti-Sema-2b immunostaining of a *w<sup>1118</sup>* wild-type third instar fillet reveals strong expression in epidermal cells. Anti-HRP immunoreactivity labels neurons in the peripheral nervous system.

(B-B') No detectable Sema-2b staining in *sema-2b<sup>C4</sup>* mutants. Scale bar represents 50 µm.

(C-C') The *2b<sup>L</sup>-τGFP* reporter labels epidermal cells that express Sema-2b. *2b<sup>L</sup>-τGFP* animals were immunostained for τGFP and anti-HRP, which labels neurons in the body wall. Some GFP positive epidermal cells are indicated by white arrowheads.

(D-D') The *2b-τMyc* reporter labels a subset of Sema-2b-expressing epidermal cells. *2b-τMyc* animals were immunostained for τMyc and anti-HRP, which labels neurons in the body wall. Some τMyc positive epidermal cells are indicated by white arrowheads. All the staining images are positioned with the anterior side on the left and dorsal side on the top.

(E-I) Dendritic patterns and quantifications of class IV da neurons in *sema-2b<sup>f02042/C4</sup>* (E, n=7), *sema-2b<sup>f02042/C4</sup>* mutant with epidermis-expressing full length Sema-2b (F, n=5), epidermis-expressing membrane tethered Sema-2b (G,

n=5), and neuronal-expressing full length Sema-2b (H, n=6). Dendritic crossings are indicated by blue arrowheads. Scale bars represent 30  $\mu\text{m}$ . Wild-type animals are  $w^{1118}$  carrying one copy of *ppk-CD4-tdTomato*. White bars represent the quantifications of contacting crossings and red bars represent the quantification of non-contacting crossings. Data are plotted as average  $\pm$  SEM. ns, not significant and \*\*\* $p < 0.001$  as assessed by one-way analysis of variance and Bonferroni test. The comparisons of the total number of crossings are labeled on top of the bars. The comparisons of the contacting crossings and non-contacting crossings are labeled in the white bars and red bars, respectively.

(J-K) Dendritic patterns of control (J) and *sema-2b<sup>C4</sup>* (K) epidermal clones (labeled by GFP) generated with MARCM. Class IV da neurons are genetically labeled by one copy of *ppk-CD4-tdTomato*. Scale bars represent 10  $\mu\text{m}$ . The boundary between two adjacent epidermal cells is marked by a white dashed line.

(L) Quantification of total crossing points among dendrites that are covered by control (n=24) and *sema-2b<sup>C4</sup>* (n=26) class IV da neurons. Data are plotted as average  $\pm$  SEM. ns, not significant as assessed by a Student's t test.

**Figure 2.4. Plexin B is the Sema-2b Receptor that regulates dendrite-ECM adhesion.**

(A-D) Dendritic patterns of wild-type (A), *plexB<sup>KG00878</sup>* (B), control RNAi (C) and *plexB RNAi* (D) class IV da neurons. Dendritic crossings are indicated by blue arrowheads. Scale bars represent 30  $\mu\text{m}$ . Wild-type animals are  $w^{1118}$  carrying one copy of *ppk-CD4-tdTomato*.

(E) Quantification of total crossing points normalized to total dendritic length in wild-type (n=4), *plexB*<sup>KG00878</sup> (n=6), RNAi control (n=6), and *plexB RNAi* (n=6) neurons. Data are plotted as average  $\pm$  SEM. ns, not significant, \*p<0.05, \*\*\*p < 0.001 as assessed by a Student's t test. The comparisons of the total number of crossings are labeled on top of the bars. The comparisons of the contacting crossings and non-contacting crossings are labeled in the white bars and red bars, respectively.

(F-H) Dendritic patterns of *sema-2b*<sup>C4/+</sup> (F), *plexB*<sup>KG00878/+</sup> (G), and *sema-2b*<sup>C4/plexB</sup><sup>KG00878</sup> (H) class IV da neurons. Dendritic crossings are indicated by blue arrowheads. Scale bars represent 30  $\mu$ m.

(I) Quantification of total crossing points normalized to total dendritic length in *sema-2b*<sup>C4/+</sup> (F), *plexB*<sup>KG00878/+</sup> (G), and *sema-2b*<sup>C4/plexB</sup><sup>KG00878</sup> (H) class IV da neurons. White bars represent the quantifications of contacting crossings and red bars represent the quantification of non-contacting crossings. Data are plotted as average  $\pm$  SEM. ns, not significant and \*\*p < 0.01, \*\*\*p<0.001 assessed by one-way analysis of variance and Bonferroni test for all pairs of columns. The comparisons of the total number of crossings in each genotype to *sema-2b*<sup>C4/+</sup> are labeled on top of the bars. The comparisons of the contacting crossings and non-contacting crossings each genotype to *sema-2b*<sup>C4/+</sup> are labeled in the white bars and red bars, respectively.

**Figure 2.5. Sema-2b genetically interacts with TORC2 complex and Trc kinase**

(A-J) Dendritic patterns of *tor<sup>ΔP</sup>/+* (A), *sema-2b<sup>C4</sup>/ tor<sup>ΔP</sup>* (B), *rictor<sup>Δ2</sup>/+* (C), *sema-2b<sup>C4</sup>/ rictor<sup>Δ2</sup>* (D), *sin1<sup>e03756</sup>/+* (E), *sema-2b<sup>C4</sup>/sin1<sup>e03756</sup>* (F), *trc<sup>1</sup>/+* (G), *sema-2b<sup>C4</sup>/trc<sup>1</sup>*(H), *fry<sup>1</sup>/+* (I), and *sema-2b<sup>C4</sup>/fry<sup>1</sup>* (J) class IV da neurons. Dendritic crossings are indicated by blue arrowheads. Scale bars represent 30 μm.

(K) Number of total crossing points normalized to total dendritic length in *sema-2b<sup>C4</sup>/+* (n=5), *tor<sup>ΔP</sup>/+* (n=4), *sema-2b<sup>C4</sup>/ tor<sup>ΔP</sup>* (n=5), *rictor<sup>Δ2</sup>/+* (n=5), *sema-2b<sup>C4</sup>/ rictor<sup>Δ2</sup>* (n=5), *sin1<sup>e03756</sup>/+* (n=5), *sema-2b<sup>C4</sup>/sin1<sup>e03756</sup>* (n=7), *trc<sup>1</sup>/+* (n=4), *sema-2b<sup>C4</sup>/trc<sup>1</sup>* (n=4), *fry<sup>1</sup>/+* (n=5), and *sema-2b<sup>C4</sup>/fry<sup>1</sup>* (n=5) neurons. White bars represent the quantifications of contacting crossings and red bars represent the quantification of contacting crossings. Data are plotted as average ± SEM. \*\*p < 0.01, and \*\*\*p < 0.001 as assessed by one-way analysis of variance and Bonferroni test.

**Figure 2.6. Trc kinase acts downstream of Semaphorin 2b/PlexB signaling to promote dendrite adhesion.**

(A-C) Anti-phospho-Trc (P-T449) immunostaining of a wild-type *w<sup>1118</sup>* third instar fillet reveals strong labeling in the wild-type class IV da neuron (A). Anti-phospho-TrcT449 shows weak labeling in *sema-2b<sup>C4</sup>* (B) and *plexB<sup>KG00878</sup>* (C) mutant class IV da neurons. Scale bar represents 50 μm. Class IV da neurons are genetically labeled by *ppk-CD4-td-Tomato*. All the staining images are positioned with the anterior side on the left and dorsal side on the top.

(D) Quantification of the level of P-T449 normalized to *ppk-CD4-td-Tomato* in the dendrites of the class IV da neurons in the wild-type, *sema-2b<sup>C4</sup>*, and *plexB<sup>KG00878</sup>*

animals. ns, not significant, \*\*p < 0.01, and \*\*\*p < 0.001 as assessed by one-way analysis of variance and Bonferroni test for all pairs of columns.

(E-G) Dendritic patterns of *sema-2b*<sup>f02042/C4</sup> mutants expressing wild-type Trc (E), phosphorylation-site mutated Trc (S292AT449A) (F), and myristoylated Trc (Myr-Trc) (G) in class IV da neurons. Dendritic crossings are indicated by blue arrowheads. Scale bars represent 30 μm.

(H) Quantification of total crossing points normalized to total dendritic length in *sema-2b*<sup>f02042/C4</sup> mutants expressing wild-type Trc (n=5), Trc<sup>S292AT449A</sup> (n=5), and Myr-Trc (n=5) in class IV da neurons. Data are plotted as average ± SEM. \*p < 0.05 and \*\*p < 0.01 as assessed by a one-way analysis of variance and Dunnett's test.

**Figure 2.7. Integrins overexpression suppresses dendrite crossing defects in *sema-2b* mutant.**

(A-B) Dendritic patterns of class IV da neurons in *sema-2b*<sup>f02042/C4</sup> mutants (A) and *sema-2b*<sup>f02042/C4</sup> mutants with integrins (*UAS-mys* and *UAS-mew*) overexpressed in class IV da neurons (B). Dendritic crossings are indicated by blue arrowheads. Scale bars represent 30 μm.

(C) Quantifications of crossing points in wild-type (n=6), *sema-2b*<sup>f02042/C4</sup> (n=5) class IV da neurons and *sema-2b*<sup>f02042/C4</sup> with integrins overexpressed in class IV da neurons (n=4). Data are plotted as average ± SEM. ns, not significant and \*\*\*p<0.001 as assessed by one-way analysis of variance and Bonferroni test for all pairs of columns. The comparisons of the total number of crossings in each

genotype and wild-type animals are labeled on top of the bars. The comparisons of the contacting crossings and non-contacting crossings are labeled in the white bars and red bars, respectively.

(D) Colocalization of Mys-FLAG and Myc-PlexB in dendrites of class IV da neurons. Mys-FLAG and Myc-PlexB are co-expressed by *ppk-Gal4* driver. Class IV da neurons are labeled by *ppk-CD4-td-GFP*. Scale bar represents 20  $\mu\text{m}$ . The line plots of two terminal dendrites are show in D' and D''.

**Figure 2.8. Mys, a  $\beta$  subunit of integrin, associates with PlexB.**

(A-B) Western blot showing co-immunoprecipitation of PlexB and Mys. Lysates from S2 cells expressing Mys-FLAG with Myc-PlexB or Dscam-Myc as depicted were incubated with anti-Myc antibody (A) or FLAG antibody bound beads (B). Immunoprecipitates were probed for the presence of Mys-FLAG (A), Myc-PlexB or Dscam-Myc (B).

(C) Western blot revealing the extracellular region of Mys is required for the association between Mys and PlexB. Lysates from S2 cells expressing either FLAG-Mys, FLAG-MysEcto<sup>TM</sup>, FLAG-MysEndo<sup>TM</sup>, and Myc-PlexB as depicted were incubated with Myc antibody. Immunoprecipitates were probed for the presence of FLAG-Mys, FLAG-MysEcto<sup>TM</sup> and FLAG-MysEndo<sup>TM</sup> using anti-FLAG antibody.

(D-F) PlexB and Mys interaction detected by *in situ* PLA on the surface of S2 cells.

(D) Diagram showing the principles of *in situ* PLA: if the two membrane proteins (Mys and PlexB) are within 40nm of each other, the secondary antibodies

conjugated with oligonucleotides will be joined together and fluorescently labeled oligonucleotides will then be added to the site by a rolling circle amplification. Both Myc-PlexB and FLAG-Mys are tagged on the extracellular regions. (E) PLA signals in each condition. The interactions were visualized as red fluorescent dots and membrane GFP marked the transfected cells. A cartoon showing the position of the focal plane is shown on the lower left of the panel. (F) Quantification of total PLA intensity per GFP positive cell (n=40 in each condition). Data are plotted as average  $\pm$  SEM. \*\*\*p<0.001 as assessed by one-way analysis of variance and Bonferroni test for all pairs of columns. Scale bars represent 10  $\mu$ m. A.u. arbitrary unit.

(G-I) PlexB and Mys interaction detected by *in situ* PLA in dendrites of class IV da neurons. PLA signals in a neuron that co-expresses FLAG-Mys and Myc-PlexB are shown in (G). PLA signals in a neuron that co-expresses Mys-FLAG and Myc-PlexB are shown in (H). (I) Quantification of the number of PLA dots normalized to the dendritic length in each genotype. Data are plotted as average  $\pm$  SEM. \*\*\*p<0.001 as assessed by a Student's t-test. Staining images are positioned with the anterior side on the left and dorsal side on the top. Scale bars represent 10  $\mu$ m.

(J) Diagram of a cross section of the ECM (green), epidermis (blue) and dendrites (red). Sema-2b ligands are produced and secreted by epidermal cells and diffuse throughout the whole dendritic field of class IV da neurons. Sema-2b signals through PlexB receptors in the neurons to regulate dendrite-ECM adhesion.

(K) A model of the downstream molecular mechanisms of how Sema-2b/PlexB



signaling regulates dendrite-ECM adhesion through the activation of Trc kinase and the binding of integrins to laminin proteins in the ECM.

**Figure 2.9. An example of a contacting and a non-contacting dendritic crossing and dendrite phenotype in class I da neuron in the *sema-2b* mutants.**

(A) Dendritic field of a wildtype class IV da neuron. Red dotted boxes mark the dendritic fields with a contacting crossing (A1-A3) and a non-contacting crossing (A4-A6). Scale bar represents 30  $\mu\text{m}$ .

(A1-A3) Example of a contacting dendritic crossing. Two overlapping dendrites (pointed out by red arrows) are located at the same focal plane (A2) along the z-axis as the focal plane moves from basal side to apical side of the dendritic field. Scale bar represents 5  $\mu\text{m}$ .

(A4-A6) Example of a non-contacting dendritic crossing. Two overlapping dendrites (pointed out by red arrows) are located at different focal planes (A4 and A6) along the z-axis as the focal plane moves from basal side to apical side of the dendritic field. Scale bar represents 5  $\mu\text{m}$ .

(B-C) Dendritic patterns of wild-type control (A) and *sema2b* mutant (B) class I da neurons. Scale bar represents 50  $\mu\text{m}$ .

(D) Quantifications of total crossing points normalized to total dendritic length in control (n=6) and *sema-2b*<sup>C4</sup> mutants (n=6) class I da neurons. White bars represent the quantifications of contacting crossings and red bars represent the quantification of non-contacting crossings. Data are plotted as mean  $\pm$  SEM. ns, not

significant, \*\*\* $p < 0.001$ , assessed by a Student's t test. The comparison of the total number of crossings in RNAi knockdown and control animals is labeled on top of the bars. The comparison of the contacting crossings and non-contacting crossings in RNAi knockdown and control animals is labeled in the white bars and red bars, respectively.

**Figure 2.10. Overall morphology of axonal projections is normal in the *sema-2b* mutant.**

(A-B) Axon projections of wild-type (A) and *sema-2b*<sup>f02042</sup> mutants (B) class IV da neurons were imaged in the ventral nerve cord using *ppk-CD4-tdTomato*. Images of class IV da axon projections were taken at 120 hr AEL. Scale bar represents 50  $\mu\text{m}$ . Both images are positioned with the anterior side on the left and left side on the bottom.

**Figure 2.11. Overall morphology of epidermal cells is normal in the *sema-2b* mutant.**

(A-B) Boundaries of epidermal cells in wild-type (A) and *sema-2b*<sup>f02042</sup> mutants (B) are labeled by Fasciclin III, and all cell nuclei are labeled by DAPI (4',6-diamidino-2-phenylindole). Larvae were dissected for immunohistochemistry at 120 hr AEL. Images are showing the midline of a larval body wall fillet with anterior side on the left and left side on the bottom.

(C) Quantification of total number of nuclei normalized to area ( $\text{mm}^2$ ) in wild-type and *sema-2b*<sup>f02042</sup> mutants. Data are plotted as mean  $\pm$  SEM. ns, not significant,

assessed by a Student's t test. Scale bar represents 50  $\mu\text{m}$ .

**Figure 2.12. BAC Sema-2b reporters colocalize with the epidermal cell marker.**

(A-A'') The  $2b^L\text{-}\tau\text{GFP}$  reporter labels Sema-2b-expressing epidermal cells.  $2b^L\text{-}\tau\text{GFP}$  animals were immunostained for  $\tau\text{GFP}$ . Epidermal cells are labeled by UAS-CD4-td-Tomato, which is governed by epidermal cell specific driver  $\text{Gal4}^{\text{A58}}$ .

(B-B'') The  $2b\text{-}\tau\text{Myc}$  reporter labels Sema-2b-expressing epidermal cells.  $2b\text{-}\tau\text{Myc}$  animals were immunostained for  $\tau\text{Myc}$ . Epidermal cells are labeled by UAS-CD4-td-Tomato, which is governed by epidermal cell specific driver  $\text{Gal4}^{\text{A58}}$ .

Scale bar represents 30  $\mu\text{m}$ . All the staining images are positioned with the anterior side on the left and dorsal side on the top.

**Figure 2.13. PlexB, but not Sema-1a, is required to prevent dendrite-crossing in the class IV da neurons .**

(A-B) Dendritic patterns of wild-type (A) and  $\text{sema-1a}^{\text{P1}}$  mutant (B) class IV da neurons.

(C-D) Dendritic patterns of RNAi control (C) and  $\text{plexB}$  RNAi (using v12167) mutant (D) class IV da neurons. Dendritic crossings are indicated by blue arrowheads.

(E) Quantifications of total crossing points normalized to total dendritic length in wild-type (n=5),  $\text{sema-1a}^{\text{P1}}$  mutant (n=4), RNAi control (n=6) and  $\text{plexB}$  RNAi (using v12167) (n=3) class IV da neurons. White bars represent the

quantifications of contacting crossings and red bars represent the quantification of contacting crossings. Data are plotted as mean  $\pm$  SEM. ns, not significant, assessed by a Student's t test. Scale bars represent 30  $\mu$ m. \*\*\*p < 0.001 as assessed by a Student's t test.

(F) Percentages of contacting and non-contacting crossings in each genotype.

(G-H) Dendritic patterns of wild-type RNAi control (G) and *p/lexB* mutant (H) class I da neurons. Scale bar represents 50  $\mu$ m.

(I) Quantifications of total crossing points normalized to total dendritic length in control (n=5) and *p/lexB* RNAi (n=5) class I da neurons. White bars represent the quantifications of contacting crossings and red bars represent the quantification of contacting crossings. Data are plotted as mean  $\pm$  SEM. ns, not significant, assessed by a Student's t test. Scale bars represent 30  $\mu$ m. \*p < 0.05 as assessed by a Student's t test. The comparison of the total number of crossings in RNAi knockdown and control animals is labeled on top of the bars. The comparison of the contacting crossings and non-contacting crossings in RNAi knockdown and control animals is labeled in the white bars and red bars, respectively.

**Figure 2.14. *fak56* and *otk* mutants do not show strong genetic interaction with *sema-2b* mutants.**

(A-C) Dendritic patterns of *fak56*<sup>CG1</sup> (A), *fak56*<sup>CG1/+</sup> (B) and *sema-2b*<sup>C4</sup>/*fak56*<sup>CG1</sup> (C) class IV da neurons.

(D) Quantifications of total crossing points normalized to total dendritic length in

*fak56<sup>CG1</sup>* (n=5), *fak56<sup>CG1</sup>/+* (n=5), *sema-2b<sup>C4</sup>/+* (n=5) and *sema-2b<sup>C4</sup>/fak56<sup>CG1</sup>* (n=6) class IV da neurons. White bars represent the quantifications of contacting crossings and red bars represent the quantification of non-contacting crossings. Data are plotted as mean  $\pm$  SEM. ns, not significant, assessed by a Student's t test between wild-type and *fak56<sup>CG1</sup>* animals and one-way analysis of variance and Bonferroni test for genetic interaction between *sema-2b<sup>C4</sup>* and *fak56<sup>CG1</sup>*. The comparison of the total number of crossings in *fak56<sup>CG1</sup>* and wild-type animals is labeled on top of the bars. The comparison of the contacting crossings and non-contacting crossings in *fak56<sup>CG1</sup>* and wild-type is labeled in the white bars and red bars, respectively. For genetic interaction assay, the comparison of the total number of crossings in each genotype and *sema-2b<sup>C4</sup>/+* animals is labeled on top of the bars. The comparison of the contacting crossings and non-contacting crossings in each genotype and *sema-2b<sup>C4</sup>/+* is labeled in the white bars and red bars, respectively.

(E-F) Dendritic patterns of *otk<sup>3</sup>/+* (E) and *sema-2b<sup>C4</sup>/otk<sup>3</sup>* (F) class IV da neurons.

(G) Quantifications of total crossing points normalized to total dendritic length in *otk<sup>3</sup>/+* (n=4) and *sema-2b<sup>C4</sup>/otk<sup>3</sup>* (n=4) neurons. White bars represent the quantifications of contacting crossings and red bars represent the quantification of non-contacting crossings. Data are plotted as mean  $\pm$  SEM. ns, not significant, assessed by a one-way analysis of variance and Bonferroni test. Scale bars represent 30  $\mu$ m.

The comparison of the total number of crossings in each genotype and *sema-2b<sup>C4</sup>/+* animals is labeled on top of the bars. The comparison of the

contacting crossings and non-contacting crossings in each genotype and *sema-2b<sup>C4</sup>/+* animals is labeled in the white bars and red bars, respectively.

**Figure 2.15. Expression of proteins in S2 cells and dendrites of class IV da neurons.**

(A) Staining of CD8GFP using a GFP antibody, PlexB using an antibody that targets the extracellular domain of PlexB, and Mys-FLAG using a FLAG antibody. Scale bar represents 3  $\mu\text{m}$ .

(B) Immunostaining of Dscam-Myc in S2 cells. White arrowhead shows the Dscam-Myc signals in the filopodia-like protrusions of the cells. Dscam-Myc transfected cells show aggregations, indicating Dscam is functional and mediate homophilic interactions between Dscam transfected cells. Scale bars represent 10  $\mu\text{m}$ .

(C) Surface staining and total staining of FLAG-Mys, FLAG-MysEcto<sup>TM</sup> and FLAG-MysEndo<sup>TM</sup> in S2 cells. Scale bars represent 10  $\mu\text{m}$ .

(D) Surface staining and total staining of FLAG-Dscam in S2 cells. Scale bars represent 10  $\mu\text{m}$ .

A cartoon showing the position of the focal plane is shown on the bottom of the panel. Red dashed line indicates the focal plane. White arrow points to the colocalization of the signals at the membrane.

(E) Western blotting showing the expression of full-length Mys and Dscam in transfected S2 cells. Anti-alpha tubulin staining is shown as loading control.

(F) Immunostaining of FLAG-Mys expressed in class IV da neurons, which is

marked by *ppk-CD4-td-GFP*. Scale bars represent 20  $\mu\text{m}$ .

### **Figure 3.1. EAS Is Required in Class IV da Neurons for Dendrite Morphogenesis**

(A-D) Sample images showing dendrite morphology for the indicated genotypes.

(E and F) Quantification of number of branches (E) and total dendritic length (F) at 48 hrs, 72 hrs, 96 hr, and 120 hrs AEL in wildtype, *eas*<sup>KO</sup> and *eas*<sup>1</sup> mutants.

Student's t tests were used to compare between wildtype and *eas*<sup>KO</sup> mutants at 48 hrs, 72 hrs, and 96 hrs AEL. one-way ANOVA analysis was used for wildtype, *eas*<sup>1</sup>, and *eas*<sup>KO</sup> mutants at 120 hrs AEL.  $n \geq 6$  per genotype.

(G) Sholl analysis showing decreased complexity of the dendritic arbor in the *eas*<sup>KO</sup> and *eas*<sup>1</sup> mutants.

(H and I) Quantification of number of branches (H) and total dendritic length (I) for the indicated genotypes, revealing that *eas* acts cell-autonomously in the class IV da neurons.  $n \geq 5$  per genotype.

(J-L) Sample images showing dendrite morphology for the indicated genotypes.

(M and N) Quantification of total dendritic length (M) and number of branches (N) for neuroal *pect* and *bbc* RNAi, two other critical genes that act together with *eas* in the CDP–ethanolamine pathway for PE synthesis.  $n \geq 5$  per genotype.

See also Figures S1 and S2. Scale bars represent 30  $\mu\text{m}$ . Data are mean  $\pm$  SEM for all figures. ns, not significant; \*\*p < 0.01; and \*\*\*p < 0.001.

### **Figure 3.2. EAS Regulates Terminal Dendrite Growth Dynamics**

(A and B) Sample images showing dendrite morphology for wildtype animals at 72 hrs (A) and 76 hrs (B) AEL.

(D and E) Sample images showing dendrite morphology for *eas*<sup>KO</sup> mutants at 72 hrs (D) and 76 hrs (E) AEL.

(C and F) Branch dynamics are depicted in traces. Increased and decreased terminal branch region are marked in green and magenta, respectively.

(G-I) Quantification of fractions of growing (G) and retracting (I) terminal dendrites, as well as dendrite growth/retraction ratios for the indicated genotypes, showing a significant decrease of dendrite stability and overall dendrite growth in *eas*<sup>KO</sup> mutants.

Scale bars represent 5  $\mu$ m. Data are mean  $\pm$  SEM for all figures. ns, not significant; and \*\*p < 0.01. Student's t test. n = 10 per genotype.

### **Figure 3.3. Aberrantly High Level of SREBP Transcriptional Activity Contributes to the Dendrite Morphogenesis Defects in *eas*<sup>KO</sup> Mutants**

(A-C) Sample images showing dendrite morphology for the indicated genotypes.

(D and E) Quantification of total dendritic length (D) and number of branches (E) for neurons expressing constitutively active forms of SREBP (*srebp.Cdel* and *srebp.1-452*), and RNAi construct targeting SREBP. Student's t test was used. n =



6 per genotype.

(F) Western blot of larval brains showing the full-length (Fl-SREBP) and constitutively active, mature (m-SREBP) forms of SREBP protein in wildtype and *eas<sup>KO</sup>* mutants. Tubulin was used as a loading control.

(G-L) Sample images showing dendrite morphology for the indicated genotypes.

(M and N) Quantification of total dendritic length (M) and number of branches (N), showing that reducing the level of SREBP and its transcriptional targets partially suppressed the dendrite outgrowth defects in *eas<sup>KO</sup>* mutants. One-way ANOVA tests were used. Results of comparison between *eas<sup>KO</sup>* mutants and each genotype are labeled on top of each column.  $n \geq 5$  per genotype.

Scale bars represent 30  $\mu\text{m}$ . Data are mean  $\pm$  SEM for all figures. ns, not significant; \*\* $p < 0.01$ ; and \*\*\* $p < 0.001$ .

**Figure 3.4. Reducing the level of *cacophony* partially suppresses dendrite morphogenesis defects in *eas<sup>KO</sup>* mutants.**

(A and C) Sample images showing dendrite morphology for *eas<sup>KO</sup>* mutants (A), *eas<sup>KO</sup>* mutants with neuronal specific *cacophony* knocked down (B), and wildtype animals with neuronal specific *cacophony* knocked down (C).

(D and E) Quantification of total dendritic length (D) and number of branches (E), showing that reducing the level of *cacophony* partially suppresses the dendrite growth defects in *eas<sup>KO</sup>* mutants.

See also Figure S3.  $n \geq 6$  per genotype. Scale bars represent 30  $\mu\text{m}$ . Data are mean  $\pm$  SEM for all figures. \*\*\* $p < 0.001$  by one-way ANOVA tests.

**Figure 3.5. Generation of *eas*<sup>KO</sup> mutants.**

(A) The *Drosophila eas* gene structure. Exons are represented by filled boxes, 5'- and 3'-UTRs by open boxes, and splicing events by straight lines. All predicted alternative splicing products are shown. Two guideRNA(gRNA) cutting sites are marked by dotted lines (deleted region indicated by gap).

(B) RT-PCR showing the complete absence of mRNA transcript in homozygous *eas*<sup>KO</sup> mutants, while the homozygous *eas*<sup>1</sup> mutants still express truncated EAS proteins.

**Figure 3.6. Loss of *eas* also leads to reduced dendritic growth in class I and III da neurons.**

(A-C) Sample images showing dendrite morphology of class I da neurons (labeled by *Gal4*<sup>2-21</sup>, *UAS-tdTomato*) for the indicated genotypes.

(D-F) Sample images showing dendrite morphology of class III da neurons (labeled by *Gal4*<sup>19-12</sup>, *UAS-tdTomato*) for the indicated genotypes.

(G and H) Quantification of total dendritic length (G) and number of branches (H) in wildtype, *eas*<sup>KO</sup> and *eas*<sup>1</sup> neurons.

Scale bars represent 30  $\mu\text{m}$ .  $n = 6$  per genotype. Data are mean  $\pm$  SEM for all figures. \*\*\* $p < 0.001$  by one-way ANOVA tests.

**Figure 3.7. Seizure-like phenotype in *eas* mutants is not suppressed by reducing SREBP signaling**

(A) Diagram showing seizure assay. Briefly, adult flies were vortexed at maximum speed for 10 seconds. Wildtype flies do not exhibit any bang sensitivity, while *eas*<sup>1</sup> and *eas*<sup>KO</sup> mutants display paralysis.

(B) Behavioral paralysis in *eas*<sup>KO</sup> mutants is not suppressed by mutations that ameliorated the dendrite morphogenesis phenotype in class IV da neurons (n ≥ 50 per genotype).

(C and D) Sample images showing dendrite morphology for the indicated genotypes.

(E and F) Quantification of total dendritic length (E) and number of branches (F) for the indicated genotypes.

Scale bars represent 30 μm. n ≥ 4 per genotype. Data are mean ± SEM for all figures. One-way ANOVA tests were used. ns, not significant.

## References

- Aguirre-Chen, C., Bulow, H.E., and Kaprielian, Z. (2011). *C. elegans* bicd-1, homolog of the Drosophila dynein accessory factor Bicaudal D, regulates the branching of PVD sensory neuron dendrites. *Development* 138, 507–518.
- Anzo, M., Sekine, S., Makihara, S., Chao, K., Miura, M., and Chihara, T. (2017). Dendritic Eph organizes dendrodendritic segregation in discrete olfactory map formation in Drosophila. *Genes & Development* 31, 1054–1065.
- Ataman, B., Boulting, G.L., Harmin, D.A., Yang, M.G., Baker-Salisbury, M., Yap, E.-L., Malik, A.N., Mei, K., Rubin, A.A., Spiegel, I., et al. (2016). Evolution of Osteocrin as an activity-regulated factor in the primate brain. *Nature* 539, 242–247.
- Ayoob, J.C. (2006). Drosophila Plexin B is a Sema-2a receptor required for axon guidance. *Development* 133, 2125–2135.
- Basile, J.R., Gavard, J., and Gutkind, J.S. (2007). Plexin-B1 utilizes RhoA and Rho kinase to promote the integrin-dependent activation of Akt and ERK and endothelial cell motility. *J. Biol. Chem.* 282, 34888–34895.
- Benzer, S. (1971). From the gene to behavior. *Jama* 218, 1015–1022.
- Beumer, K.J., Rohrbough, J., Prokop, A., and Broadie, K. (1999). A role for PS

integrins in morphological growth and synaptic function at the postembryonic neuromuscular junction of *Drosophila*. *Development* *126*, 5833–5846.

Blochlinger, K., Bodmer, R., Jan, L.Y., and Jan, Y.N. (1990). Patterns of expression of cut, a protein required for external sensory organ development in wild-type and cut mutant *Drosophila* embryos. *Genes & Development* *4*, 1322–1331.

Buchovecky, C.M., Turley, S.D., Brown, H.M., Kyle, S.M., McDonald, J.G., Liu, B., Pieper, A.A., Huang, W., Katz, D.M., Russell, D.W., et al. (2013). A suppressor screen in *Mecp2* mutant mice implicates cholesterol metabolism in Rett syndrome. *Nature Publishing Group* *45*, 1013–1020.

Chao, M.V. (2003). Neurotrophins and their receptors: a convergence point for many signalling pathways. *Nat. Rev. Neurosci.* *4*, 299–309.

Chen, W.V., and Maniatis, T. (2013). Clustered protocadherins. *Development* *140*, 3297–3302.

Cho, J.Y., Chak, K., Andreone, B.J., Wooley, J.R., and Kolodkin, A.L. (2012). The extracellular matrix proteoglycan perlecan facilitates transmembrane semaphorin-mediated repulsive guidance. *Genes & Development* *26*, 2222–2235.

Chun-Jen Lin, C., Summerville, J.B., Howlett, E., and Stern, M. (2011). The

metabotropic glutamate receptor activates the lipid kinase PI3K in *Drosophila* motor neurons through the calcium/calmodulin-dependent protein kinase II and the nonreceptor tyrosine protein kinase DFak. *Genetics* *188*, 601–613.

Clifford, M.A., Athar, W., Leonard, C.E., Russo, A., Sampognaro, P.J., Van der Goes, M.-S., Burton, D.A., Zhao, X., Lalchandani, R.R., Sahin, M., et al. (2014). EphA7 signaling guides cortical dendritic development and spine maturation. *Proc. Natl. Acad. Sci. U.S.a.* *111*, 4994–4999.

Cong, J., Geng, W., He, B., Liu, J., Charlton, J., and Adler, P.N. (2001). The furry gene of *Drosophila* is important for maintaining the integrity of cellular extensions during morphogenesis. *Development* *128*, 2793–2802.

Corty, M.M., and Freeman, M.R. (2013). Architects in neural circuit design: Glia control neuron numbers and connectivity. *The Journal of Cell Biology* *203*, 395–405.

Corty, M.M., Matthews, B.J., and Grueber, W.B. (2009). Molecules and mechanisms of dendrite development in *Drosophila*. *Development* *136*, 1049–1061.

Crozatier, M., and Vincent, A. (2008). Control of multidendritic neuron differentiation in *Drosophila*: the role of Collier. *Developmental Biology* *315*, 232–242.

Cubelos, B., Sebastián-Serrano, A., Beccari, L., Calcagnotto, M.E., Cisneros, E., Kim, S., Dopazo, A., Alvarez-Dolado, M., Redondo, J.M., Bovolenta, P., et al. (2010). Cux1 and Cux2 regulate dendritic branching, spine morphology, and synapses of the upper layer neurons of the cortex. *Neuron* 66, 523–535.

de Anda, F.C., Rosario, A.L., Durak, O., Tran, T., Gräff, J., Meletis, K., Rei, D., Soda, T., Madabhushi, R., Ginty, D.D., et al. (2012). Autism spectrum disorder susceptibility gene TAOK2 affects basal dendrite formation in the neocortex. *Nat. Neurosci.* 15, 1022–1031.

Deans, M.R., Krol, A., Abraira, V.E., Copley, C.O., Tucker, A.F., and Goodrich, L.V. (2011). Control of Neuronal Morphology by the Atypical Cadherin Fat3. *Neuron* 71, 820–832.

Dietzl, G., Chen, D., Schnorrer, F., Su, K.-C., Barinova, Y., Fellner, M., Gasser, B., Kinsey, K., Oppel, S., Scheiblauer, S., et al. (2007). A genome-wide transgenic RNAi library for conditional gene inactivation in *Drosophila*. *Nature* 448, 151–156.

Díaz-Balzac, C.A., Rahman, M., Lázaro-Peña, M.I., Martin Hernandez, L.A., Salzberg, Y., Aguirre-Chen, C., Kaprielian, Z., and Bülow, H.E. (2016). Muscle- and Skin-Derived Cues Jointly Orchestrate Patterning of Somatosensory Dendrites. *Curr. Biol.* 26, 2379–2387.

Dobrosotskaya, I.Y., Seegmiller, A.C., Brown, M.S., Goldstein, J.L., and Rawson,

R.B. (2002). Regulation of SREBP processing and membrane lipid production by phospholipids in *Drosophila*. *Science* 296, 879–883.

Dong, X., Liu, O.W., Howell, A.S., and Shen, K. (2013). An extracellular adhesion molecule complex patterns dendritic branching and morphogenesis. *Cell* 155, 296–307.

Dong, X., Shen, K., and Bülow, H.E. (2015). Intrinsic and extrinsic mechanisms of dendritic morphogenesis. *Annu. Rev. Physiol.* 77, 271–300.

Emoto, K., He, Y., Ye, B., Grueber, W.B., Adler, P.N., Jan, L.Y., and Jan, Y.N. (2004). Control of Dendritic Branching and Tiling by the Tricornered-Kinase/Furry Signaling Pathway in *Drosophila* Sensory Neurons. *Cell* 119, 245–256.

Fast, P.G. (1966). A comparative study of the phospholipids and fatty acids of some insects. *Lipids* 1, 209–215.

Fuentes-Medel, Y., Ashley, J., Barria, R., Maloney, R., Freeman, M., and Budnik, V. (2012). Integration of a retrograde signal during synapse formation by glia-secreted TGF- $\beta$  ligand. *Curr. Biol.* 22, 1831–1838.

Fuerst, P.G., Koizumi, A., Masland, R.H., and Burgess, R.W. (2008). Neurite arborization and mosaic spacing in the mouse retina require DSCAM. *Nature* 451, 470–474.



Furrer, M.-P., Kim, S., Wolf, B., and Chiba, A. (2003). Robo and Frazzled/DCC mediate dendritic guidance at the CNS midline. *Nat. Neurosci.* 6, 223–230.

Galko, M.J., and Krasnow, M.A. (2004). Cellular and Genetic Analysis of Wound Healing in *Drosophila* Larvae. *PLoS Biol.* 2, e239.

Gallegos, M.E., and Bargmann, C.I. (2004). Mechanosensory Neurite Termination and Tiling Depend on SAX-2 and the SAX-1 Kinase. *Neuron* 44, 239–249.

Gao, F.B., Kohwi, M., Brenman, J.E., Jan, L.Y., and Jan, Y.N. (2000). Control of dendritic field formation in *Drosophila*: the roles of flamingo and competition between homologous neurons. *Neuron* 28, 91–101.

Garrett, A.M., Schreiner, D., Lobas, M.A., and Weiner, J.A. (2012).  $\gamma$ -Protocadherins Control Cortical Dendrite Arborization by Regulating the Activity of a FAK/PKC/MARCKS Signaling Pathway. *Neuron* 74, 269–276.

Gaudillière, B., Konishi, Y., la Iglesia, de, N., Yao, G.-L., and Bonni, A. (2004). A CaMKII-NeuroD Signaling Pathway Specifies Dendritic Morphogenesis. *Neuron* 41, 229–241.

Geiger, J.C., Lipka, J., Segura, I., Hoyer, S., Schlager, M.A., Wulf, P.S., Weinges, S., Demmers, J., Hoogenraad, C.C., and Acker-Palmer, A. (2014). The GRIP1/14-3-3 pathway coordinates cargo trafficking and dendrite development.

Developmental Cell 28, 381–393.

Geng, W., He, B., Wang, M., and Adler, P.N. (2000). The tricornered gene, which is required for the integrity of epidermal cell extensions, encodes the Drosophila nuclear DBF2-related kinase. *Genetics* 156, 1817–1828.

Giangrande, A., Murray, M.A., and Palka, J. (1993). Development and organization of glial cells in the peripheral nervous system of *Drosophila melanogaster*. *Development* 117, 895–904.

Gibson, D.A., Tymanskyj, S., Yuan, R.C., Leung, H.C., Lefebvre, J.L., Sanes, J.R., Chédotal, A., and Ma, L. (2014). Dendrite self-avoidance requires cell-autonomous slit/robo signaling in cerebellar purkinje cells. *Neuron* 81, 1040–1056.

Godenschwege, T.A., Simpson, J.H., Shan, X., Bashaw, G.J., Goodman, C.S., and Murphey, R.K. (2002). Ectopic expression in the giant fiber system of *Drosophila* reveals distinct roles for roundabout (Robo), Robo2, and Robo3 in dendritic guidance and synaptic connectivity. *J. Neurosci.* 22, 3117–3129.

Gorczyca, D.A., Younger, S., Meltzer, S., Kim, S.E., Cheng, L., Song, W., Lee, H.Y., Jan, L.Y., and Jan, Y.N. (2014). Identification of Ppk26, a DEG/ENaC Channel Functioning with Ppk1 in a Mutually Dependent Manner to Guide Locomotion Behavior in *Drosophila*. *CellReports* 9, 1446–1458.

Grueber, W.B., Jan, L.Y., and Jan, Y.N. (2002). Tiling of the *Drosophila* epidermis by multidendritic sensory neurons. *Development* *129*, 2867–2878.

Grueber, W.B., Jan, L.Y., and Jan, Y.N. (2003). Different levels of the homeodomain protein cut regulate distinct dendrite branching patterns of *Drosophila* multidendritic neurons. *Cell* *112*, 805–818.

Grueber, W.B., Ye, B., Yang, C.-H., Younger, S., Borden, K., Jan, L.Y., and Jan, Y.N. (2007). Projections of *Drosophila* multidendritic neurons in the central nervous system: links with peripheral dendrite morphology. *Development* *134*, 55–64.

Guo, Y., Wang, Y., Zhang, W., Meltzer, S., Zanini, D., Yu, Y., Li, J., Cheng, T., Guo, Z., Wang, Q., et al. (2016). Transmembrane channel-like (tmc) gene regulates *Drosophila* larval locomotion. *Proc. Natl. Acad. Sci. U.S.a.* *113*, 7243–7248.

Han, C., Jan, L.Y., and Jan, Y.N. (2011). Enhancer-driven membrane markers for analysis of nonautonomous mechanisms reveal neuron-glia interactions in *Drosophila*. *Proc. Natl. Acad. Sci. U.S.a.* *108*, 9673–9678.

Han, C., Wang, D., Soba, P., Zhu, S., Lin, X., Jan, L.Y., and Jan, Y.N. (2012). Integrins regulate repulsion-mediated dendritic patterning of *drosophila* sensory neurons by restricting dendrites in a 2D space. *Neuron* *73*, 64–78.

Harony-Nicolas, H., and Buxbaum, J.D. (2015). Animal Models for Neurodevelopmental Disorders. In *The Genetics of Neurodevelopmental Disorders*, (Hoboken, NJ, USA: John Wiley & Sons, Inc), pp. 261–274.

Hattori, Y., Sugimura, K., and Uemura, T. (2007). Selective expression of Knot/Collier, a transcriptional regulator of the EBF/Olf-1 family, endows the *Drosophila* sensory system with neuronal class-specific elaborated dendritic patterns. *Genes to Cells* 12, 1011–1022.

Hattori, Y., Usui, T., Satoh, D., Moriyama, S., Shimono, K., Itoh, T., Shirahige, K., and Uemura, T. (2013). Sensory-neuron subtype-specific transcriptional programs controlling dendrite morphogenesis: genome-wide analysis of *Abrupt* and *Knot/Collier*. *Developmental Cell* 27, 530–544.

Hekmat-Scafe, D.S., Dang, K.N., and Tanouye, M.A. (2005). Seizure suppression by gain-of-function *escargot* mutations. *Genetics* 169, 1477–1493.

Hekmat-Scafe, D.S., Mercado, A., Fajilan, A.A., Lee, A.W., Hsu, R., Mount, D.B., and Tanouye, M.A. (2010). Seizure sensitivity is ameliorated by targeted expression of K<sup>+</sup>-Cl<sup>-</sup> cotransporter function in the mushroom body of the *Drosophila* brain. *Genetics* 184, 171–183.

Hergovich, A., Stegert, M.R., Schmitz, D., and Hemmings, B.A. (2006). NDR kinases regulate essential cell processes from yeast to humans. *Nat Rev Mol Cell*

Biol 7, 253–264.

Hong, W., Mosca, T.J., and Luo, L. (2012). Teneurins instruct synaptic partner matching in an olfactory map. *Nature* 484, 201–207.

Hoogenraad, C.C., Milstein, A.D., Ethell, I.M., Henkemeyer, M., and Sheng, M. (2005). GRIP1 controls dendrite morphogenesis by regulating EphB receptor trafficking. *Nat. Neurosci.* 8, 906–915.

Horton, A.C., Rácz, B., Monson, E.E., Lin, A.L., Weinberg, R.J., and Ehlers, M.D. (2005). Polarized Secretory Trafficking Directs Cargo for Asymmetric Dendrite Growth and Morphogenesis. *Neuron* 48, 757–771.

Hu, H., Marton, T.F., and Goodman, C.S. (2001). Plexin B mediates axon guidance in *Drosophila* by simultaneously inhibiting active Rac and enhancing RhoA signaling. *Neuron* 32, 39–51.

Hughes, M.E., Bortnick, R., Tsubouchi, A., Bäumer, P., Kondo, M., Uemura, T., and Schmucker, D. (2007). Homophilic Dscam interactions control complex dendrite morphogenesis. *Neuron* 54, 417–427.

Jackson, C.L., Walch, L., and Verbavatz, J.-M. (2016). Lipids and Their Trafficking: An Integral Part of Cellular Organization. *Developmental Cell* 39, 139–153.

Jan, Y.N., and Jan, L.Y. (2010). Branching out: mechanisms of dendritic

arborization. *Nat. Rev. Neurosci.* *11*, 316–328.

Jeon, T.-I., and Osborne, T.F. (2012). SREBPs: metabolic integrators in physiology and metabolism. *Trends Endocrinol. Metab.* *23*, 65–72.

Jinushi-Nakao, S., Arvind, R., Amikura, R., Kinameri, E., Liu, A.W., and Moore, A.W. (2007). Knot/Collier and cut control different aspects of dendrite cytoskeleton and synergize to define final arbor shape. *Neuron* *56*, 963–978.

Jones, H.E., Harwood, J.L., Bowen, I.D., and Griffiths, G. (1992). Lipid composition of subcellular membranes from larvae and prepupae of *Drosophila melanogaster*. *Lipids* *27*, 984–987.

Joo, W.J., Sweeney, L.B., Liang, L., and Luo, L. (2013). Linking Cell Fate, Trajectory Choice, and Target Selection: Genetic Analysis of Sema-2b in Olfactory Axon Targeting. *Neuron* *78*, 673–686.

Joo, W., Hippenmeyer, S., and Luo, L. (2014). Neurodevelopment. Dendrite morphogenesis depends on relative levels of NT-3/TrkC signaling. *Science* *346*, 626–629.

Kanamori, T., Kanai, M.I., Dairyo, Y., Yasunaga, K.-I., Morikawa, R.K., and Emoto, K. (2013). Compartmentalized calcium transients trigger dendrite pruning in *Drosophila* sensory neurons. *Science* *340*, 1475–1478.

Kaneko, M., Yamaguchi, K., Eiraku, M., Sato, M., Takata, N., Kiyohara, Y., Mishina, M., Hirase, H., Hashikawa, T., and Kengaku, M. (2011). Remodeling of monopolar Purkinje cell dendrites during cerebellar circuit formation. *PLoS ONE* *6*, e20108.

Kaufmann, W.E., and Moser, H.W. (2000). Dendritic anomalies in disorders associated with mental retardation. *Cereb. Cortex* *10*, 981–991.

KENNEDY, E.P. (1957). Metabolism of lipides. *Annu. Rev. Biochem.* *26*, 119–148.

Kim, I.-J., Zhang, Y., Meister, M., and Sanes, J.R. (2010). Laminar restriction of retinal ganglion cell dendrites and axons: subtype-specific developmental patterns revealed with transgenic markers. *J. Neurosci.* *30*, 1452–1462.

Kim, M.D., Jan, L.Y., and Jan, Y.N. (2006). The bHLH-PAS protein Spineless is necessary for the diversification of dendrite morphology of *Drosophila* dendritic arborization neurons. *Genes & Development* *20*, 2806–2819.

Kim, M.E., Shrestha, B.R., Blazeski, R., Mason, C.A., and Grueber, W.B. (2012a). Integrins establish dendrite-substrate relationships that promote dendritic self-avoidance and patterning in *Drosophila* sensory neurons. *Neuron* *73*, 79–91.

Kim, S.E., Coste, B., Chadha, A., Cook, B., and Patapoutian, A. (2012b). The role

of *Drosophila* Piezo in mechanical nociception. *Nature* 483, 209–212.

Kliman, M., Vijayakrishnan, N., Wang, L., Tapp, J.T., Broadie, K., and McLean, J.A. (2010). Structural mass spectrometry analysis of lipid changes in a *Drosophila* epilepsy model brain. *Mol. BioSyst.* 6, 958–959.

Koike-Kumagai, M., Yasunaga, K.-I., Morikawa, R., Kanamori, T., and Emoto, K. (2009). The target of rapamycin complex 2 controls dendritic tiling of *Drosophila* sensory neurons through the Tricornered kinase signalling pathway. *The EMBO Journal* 28, 3879–3892.

Komiyama, T., Sweeney, L.B., Schuldiner, O., Garcia, K.C., and Luo, L. (2007). Graded expression of semaphorin-1a cell-autonomously directs dendritic targeting of olfactory projection neurons. *Cell* 128, 399–410.

Koropouli, E., and Kolodkin, A.L. (2014). Semaphorins and the dynamic regulation of synapse assembly, refinement, and function. *Current Opinion in Neurobiology* 27, 1–7.

Kroll, J.R., and Tanouye, M.A. (2013). Rescue of easily shocked mutant seizure sensitivity in *Drosophila* adults. *J. Comp. Neurol.* 521, 3500–3507.

Kruger, R.P., Aurandt, J., and Guan, K.-L. (2005). Semaphorins command cells to move. *Nat Rev Mol Cell Biol* 6, 789–800.



Kulkarni, V.A., and Firestein, B.L. (2012). The dendritic tree and brain disorders. *Mol. Cell. Neurosci.* *50*, 10–20.

Kunte, A.S., Matthews, K.A., and Rawson, R.B. (2006). Fatty acid auxotrophy in *Drosophila* larvae lacking SREBP. *Cell Metab.* *3*, 439–448.

Lanoue, V., Usardi, A., Sigoillot, S.M., Talleur, M., Iyer, K., Mariani, J., Isope, P., Vodjdani, G., Heintz, N., and Selimi, F. (2013). The adhesion-GPCR BAI3, a gene linked to psychiatric disorders, regulates dendrite morphogenesis in neurons. *Molecular Psychiatry* *18*, 943–950.

Lawrence Zipursky, S., and Grueber, W.B. (2013). The Molecular Basis of Self-Avoidance. *Annu. Rev. Neurosci.* *36*, 547–568.

Lee, A. (2003). Control of dendritic development by the *Drosophila* fragile X-related gene involves the small GTPase Rac1. *Development* *130*, 5543–5552.

Lee, T., Winter, C., Marticke, S.S., Lee, A., and Luo, L. (2000). Essential roles of *Drosophila* RhoA in the regulation of neuroblast proliferation and dendritic but not axonal morphogenesis. *Neuron* *25*, 307–316.

Lefebvre, J.L., Kostadinov, D., Chen, W.V., Maniatis, T., and Sanes, J.R. (2012). Protocadherins mediate dendritic self-avoidance in the mammalian nervous system. *Nature* *488*, 517–521.

Lefebvre, J.L., Sanes, J.R., and Kay, J.N. (2015). Development of Dendritic Form and Function. *Annu. Rev. Cell Dev. Biol.* *31*, 741–777.

Li, N., Zhao, C.-T., Wang, Y., and Yuan, X.-B. (2010). The transcription factor Cux1 regulates dendritic morphology of cortical pyramidal neurons. *PLoS ONE* *5*, e10596.

Li, W., and Gao, F.-B. (2003). Actin filament-stabilizing protein tropomyosin regulates the size of dendritic fields. *J. Neurosci.* *23*, 6171–6175.

Li, W., Wang, F., Menut, L., and Gao, F.-B. (2004). BTB/POZ-Zinc Finger Protein Abrupt Suppresses Dendritic Branching in a Neuronal Subtype-Specific and Dosage-Dependent Manner. *Neuron* *43*, 823–834.

Li, Z., Van Aelst, L., and Cline, H.T. (2000). Rho GTPases regulate distinct aspects of dendritic arbor growth in *Xenopus* central neurons in vivo. *Nat. Neurosci.* *3*, 217–225.

Lim, H.-Y., Wang, W., Wessells, R.J., Ocorr, K., and Bodmer, R. (2011). Phospholipid homeostasis regulates lipid metabolism and cardiac function through SREBP signaling in *Drosophila*. *Genes & Development* *25*, 189–200.

Liu, L., Zhang, K., Sandoval, H., Yamamoto, S., Jaiswal, M., Sanz, E., Li, Z., Hui, J., Graham, B.H., Quintana, A., et al. (2015). Glial Lipid Droplets and ROS

Induced by Mitochondrial Defects Promote Neurodegeneration. *Cell* 160, 177–190.

London, M., and Häusser, M. (2005). Dendritic computation. *Annu. Rev. Neurosci.* 28, 503–532.

López-Muñoz, F., Boya, J., and Alamo, C. (2006). Neuron theory, the cornerstone of neuroscience, on the centenary of the Nobel Prize award to Santiago Ramón y Cajal. *Brain Research Bulletin* 70, 391–405.

Majdazari, A., Stubbusch, J., Müller, C.M., Hennchen, M., Weber, M., Deng, C.-X., Mishina, Y., Schütz, G., Deller, T., and Rohrer, H. (2013). Dendrite complexity of sympathetic neurons is controlled during postnatal development by BMP signaling. *J. Neurosci.* 33, 15132–15144.

Martin-Bermudo, M.D. (1997). Specificity of PS integrin function during embryogenesis resides in the alpha subunit extracellular domain. *The EMBO Journal* 16, 4184–4193.

Martínez-Cerdeño, V. (2017). Dendrite and spine modifications in autism and related neurodevelopmental disorders in patients and animal models. *Dev Neurobiol* 77, 393–404.

Matsubara, D., Horiuchi, S.-Y., Shimono, K., Usui, T., and Uemura, T. (2011). The

seven-pass transmembrane cadherin Flamingo controls dendritic self-avoidance via its binding to a LIM domain protein, Espinas, in *Drosophila* sensory neurons. *Genes & Development* 25, 1982–1996.

Matsui, A., Tran, M., Yoshida, A.C., Kikuchi, S.S., U, M., Ogawa, M., and Shimogori, T. (2013). BTBD3 controls dendrite orientation toward active axons in mammalian neocortex. *Science* 342, 1114–1118.

Matsuoka, R.L., Chivatakarn, O., Badea, T.C., Samuels, I.S., Cahill, H., Katayama, K.-I., Kumar, S.R., Suto, F., Chédotal, A., Peachey, N.S., et al. (2011a). Class 5 Transmembrane Semaphorins Control Selective Mammalian Retinal Lamination and Function. *Neuron* 71, 460–473.

Matsuoka, R.L., Nguyen-Ba-Charvet, K.T., Parray, A., Badea, T.C., Chédotal, A., and Kolodkin, A.L. (2011b). Transmembrane semaphorin signalling controls laminar stratification in the mammalian retina. *Nature* 470, 259–263.

Matthes, D.J., Sink, H., Kolodkin, A.L., and Goodman, C.S. (1995). Semaphorin II can function as a selective inhibitor of specific synaptic arborizations. *Cell* 81, 631–639.

Matthews, B.J., and Grueber, W.B. (2011). Dscam1-Mediated Self-Avoidance Counters Netrin-Dependent Targeting of Dendrites in *Drosophila*. *Current Biology* 21, 1480–1487.

Matthews, B.J., Kim, M.E., Flanagan, J.J., Hattori, D., Clemens, J.C., Zipursky, S.L., and Grueber, W.B. (2007). Dendrite self-avoidance is controlled by Dscam. *Cell* 129, 593–604.

McAllister, A.K., Lo, D.C., and Katz, L.C. (1995). Neurotrophins regulate dendritic growth in developing visual cortex. *Neuron* 15, 791–803.

Montani, C., Ramos-Brossier, M., Ponzoni, L., Gritti, L., Cwetsch, A.W., Braidà, D., Saillour, Y., Terragni, B., Mantegazza, M., Sala, M., et al. (2017). The X-Linked Intellectual Disability Protein IL1RAPL1 Regulates Dendrite Complexity. *J. Neurosci.* 37, 6606–6627.

Morin, X., Daneman, R., Zavortink, M., and Chia, W. (2001). A protein trap strategy to detect GFP-tagged proteins expressed from their endogenous loci in *Drosophila*. *Proceedings of the National Academy of Sciences* 98, 15050–15055.

Mukaetova-Ladinska, E.B., Arnold, H., Jaros, E., Perry, R., and Perry, E. (2004). Depletion of MAP2 expression and laminar cytoarchitectonic changes in dorsolateral prefrontal cortex in adult autistic individuals. *Neuropathol. Appl. Neurobiol.* 30, 615–623.

Nakamura, F., Ugajin, K., Yamashita, N., Okada, T., Uchida, Y., Taniguchi, M., Ohshima, T., and Goshima, Y. (2009). Increased proximal bifurcation of CA1 pyramidal apical dendrites in *sema3A* mutant mice. *J. Comp. Neurol.* 516, 360–

375.

Nakayama, A.Y., Harms, M.B., and Luo, L. (2000). Small GTPases Rac and Rho in the maintenance of dendritic spines and branches in hippocampal pyramidal neurons. *Journal of Neuroscience* 20, 5329–5338.

Ng, J., Nardine, T., Harms, M., Tzu, J., Goldstein, A., Sun, Y., Dietzl, G., Dickson, B.J., and Luo, L. (2002). Rac GTPases control axon growth, guidance and branching. *Nature* 416, 442–447.

Nyako, M., Marks, C., Sherma, J., and Reynolds, E.R. (2001). Tissue-specific and developmental effects of the easily shocked mutation on ethanolamine kinase activity and phospholipid composition in *Drosophila melanogaster*. *Biochem. Genet.* 39, 339–349.

O'Malley, A.M., Shanley, D.K., Kelly, A.T., and Barry, D.S. (2014). Towards an understanding of semaphorin signalling in the spinal cord. *Gene* 553, 69–74.

Ori-McKenney, K.M., Jan, L.Y., and Jan, Y.N. (2012). Golgi Outposts Shape Dendrite Morphology by Functioning as Sites of Acentrosomal Microtubule Nucleation in Neurons. *Neuron* 76, 921–930.

Osório, C., Chacón, P.J., Kisiswa, L., White, M., Wyatt, S., Rodríguez-Tébar, A., and Davies, A.M. (2013). Growth differentiation factor 5 is a key physiological

regulator of dendrite growth during development. *Development* *140*, 4751–4762.

Parker, L., Howlett, I.C., Rusan, Z.M., and Tanouye, M.A. (2011). Seizure and epilepsy: studies of seizure disorders in *Drosophila*. *Int. Rev. Neurobiol.* *99*, 1–21.

Parrish, J.Z., Emoto, K., Jan, L.Y., and Jan, Y.N. (2007a). Polycomb genes interact with the tumor suppressor genes *hippo* and *warts* in the maintenance of *Drosophila* sensory neuron dendrites. *Genes & Development* *21*, 956–972.

Parrish, J.Z., Emoto, K., Kim, M.D., and Jan, Y.N. (2007b). Mechanisms that regulate establishment, maintenance, and remodeling of dendritic fields. *Annu. Rev. Neurosci.* *30*, 399–423.

Parrish, J.Z., Kim, M.D., Jan, L.Y., and Jan, Y.N. (2006). Genome-wide analyses identify transcription factors required for proper morphogenesis of *Drosophila* sensory neuron dendrites. *Genes & Development* *20*, 820–835.

Pasterkamp, R.J. (2012). Getting neural circuits into shape with semaphorins. *Nat. Rev. Neurosci.* *13*, 605–618.

Pasterkamp, R.J., and Kolodkin, A.L. (2013). SnapShot: Axon Guidance. *Cell* *153*, 494–494.e2.

Pavlidis, P., Ramaswami, M., and Tanouye, M.A. (1994a). The *Drosophila* easily shocked gene: a mutation in a phospholipid synthetic pathway causes seizure,

neuronal failure, and paralysis. *Cell* 79, 23–33.

Pavlidis, P., Ramaswami, M., and Tanouye, M.A. (1994b). The *Drosophila* easily shocked gene: a mutation in a phospholipid synthetic pathway causes seizure, neuronal failure, and paralysis. *Cell* 79, 23–33.

Peng, I.-F., and Wu, C.-F. (2007). *Drosophila* cacophony channels: a major mediator of neuronal Ca<sup>2+</sup> currents and a trigger for K<sup>+</sup> channel homeostatic regulation. *J. Neurosci.* 27, 1072–1081.

Perry, V.H., and Linden, R. (1982). Evidence for dendritic competition in the developing retina. *Nature* 297, 683–685.

Pfeiffer, B.D., Truman, J.W., and Rubin, G.M. (2012). Using translational enhancers to increase transgene expression in *Drosophila*. *Proc. Natl. Acad. Sci. U.S.a.* 109, 6626–6631.

Pino, D., Choe, Y., and Pleasure, S.J. (2011). Wnt5a controls neurite development in olfactory bulb interneurons. *ASN Neuro* 3, e00059.

Podkowa, M., Christova, T., Zhao, X., Jian, Y., and Attisano, L. (2013). p21-Activated kinase (PAK) is required for Bone Morphogenetic Protein (BMP)-induced dendritogenesis in cortical neurons. *Mol. Cell. Neurosci.* 57, 83–92.



Polleux, F., Morrow, T., and Ghosh, A. (2000). Semaphorin 3A is a chemoattractant for cortical apical dendrites. *Nature* *404*, 567–573.

Port, F., Chen, H.-M., Lee, T., and Bullock, S.L. (2014). Optimized CRISPR/Cas tools for efficient germline and somatic genome engineering in *Drosophila*. *Proc. Natl. Acad. Sci. U.S.A.* *111*, E2967–E2976.

Puram, S.V., and Bonni, A. (2013). Cell-intrinsic drivers of dendrite morphogenesis. *Development* *140*, 4657–4671.

Ramón y Cajal, S. (1909). *Histologie du système nerveux de l'homme & des vertébrés.* (Paris :: Maloine,).

Rawson, R.B. (2003). The SREBP pathway — insights from Insigs and insects. *Nat Rev Mol Cell Biol* *4*, 631–640.

Raymond, G.V., Bauman, M.L., and Kemper, T.L. (1996). Hippocampus in autism: a Golgi analysis. *Acta Neuropathol.* *91*, 117–119.

Redmond, L., and Ghosh, A. (2005). Regulation of dendritic development by calcium signaling. *Cell Calcium* *37*, 411–416.

Redmond, L., Kashani, A.H., and Ghosh, A. (2002). Calcium regulation of dendritic growth via CaM kinase IV and CREB-mediated transcription. *Neuron* *34*, 999–1010.

Rosso, S.B., Sussman, D., Wynshaw-Boris, A., and Salinas, P.C. (2005). Wnt signaling through Dishevelled, Rac and JNK regulates dendritic development. *Nat. Neurosci.* *8*, 34–42.

Rubinstein, R., Thu, C.A., Goodman, K.M., Wolcott, H.N., Bahna, F., Manneppalli, S., Ahlsen, G., Chevee, M., Halim, A., Clausen, H., et al. (2015). Molecular logic of neuronal self-recognition through protocadherin domain interactions. *Cell* *163*, 629–642.

Rudelli, R.D., Brown, W.T., Wisniewski, K., Jenkins, E.C., Laure-Kamionowska, M., Connell, F., and Wisniewski, H.M. (1985). Adult fragile X syndrome. Clinico-neuropathologic findings. *Acta Neuropathol.* *67*, 289–295.

Sagasti, A., Guido, M.R., Raible, D.W., and Schier, A.F. (2005). Repulsive Interactions Shape the Morphologies and Functional Arrangement of Zebrafish Peripheral Sensory Arbors. *Current Biology* *15*, 804–814.

Salzberg, Y., Díaz-Balzac, C.A., Ramirez-Suarez, N.J., Attreed, M., Tecle, E., Desbois, M., Kaprielian, Z., and Bülow, H.E. (2013). Skin-Derived Cues Control Arborization of Sensory Dendrites in *Caenorhabditis elegans*. *Cell* *155*, 308–320.

Sanes, J.R., and Zipursky, S.L. (2010). Design principles of insect and vertebrate visual systems. *Neuron* *66*, 15–36.

Saras, A., and Tanouye, M.A. (2016). Mutations of the Calcium Channel Gene cacophony Suppress Seizures in *Drosophila*. *PLoS Genet.* *12*, e1005784.

Satoh, D., Sato, D., Tsuyama, T., Saito, M., Ohkura, H., Rolls, M.M., Ishikawa, F., and Uemura, T. (2008). Spatial control of branching within dendritic arbors by dynein-dependent transport of Rab5-endosomes. *Nat. Cell Biol.* *10*, 1164–1171.

Schneider, I. (1972). Cell lines derived from late embryonic stages of *Drosophila melanogaster*. *J Embryol Exp Morphol* *27*, 353–365.

Scott, E.K., Reuter, J.E., and Luo, L. (2003). Small GTPase Cdc42 is required for multiple aspects of dendritic morphogenesis. *J. Neurosci.* *23*, 3118–3123.

Sears, J.C., and Broihier, H.T. (2016). FoxO regulates microtubule dynamics and polarity to promote dendrite branching in *Drosophila* sensory neurons. *Developmental Biology* *418*, 40–54.

Seegmiller, A.C., Dobrosotskaya, I., Goldstein, J.L., Ho, Y.K., Brown, M.S., and Rawson, R.B. (2002). The SREBP pathway in *Drosophila*: regulation by palmitate, not sterols. *Developmental Cell* *2*, 229–238.

Serini, G., Valdembrì, D., Zanivan, S., Morterra, G., Burkhardt, C., Caccavari, F., Zammataro, L., Primo, L., Tamagnone, L., Logan, M., et al. (2003). Class 3 semaphorins control vascular morphogenesis by inhibiting integrin function.

Nature 424, 391–397.

Shima, Y., Kawaguchi, S.-Y., Kosaka, K., Nakayama, M., Hoshino, M., Nabeshima, Y., Hirano, T., and Uemura, T. (2007). Opposing roles in neurite growth control by two seven-pass transmembrane cadherins. *Nat. Neurosci.* 10, 963–969.

Shima, Y., Kengaku, M., Hirano, T., Takeichi, M., and Uemura, T. (2004). Regulation of Dendritic Maintenance and Growth by a Mammalian 7-Pass Transmembrane Cadherin. *Developmental Cell* 7, 205–216.

Singhania, A., and Grueber, W.B. (2014). Development of the embryonic and larval peripheral nervous system of *Drosophila*. *Wiley Interdiscip Rev Dev Biol* 3, 193–210.

Sloan, S.A., and Barres, B.A. (2014). Mechanisms of astrocyte development and their contributions to neurodevelopmental disorders. *Current Opinion in Neurobiology* 27, 75–81.

Smith, C.J., Watson, J.D., Spencer, W.C., O'Brien, T., Cha, B., Albeg, A., Treinin, M., and Miller, D.M., III (2010). Time-lapse imaging and cell-specific expression profiling reveal dynamic branching and molecular determinants of a multi-dendritic nociceptor in *C. elegans*. *Developmental Biology* 345, 18–33.

Smith, C.J., Watson, J.D., VanHoven, M.K., Colón-Ramos, D.A., and Miller, D.M. (2012). Netrin (UNC-6) mediates dendritic self-avoidance. *Nat. Neurosci.* *15*, 731–737.

Soba, P., Han, C., Zheng, Y., Perea, D., Miguel-Aliaga, I., Jan, L.Y., and Jan, Y.N. (2015). The Ret receptor regulates sensory neuron dendrite growth and integrin mediated adhesion. *Elife* *4*, e05491.

Soba, P., Zhu, S., Emoto, K., Younger, S., Yang, S.-J., Yu, H.-H., Lee, T., Jan, L.Y., and Jan, Y.N. (2007). *Drosophila* sensory neurons require Dscam for dendritic self-avoidance and proper dendritic field organization. *Neuron* *54*, 403–416.

Song, W., Onishi, M., Jan, L.Y., and Jan, Y.N. (2007). Peripheral multidendritic sensory neurons are necessary for rhythmic locomotion behavior in *Drosophila* larvae. *Proceedings of the National Academy of Sciences* *104*, 5199–5204.

Song, W., Veenstra, J.A., and Perrimon, N. (2014). Control of Lipid Metabolism by Tachykinin in *Drosophila*. *CellReports* *9*, 40–47.

Söderberg, O., Gullberg, M., Jarvius, M., Ridderstråle, K., Leuchowius, K.-J., Jarvius, J., Wester, K., Hydbring, P., Bahram, F., Larsson, L.-G., et al. (2006). Direct observation of individual endogenous protein complexes in situ by proximity ligation. *Nat Meth* *3*, 995–1000.

Spruston, N. (2008). Pyramidal neurons: dendritic structure and synaptic integration. *Nat. Rev. Neurosci.* *9*, 206–221.

Stankiewicz, T.R., and Linseman, D.A. (2014). Rho family GTPases: key players in neuronal development, neuronal survival, and neurodegeneration. *Front Cell Neurosci* *8*, 314.

Sugimura, K., Satoh, D., Estes, P., Crews, S., and Uemura, T. (2004). Development of Morphological Diversity of Dendrites in *Drosophila* by the BTB-Zinc Finger Protein *Abrupt*. *Neuron* *43*, 809–822.

Sun, L.O., Jiang, Z., Rivlin-Etzion, M., Hand, R., Brady, C.M., Matsuoka, R.L., Yau, K.-W., Feller, M.B., and Kolodkin, A.L. (2013). On and off retinal circuit assembly by divergent molecular mechanisms. *Science* *342*, 1241974–1241974.

Sweeney, L.B., Chou, Y.-H., Wu, Z., Joo, W., Komiyama, T., Potter, C.J., Kolodkin, A.L., Garcia, K.C., and Luo, L. (2011). Secreted semaphorins from degenerating larval ORN axons direct adult projection neuron dendrite targeting. *Neuron* *72*, 734–747.

Tamagnone, L., and Comoglio, P.M. (2004). To move or not to move? Semaphorin signalling in cell migration. *EMBO Rep.* *5*, 356–361.

Tamiji, J., and Crawford, D.A. (2010). The neurobiology of lipid metabolism in

autism spectrum disorders. *Neurosignals* 18, 98–112.

Teichmann, H.M., and Shen, K. (2011). UNC-6 and UNC-40 promote dendritic growth through PAR-4 in *Caenorhabditis elegans* neurons. *Nat. Neurosci.* 14, 165–172.

Thibault, S.T., Singer, M.A., Miyazaki, W.Y., Milash, B., Dompe, N.A., Singh, C.M., Buchholz, R., Demsky, M., Fawcett, R., Francis-Lang, H.L., et al. (2004). A complementary transposon tool kit for *Drosophila melanogaster* using P and piggyBac. *Nat. Genet.* 36, 283–287.

Tint, G.S., Irons, M., Elias, E.R., Batta, A.K., Frieden, R., Chen, T.S., and Salen, G. (1994). Defective cholesterol biosynthesis associated with the Smith-Lemli-Opitz syndrome. *N. Engl. J. Med.* 330, 107–113.

Tracey, W.D., Wilson, R.I., Laurent, G., and Benzer, S. (2003). *painless*, a *Drosophila* gene essential for nociception. *Cell* 113, 261–273.

Tran, T.S., Kolodkin, A.L., and Bharadwaj, R. (2007). Semaphorin regulation of cellular morphology. *Annu. Rev. Cell Dev. Biol.* 23, 263–292.

Tsubouchi, A., Caldwell, J.C., and Tracey, W.D. (2012). Dendritic filopodia, Ripped Pocket, NOMPC, and NMDARs contribute to the sense of touch in *Drosophila* larvae. *Curr. Biol.* 22, 2124–2134.

Uhlén, M., Fagerberg, L., Hallström, B.M., Lindskog, C., Oksvold, P., Mardinoglu, A., Sivertsson, Å., Kampf, C., Sjöstedt, E., Asplund, A., et al. (2015). Proteomics. Tissue-based map of the human proteome. *Science* *347*, 1260419–1260419.

Ultanir, S.K., Hertz, N.T., Li, G., Ge, W.-P., Burlingame, A.L., Pleasure, S.J., Shokat, K.M., Jan, L.Y., and Jan, Y.N. (2012). Chemical Genetic Identification of NDR1/2 Kinase Substrates AAK1 and Rabin8 Uncovers Their Roles in Dendrite Arborization and Spine Development. *Neuron* *73*, 1127–1142.

Vaillant, A.R., Zanassi, P., Walsh, G.S., Aumont, A., Alonso, A., and Miller, F.D. (2002). Signaling Mechanisms Underlying Reversible, Activity-Dependent Dendrite Formation. *Neuron* *34*, 985–998.

Valnegri, P., Puram, S.V., and Bonni, A. (2015). Regulation of dendrite morphogenesis by extrinsic cues. *Trends Neurosci.* *38*, 439–447.

Vance, J.E. (2014). Phospholipid Synthesis and Transport in Mammalian Cells. *Traffic* *16*, 1–18.

Wang, J., Ma, X., Yang, J.S., Zheng, X., Zugates, C.T., Lee, C.-H.J., and Lee, T. (2004). Transmembrane/Juxtamembrane Domain-Dependent Dscam Distribution and Function during Mushroom Body Neuronal Morphogenesis. *Neuron* *43*, 663–672.



Wayman, G.A., Lee, Y.-S., Tokumitsu, H., Silva, A.J., and Soderling, T.R. (2009).

Calmodulin-Kinases: Modulators of Neuronal Development and Plasticity. *Neuron* 64, 590.

Wässle, H. (2004). Parallel processing in the mammalian retina. *Nat. Rev.*

*Neurosci.* 5, 747–757.

Weiss, L.A., Shen, Y., Korn, J.M., Arking, D.E., Miller, D.T., Fossdal, R.,

Saemundsen, E., Stefansson, H., Ferreira, M.A.R., Green, T., et al. (2008).

Association between microdeletion and microduplication at 16p11.2 and autism.

*N. Engl. J. Med.* 358, 667–675.

Whitford, K.L., Marillat, V., Stein, E., Goodman, C.S., Tessier-Lavigne, M.,

Chédotal, A., and Ghosh, A. (2002). Regulation of cortical dendrite development

by Slit-Robo interactions. *Neuron* 33, 47–61.

Wojtowicz, W.M., Flanagan, J.J., Millard, S.S., Zipursky, S.L., and Clemens, J.C.

(2004). Alternative Splicing of *Drosophila* Dscam Generates Axon Guidance

Receptors that Exhibit Isoform-Specific Homophilic Binding. *Cell* 118, 619–633.

Wong, C., and Crawford, D.A. (2014). Lipid Signalling in the Pathology of Autism

Spectrum Disorders. In *Comprehensive Guide to Autism*, (New York, NY:

Springer New York), pp. 1259–1283.

Wong, R.O.L., and Ghosh, A. (2002). Activity-dependent regulation of dendritic growth and patterning. *Nat. Rev. Neurosci.* *3*, 803–812.

Wu, G.Y., Deisseroth, K., and Tsien, R.W. (2001). Spaced stimuli stabilize MAPK pathway activation and its effects on dendritic morphology. *Nat. Neurosci.* *4*, 151–158.

Wu, Y., Helt, J.-C., Wexler, E., Petrova, I.M., Noordermeer, J.N., Fradkin, L.G., and Hing, H. (2014). Wnt5 and *drl/ryk* gradients pattern the *Drosophila* olfactory dendritic map. *J. Neurosci.* *34*, 14961–14972.

Wu, Z., Sawada, T., Shiba, K., Liu, S., Kanao, T., Takahashi, R., Hattori, N., Imai, Y., and Lu, B. (2013). Tricornered/NDR kinase signaling mediates PINK1-directed mitochondrial quality control and tissue maintenance. *Genes & Development* *27*, 157–162.

Wu, Z., Sweeney, L.B., Ayoob, J.C., Chak, K., Andreone, B.J., Ohyama, T., Kerr, R., Luo, L., Zlatic, M., and Kolodkin, A.L. (2011). A combinatorial semaphorin code instructs the initial steps of sensory circuit assembly in the *Drosophila* CNS. *Neuron* *70*, 281–298.

Xiang, Y., Yuan, Q., Vogt, N., Looger, L.L., Jan, L.Y., and Jan, Y.N. (2010). Light-avoidance-mediating photoreceptors tile the *Drosophila* larval body wall. *Nature* *468*, 921–926.

Xu, B., Zang, K., Ruff, N.L., Zhang, Y.A., McConnell, S.K., Stryker, M.P., and Reichardt, L.F. (2000). Cortical degeneration in the absence of neurotrophin signaling: dendritic retraction and neuronal loss after removal of the receptor TrkB. *Neuron* 26, 233–245.

Xu, N.-J., Sun, S., Gibson, J.R., and Henkemeyer, M. (2011). A dual shaping mechanism for postsynaptic ephrin-B3 as a receptor that sculpts dendrites and synapses. *Nat. Neurosci.* 14, 1421–1429.

Yacoubian, T.A., and Lo, D.C. (2000). Truncated and full-length TrkB receptors regulate distinct modes of dendritic growth. *Nat. Neurosci.* 3, 342–349.

Yadav, S., Oses-Prieto, J.A., Peters, C.J., Zhou, J., Pleasure, S.J., Burlingame, A.L., Jan, L.Y., and Jan, Y.N. (2017). TAOK2 Kinase Mediates PSD95 Stability and Dendritic Spine Maturation through Septin7 Phosphorylation. *Neuron* 93, 379–393.

Yalgin, C., Ebrahimi, S., Delandre, C., Yoong, L.F., Akimoto, S., Tran, H., Amikura, R., Spokony, R., Torben-Nielsen, B., White, K.P., et al. (2015). Centrosomin represses dendrite branching by orienting microtubule nucleation. *Nat. Neurosci.* 18, 1437–1445.

Yamagata, M., and Sanes, J.R. (2008). Dscam and Sidekick proteins direct lamina-specific synaptic connections in vertebrate retina. *Nature* 451, 465–469.

Yan, Z., Zhang, W., He, Y., Gorczyca, D., Xiang, Y., Cheng, L.E., Meltzer, S., Jan, L.Y., and Jan, Y.N. (2013). *Drosophila* NOMPC is a mechanotransduction channel subunit for gentle-touch sensation. *Nature* *493*, 221–225.

Yau, K.W., van Beuningen, S.F.B., Cunha-Ferreira, I., Cloin, B.M.C., van Battum, E.Y., Will, L., Schätzle, P., Tas, R.P., van Krugten, J., Katrukha, E.A., et al. (2014). Microtubule minus-end binding protein CAMSAP2 controls axon specification and dendrite development. *Neuron* *82*, 1058–1073.

Ye, B., Zhang, Y., Song, W., Younger, S.H., Jan, L.Y., and Jan, Y.N. (2007). Growing dendrites and axons differ in their reliance on the secretory pathway. *Cell* *130*, 717–729.

Zhang, J., and Liu, Q. (2015). Cholesterol metabolism and homeostasis in the brain. *Protein Cell* *6*, 254–264.

Zheng, Y., Wildonger, J., Ye, B., Zhang, Y., Kita, A., Younger, S.H., Zimmerman, S., Jan, L.Y., and Jan, Y.N. (2008). Dynein is required for polarized dendritic transport and uniform microtubule orientation in axons. *Nat. Cell Biol.* *10*, 1172–1180.

Zhou, B., Cai, Q., Xie, Y., and Sheng, Z.-H. (2012). Snapin recruits dynein to BDNF-TrkB signaling endosomes for retrograde axonal transport and is essential for dendrite growth of cortical neurons. *CellReports* *2*, 42–51.

Zhu, H., Hummel, T., Clemens, J.C., Berdnik, D., Zipursky, S.L., and Luo, L. (2006). Dendritic patterning by Dscam and synaptic partner matching in the *Drosophila* antennal lobe. *Nat. Neurosci.* *9*, 349–355.

Zipursky, S.L., and Sanes, J.R. (2010). Chemoaffinity Revisited: Dscams, Protocadherins, and Neural Circuit Assembly. *Cell* *143*, 343–353.

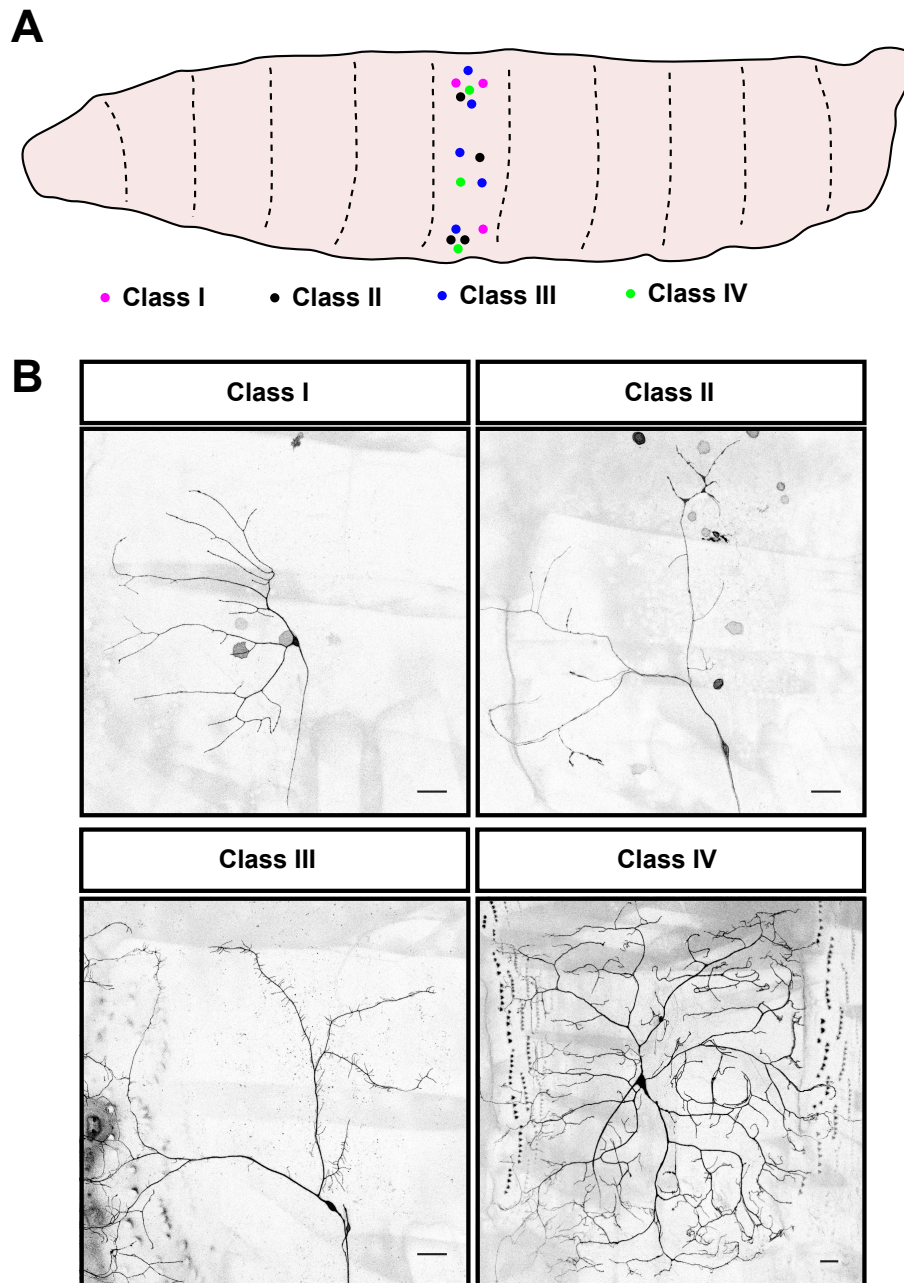
Zlatic, M., Li, F., Strigini, M., Grueber, W., and Bate, M. (2009). Positional cues in the *Drosophila* nerve cord: semaphorins pattern the dorso-ventral axis. *PLoS Biol.* *7*, e1000135.

Zou, W., Shen, A., Dong, X., Tugizova, M., Xiang, Y.K., and Shen, K. (2016). A multi-protein receptor-ligand complex underlies combinatorial dendrite guidance choices in *C. elegans*. *Elife* *5*, 308.

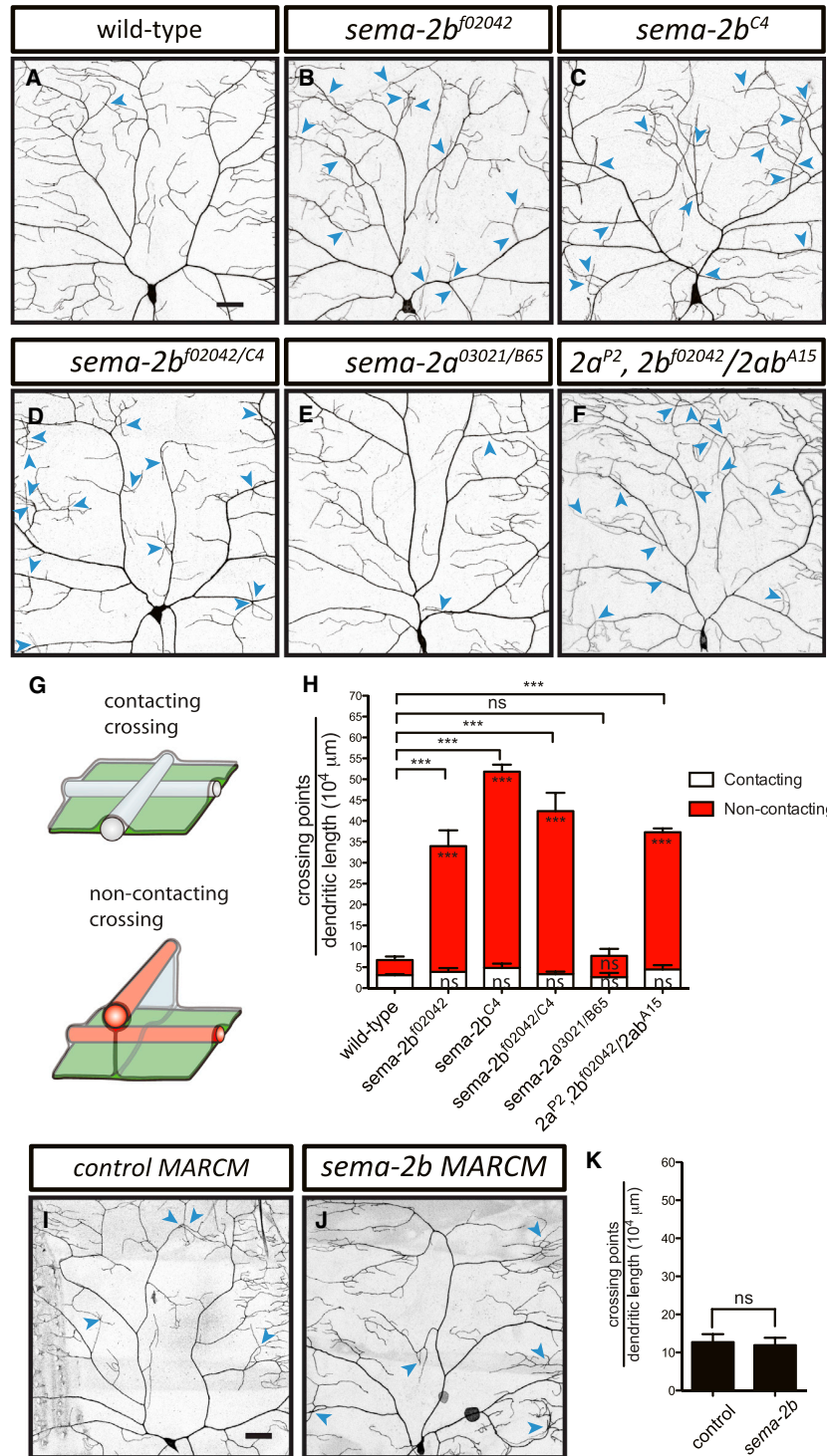
## Figures

Figure 1.1 Distributions and dendrite morphologies of classes I-IV

*Drosophila* dendritic arborization (da) neurons.



**Figure 2.1 Sema-2b, but not Sema-2a loss of function leads to an increase in dendritic self-crossings.**



**Figure 2.2 Enclosure of terminal dendrites by epidermal cells in *sema-2b* mutants.**

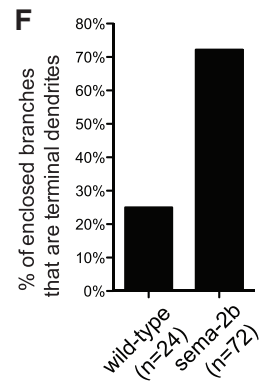
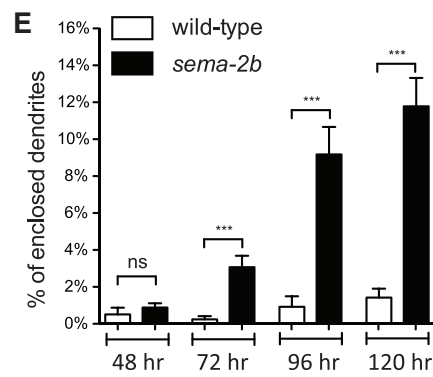
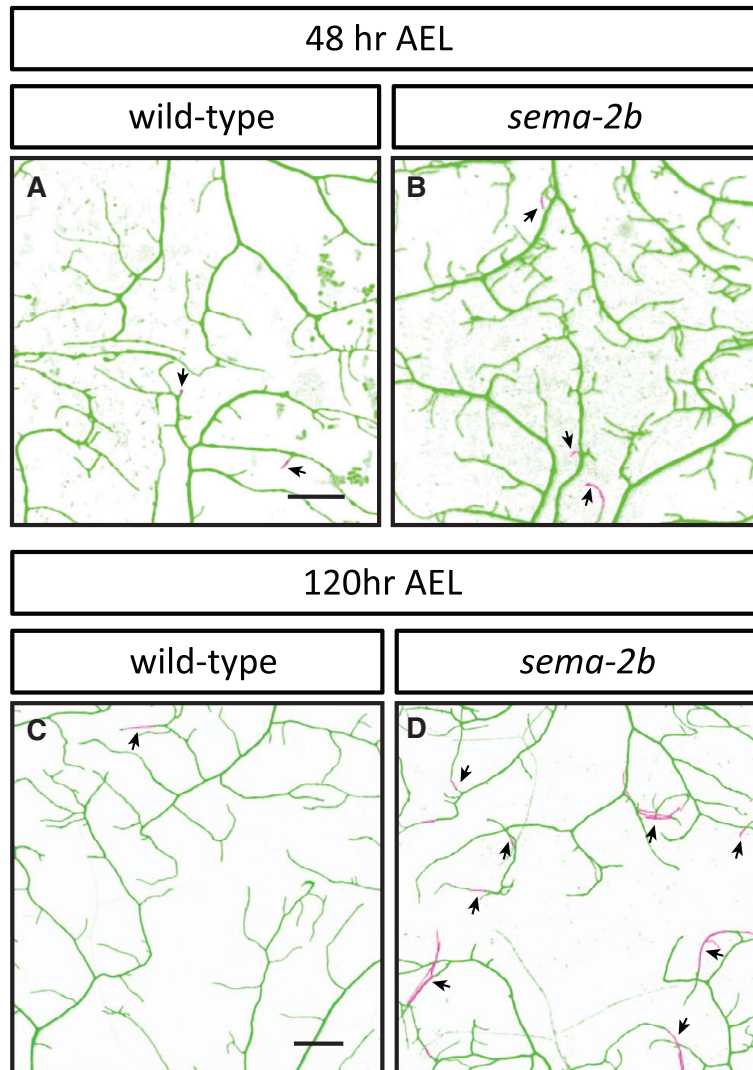




**Figure 2.3 Sema-2b is derived from epidermal cells and acts at short range to regulate dendrite adhesion.**

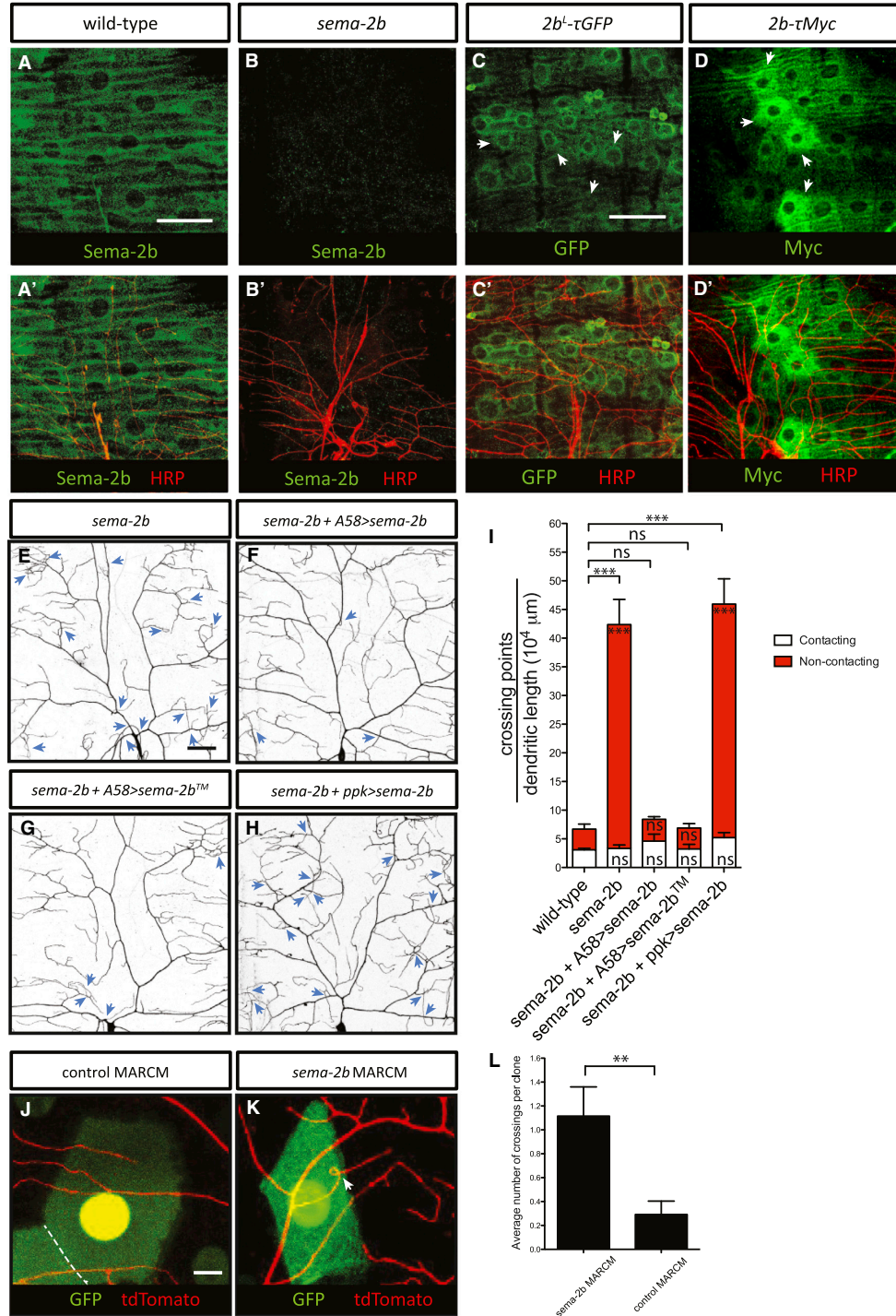


**Figure 2.4 Plexin B is the Sema-2b Receptor that regulates dendrite-ECM adhesion.**

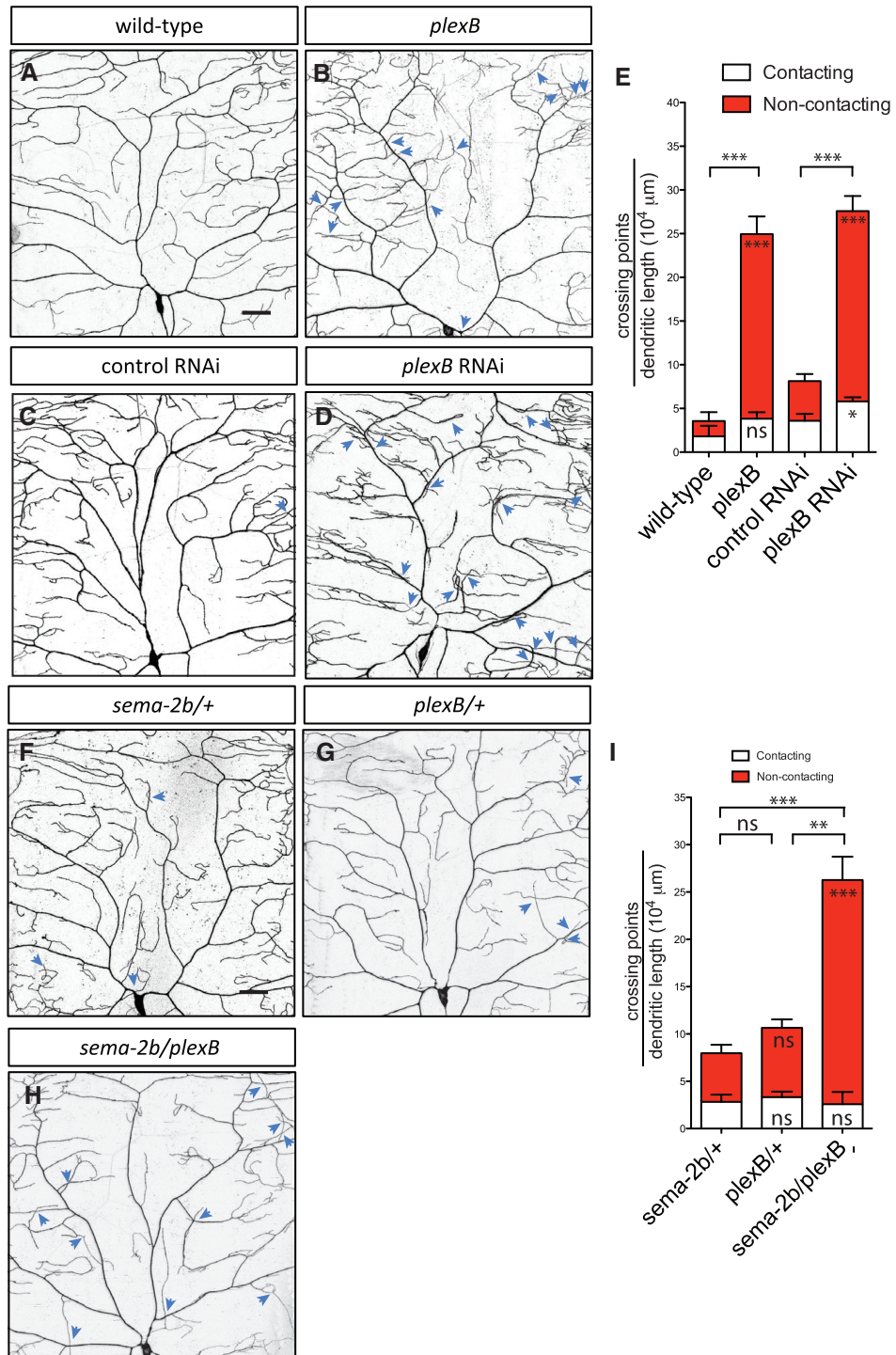


**Figure 2.5 Sema-2b genetically interacts with TORC2 complex and Trc kinase.**

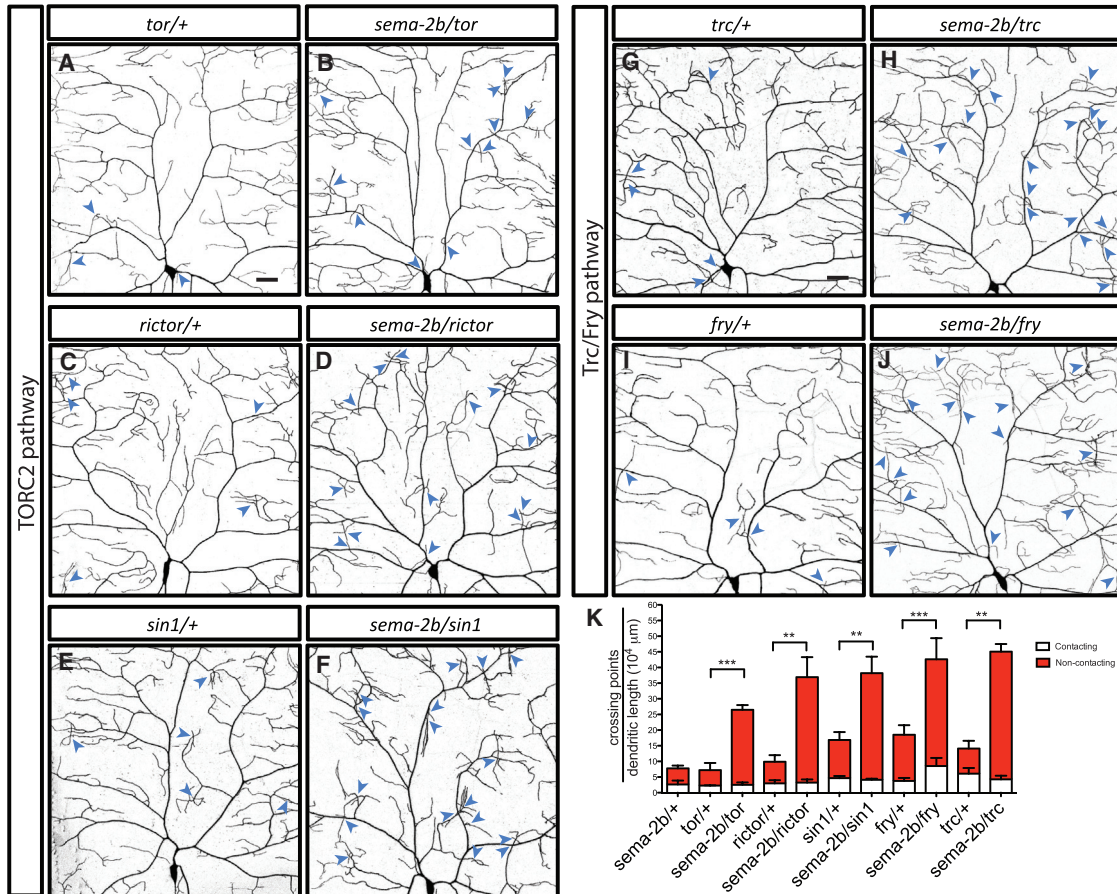


**Figure 2.6 Trc kinase acts downstream of Sema-2b/PlexB signaling to promote dendrite adhesion.**

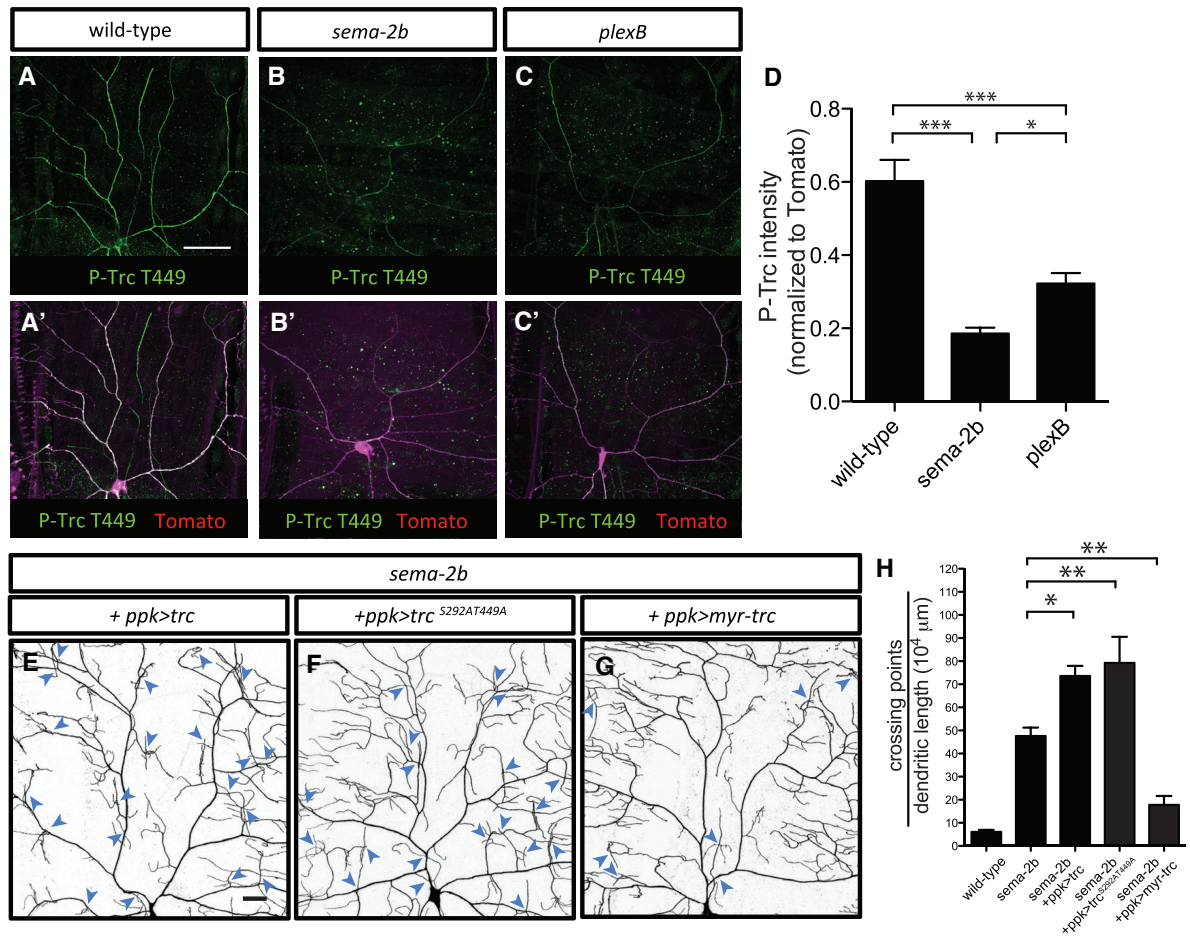


**Figure 2.7 Integrins overexpression suppresses dendrite crossing defects in *sema-2b* mutant.**

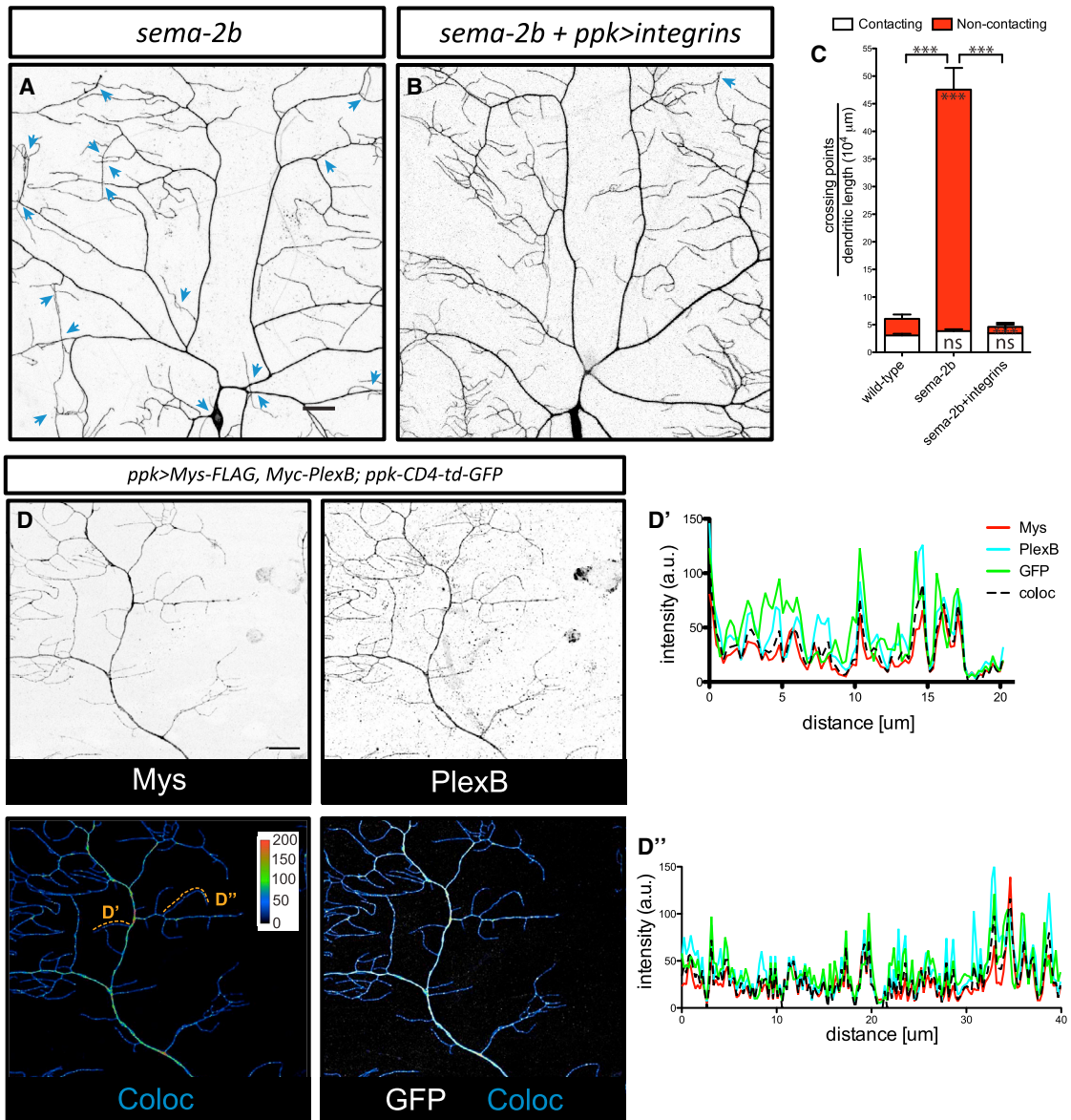


**Figure 2.8 Mys, a  $\beta$  subunit of integrin, associates with PlexB.**

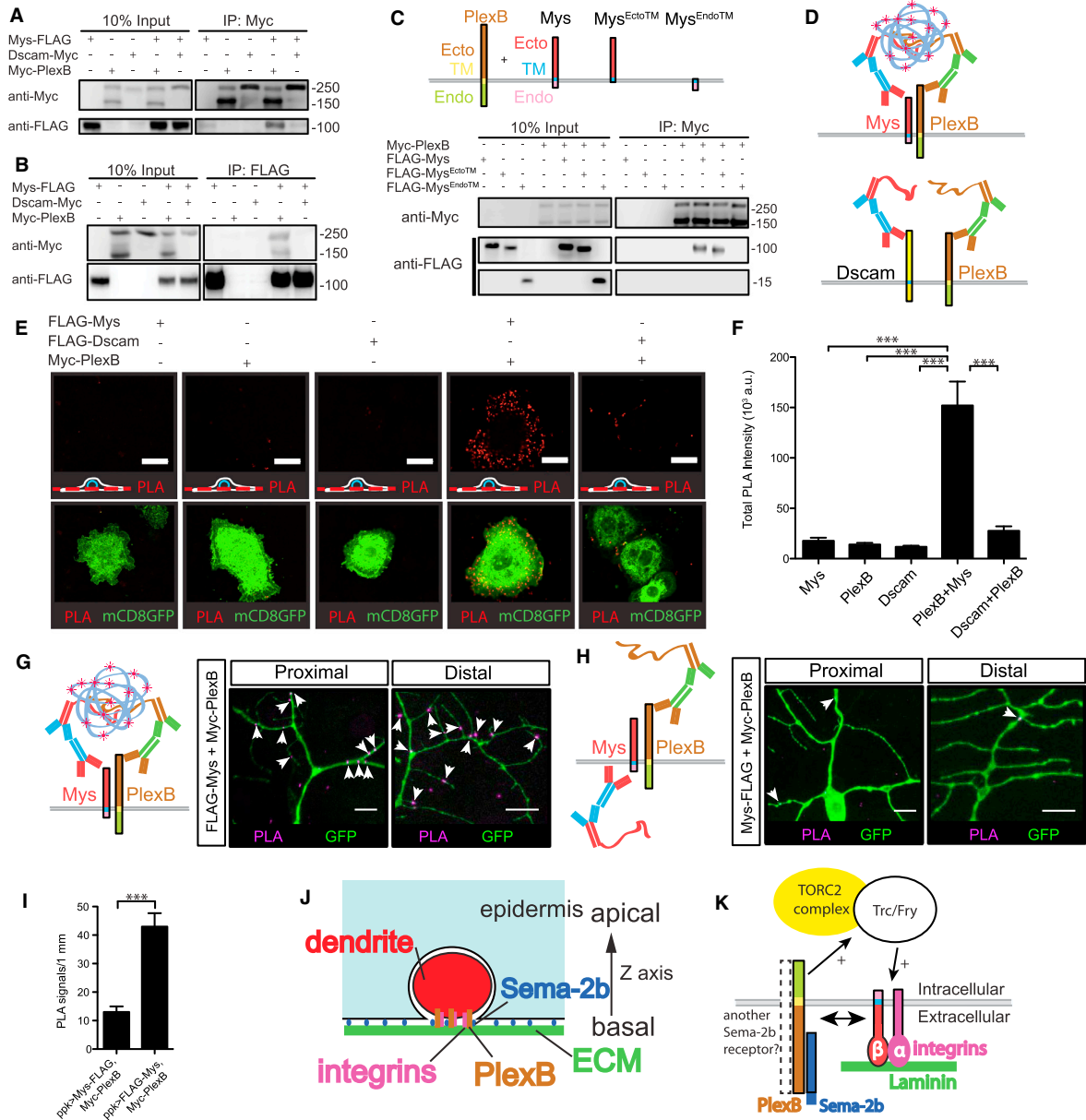


**Figure 2.9** An example of a contacting and a non-contacting dendritic crossing and dendrite phenotype in class I da neuron in the *sema-2b*

mutants.

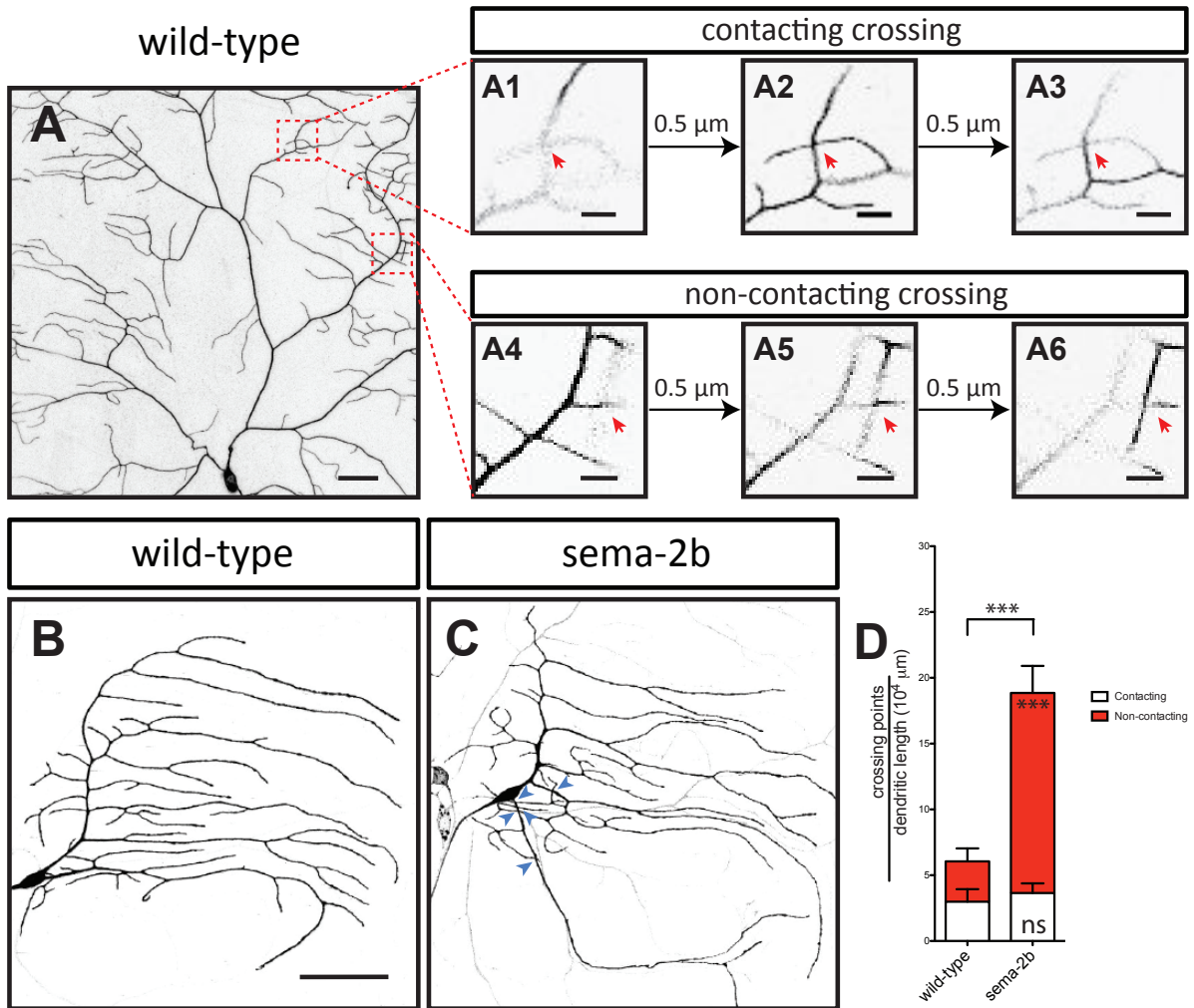


Figure 2.10 Overall morphology of axonal projections is normal in the *sema-2b* mutant.

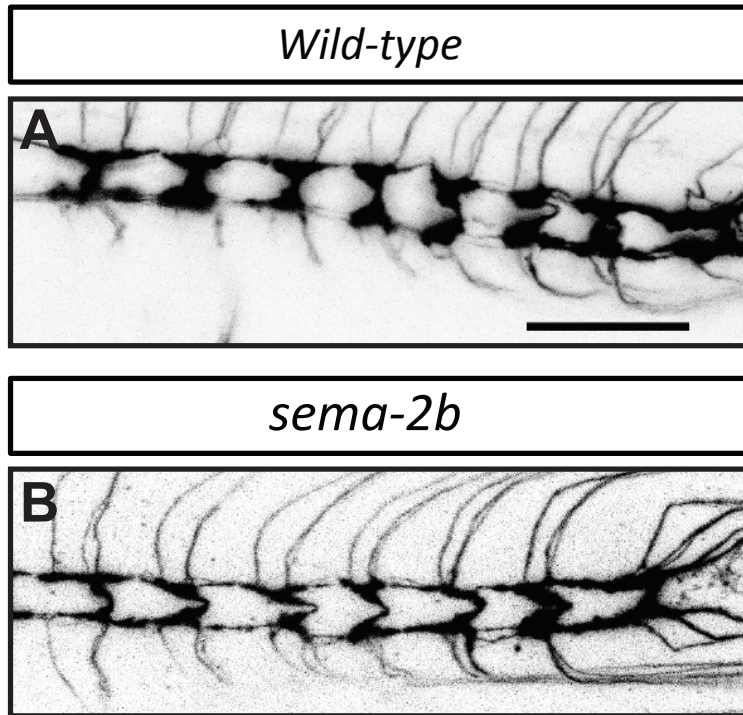




Figure 2.11 Overall morphology of epidermal cells is normal in the *sema-2b* mutant.

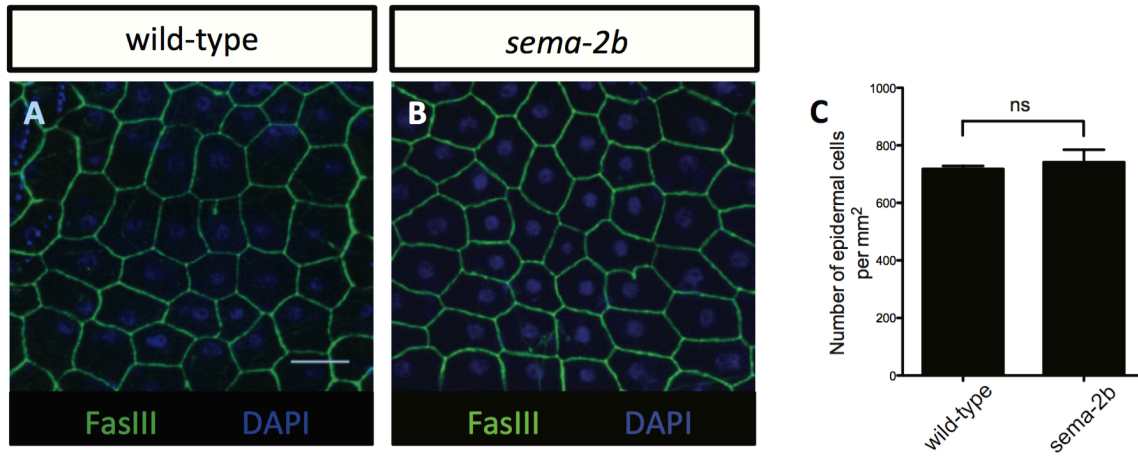
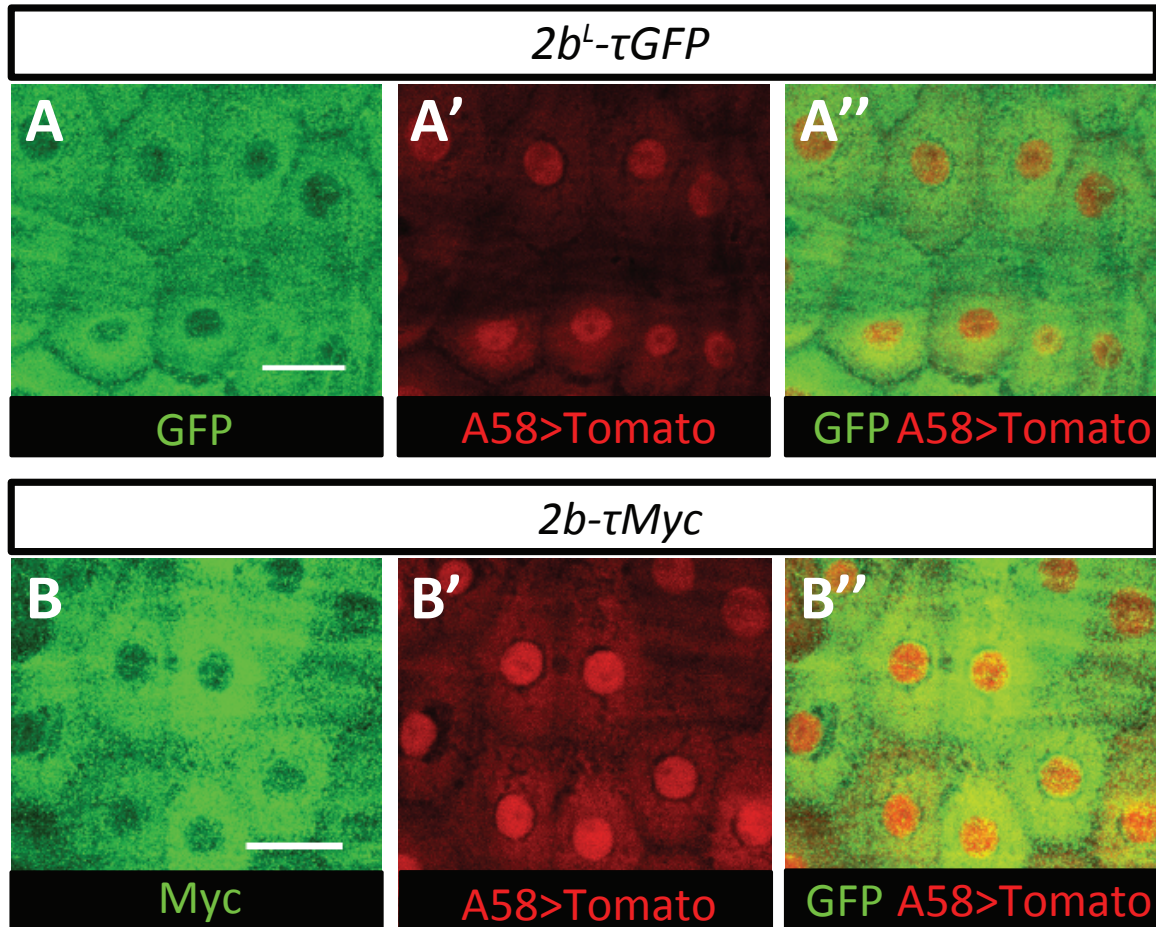
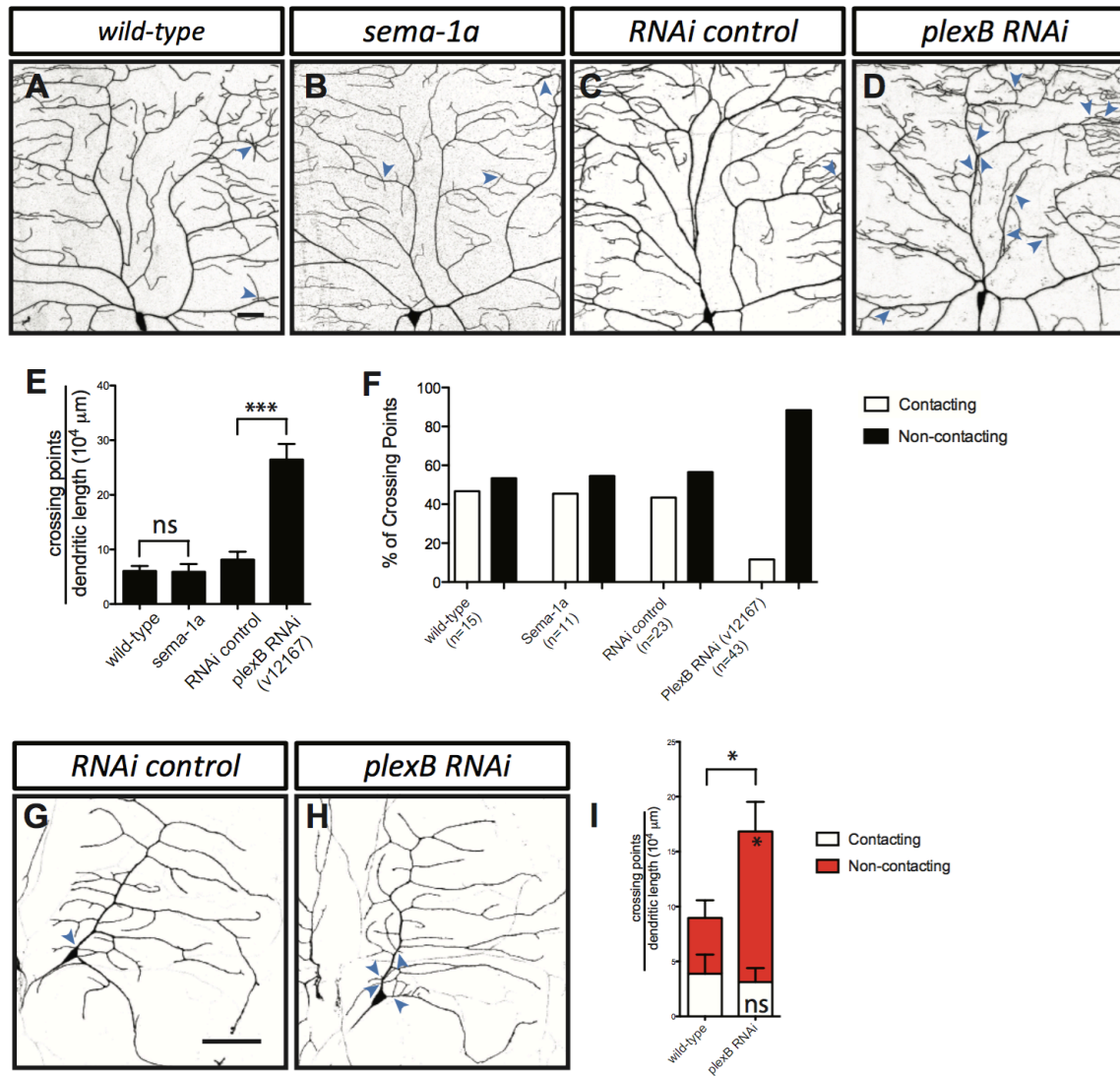


Figure 2.12 BAC Sema-2b reporters colocalize with the epidermal cell marker.



**Figure 2.13 PlexB, but not Sema-1a, is required to prevent dendrite-crossing in the class IV da neurons.**



**Figure 2.14 *fak56* and *otk* mutants do not show strong genetic interaction with *sema-2b* mutants.**

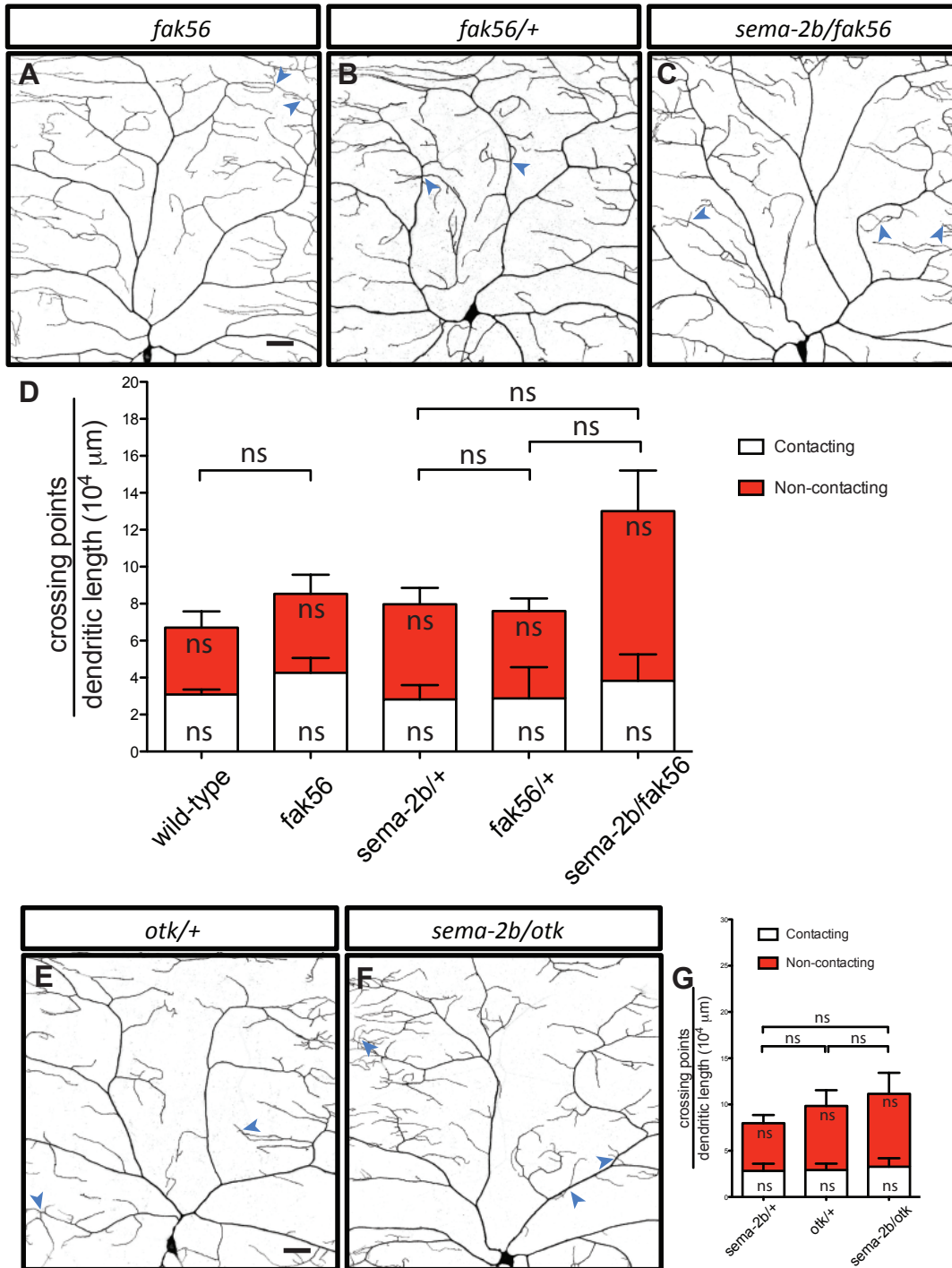


**Figure 2.15 Expression of proteins in S2 cells and dendrites of class IV da neurons.**

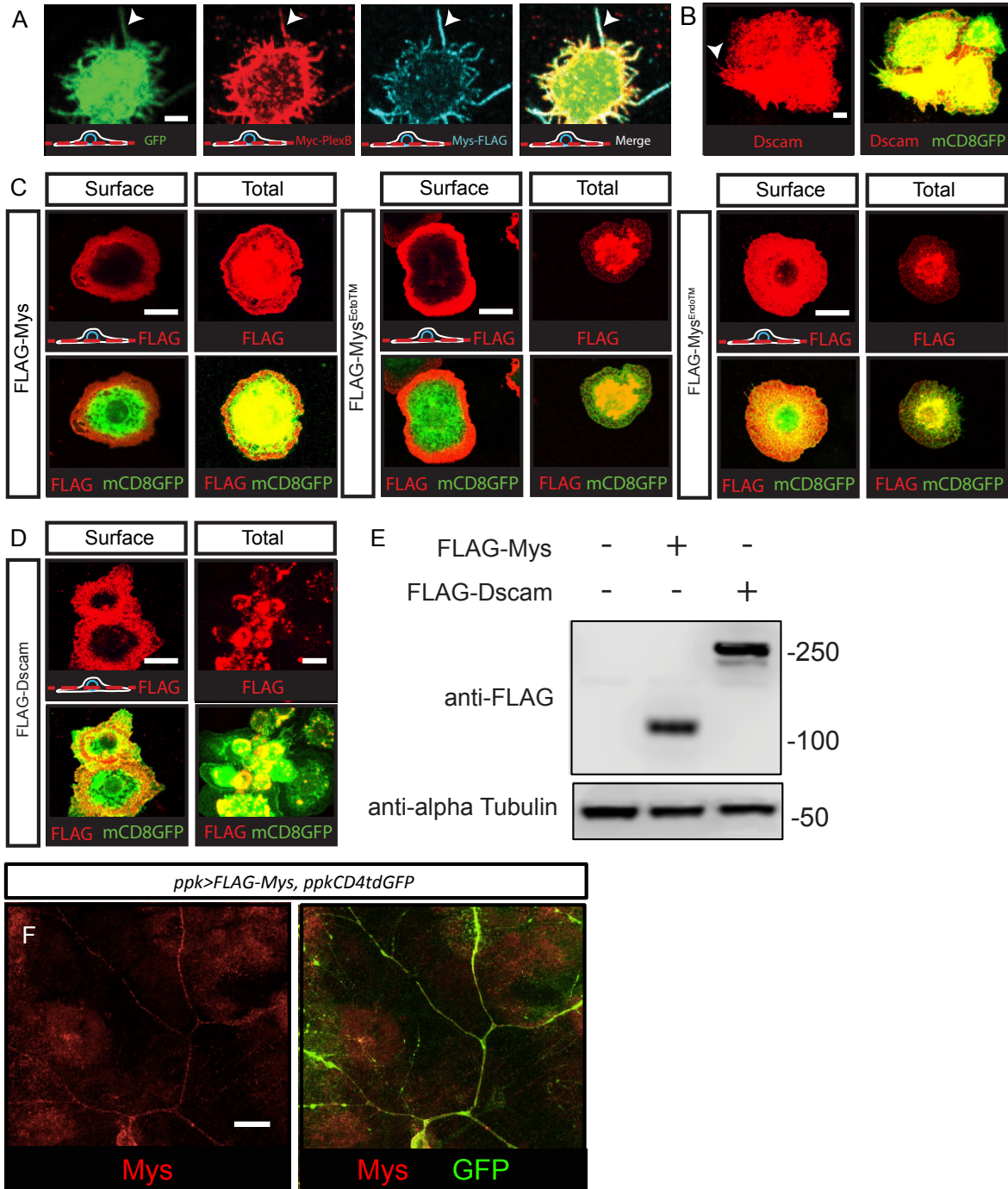


**Figure 3.1 EAS Is Required in Class IV da Neurons for Dendrite Morphogenesis.**

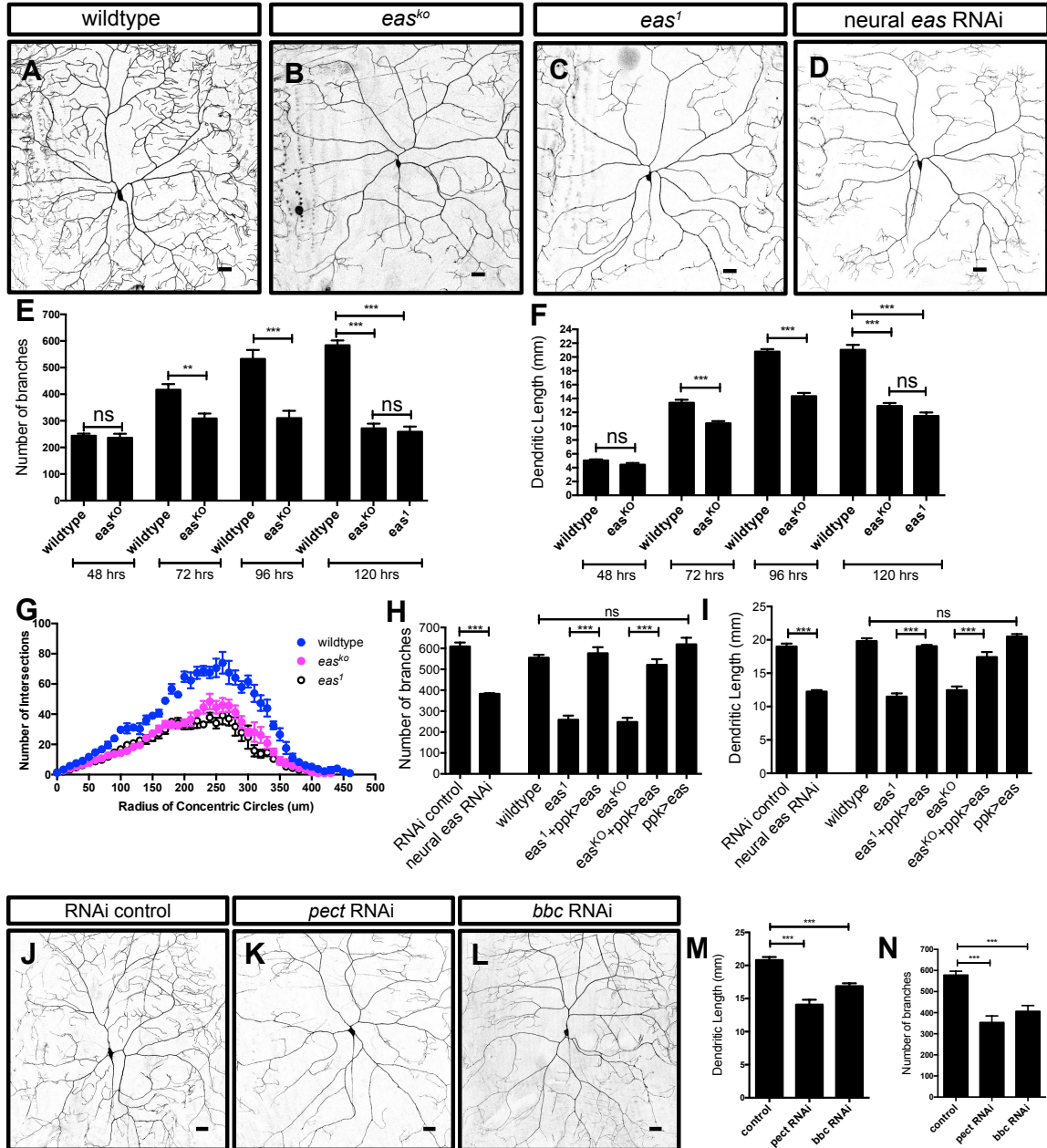
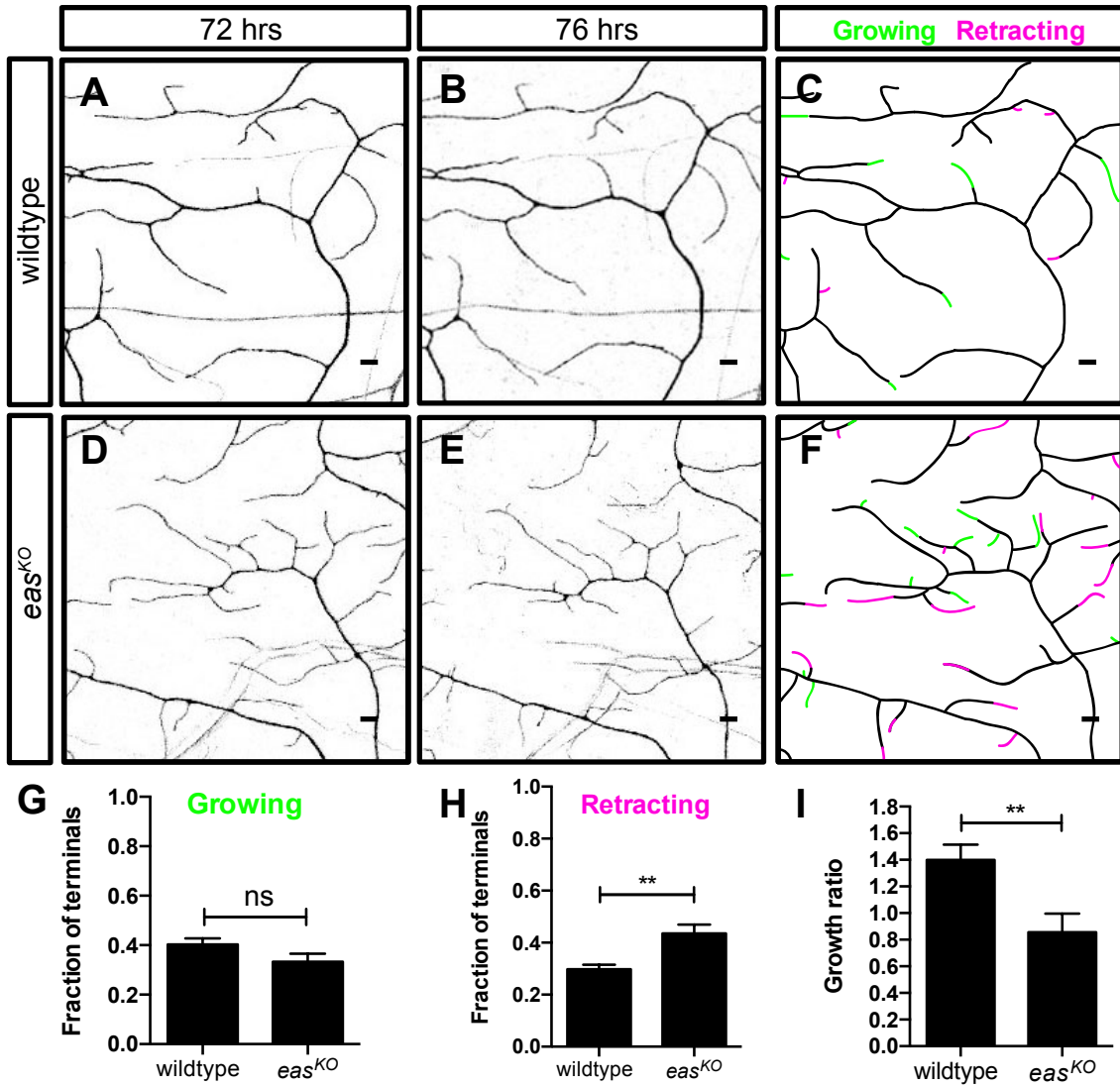
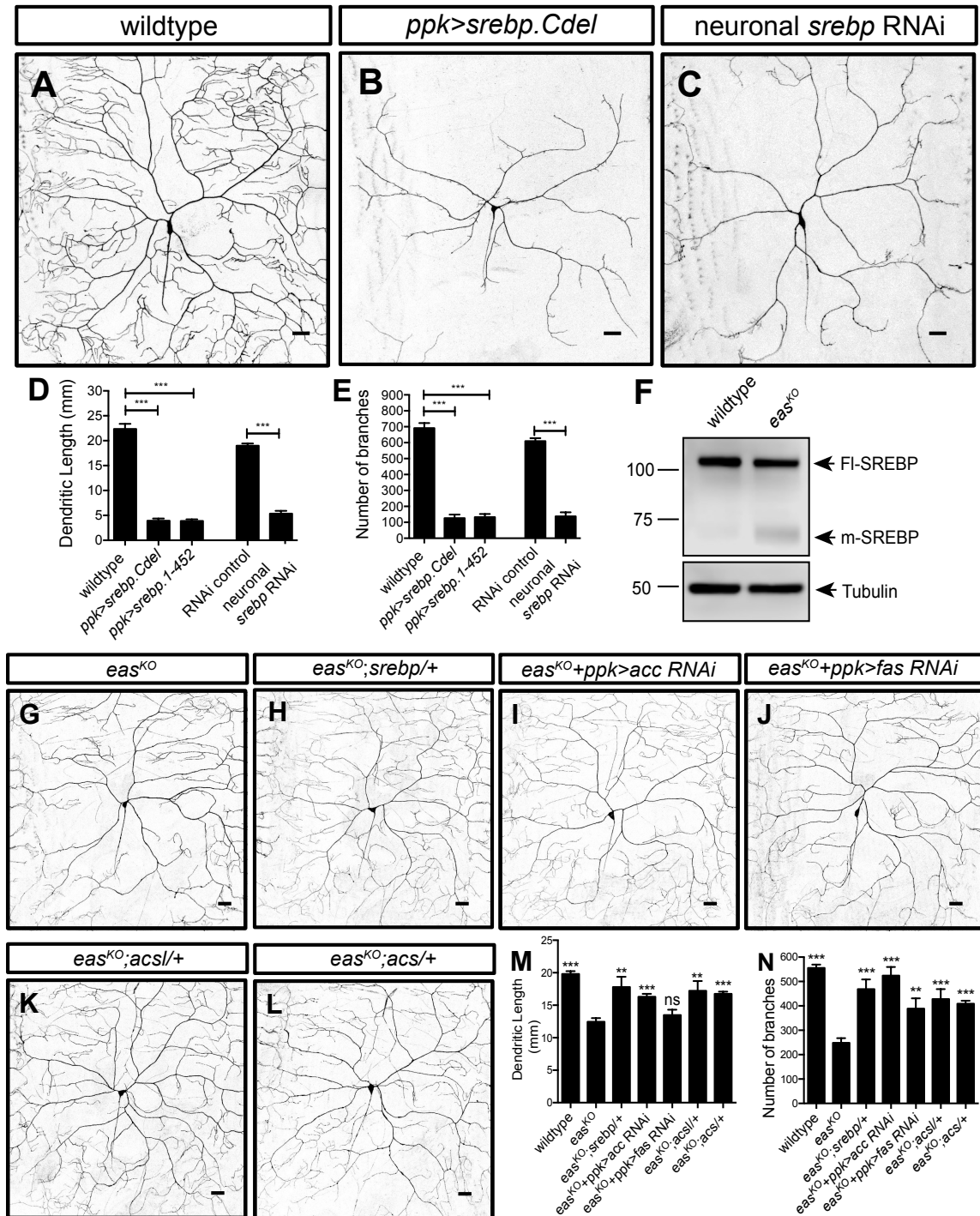


Figure 3.2 EAS Regulates Terminal Dendrite Growth Dynamics.



**Figure 3.3 Aberrantly High Level of SREBP Transcriptional Activity  
Contributes to the Dendrite Morphogenesis Defects in *eas*<sup>KO</sup> Mutants.**





**Figure 3.4 Reducing the level of cacophony partially suppresses dendrite morphogenesis defects in *eas*<sup>KO</sup> mutants.**

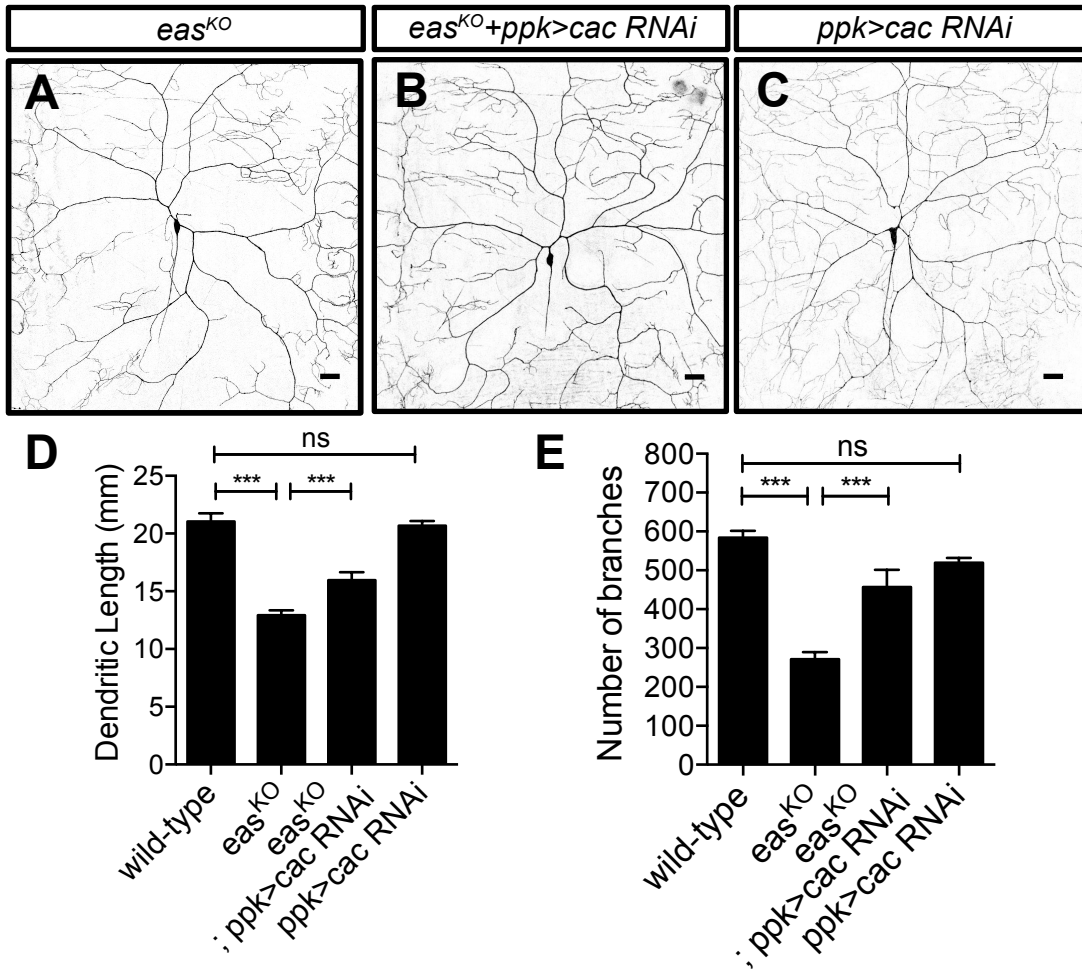




**Figure 3.6 Loss of eas also leads to reduced dendritic growth in class I and III da neurons.**

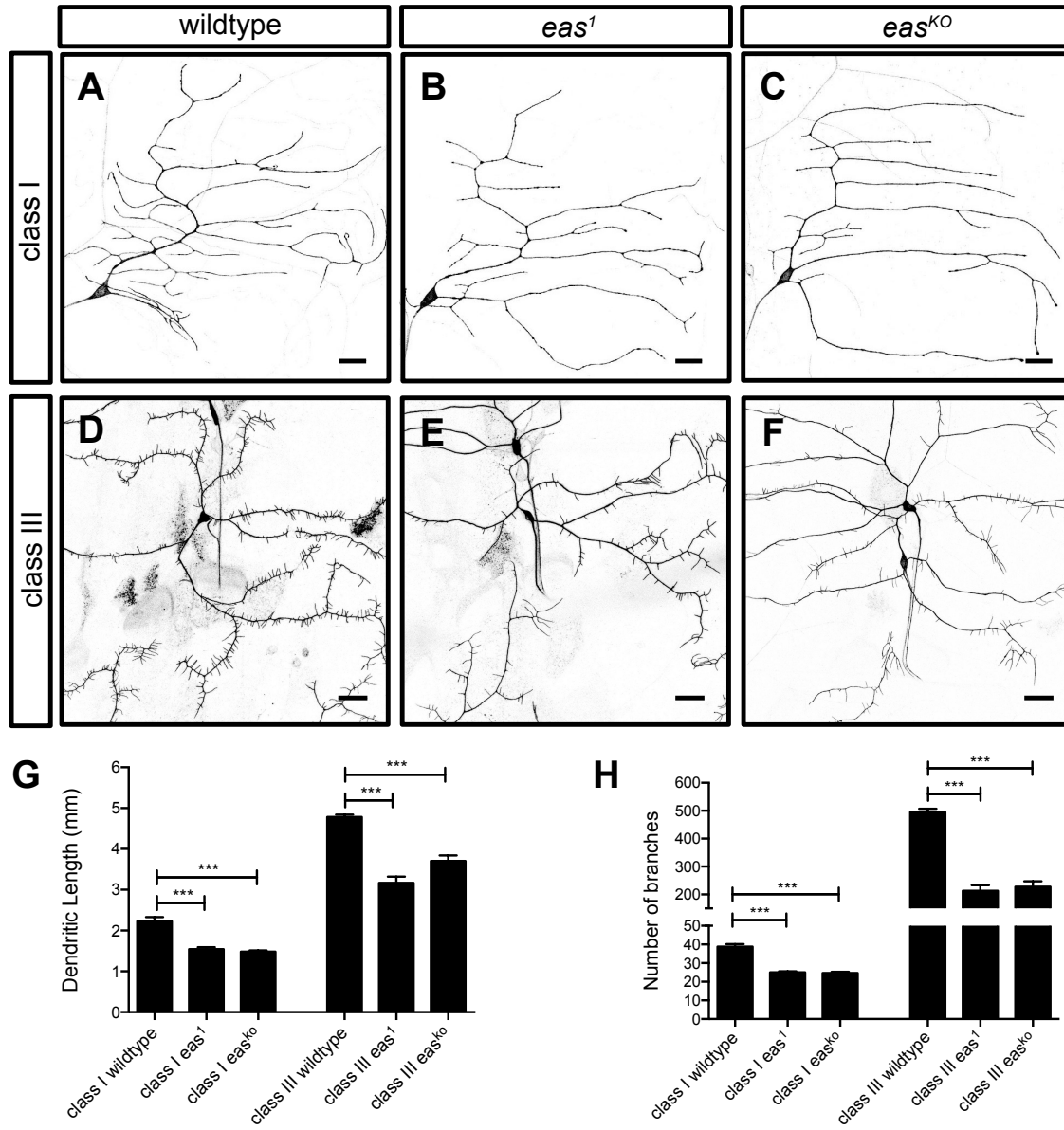
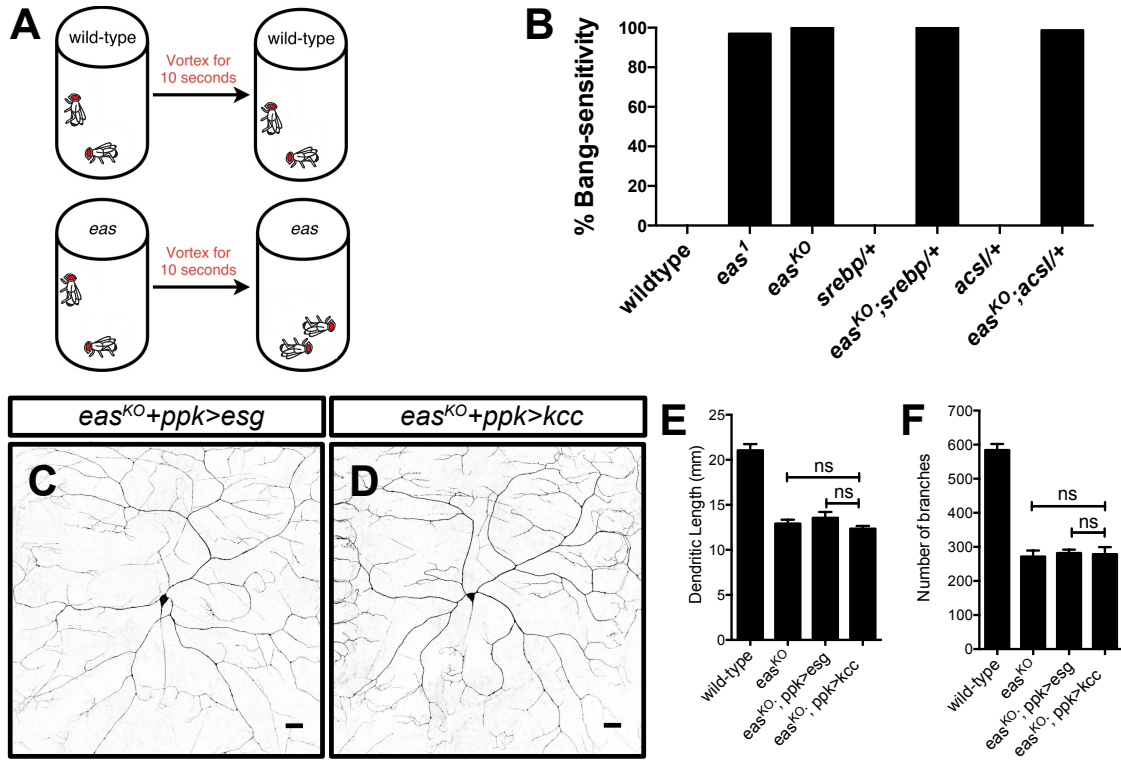


**Figure 3.7 Seizure-like phenotype in *eas* mutants is not suppressed by reducing SREBP signaling.**

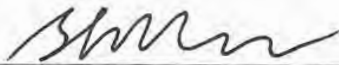


**Publishing Agreement**

*It is the policy of the University to encourage the distribution of all theses, dissertations, and manuscripts. Copies of all UCSF theses, dissertations, and manuscripts will be routed to the library via the Graduate Division. The library will make all theses, dissertations, and manuscripts accessible to the public and will preserve these to the best of their abilities, in perpetuity.*

***Please sign the following statement:***

*I hereby grant permission to the Graduate Division of the University of California, San Francisco to release copies of my thesis, dissertation, or manuscript to the Campus Library to provide access and preservation, in whole or in part, in perpetuity.*



\_\_\_\_\_  
Author Signature

8117117

\_\_\_\_\_  
Date